BARRICADED AND UNBARRICADED BLAST MEASUREMENTS

by

A. B. Wenzel
R. L. Bessey

Conducted for

Research Triangle Institute
Research Triangle Park, North Carolina

under

Contract No. DAHC04-69-C-0028
Subcontract 1-OU-431

by

Southwest Research Institute

October 1969

SOUTHWEST RESEARCH INSTITUTE
SAN ANTONIO HOUSTON

SOUTHWEST RESEARCH INSTITUTE
Post Office Drawer 28510, 8500 Culebra Road
San Antonio, Texas 78228

BARRICADED AND UNBARRICADED BLAST MEASUREMENTS,

by
A. B. Wenzel
R. L. Bessey

Conducted for
Research Triangle Institute
Research Triangle Park, North Carolina
under
Contract No. DAHC04-69-C-0028
Subcontract 1-OU-431
by
Southwest Research Institute
October 1969
91 p.

Approved:

H. N. Abramson

H. N. Abramson, Director
(Department of Mechanical Sciences)

TABLE OF CONTENTS

ABSTRACT

The objectives of this program were to conduct scaled experiments to measure air blast parameters from barricaded and unbarricaded high explosive charges, and to compare the results of those experiments with the Research Triangle Institute's analytical program presently being developed. Blast parameter measurements were made for the free field (no barricade present), near field (barricade located near the explosive charge), and the far field (barricade located a considerable distance away from the explosive charge) cases. The experiments utilized 1-lb and 64-lb spherical Pentolite charges, and single revetted and mound barricade configurations. The effects of the barricades on the blast parameters (peak pressures, scaled impulses, scaled time of arrivals, and shock overpressure duration) were investigated and compared with the blast parameters for the unbarricaded condition.

ACKNOWLEDGEMENTS

The authors are grateful to Dr. W. E. Baker for his helpful comments and suggestions during the course of this investigation.

Also, special recognition is given to Mr. W. G. Martin, Mr. W. B. Pepper, and Mr. E. R. Garcia, Jr., for conducting the experimental program; Mr. L. R. Garza for his help in the design of the barricades; F. O. Hoese for his assistance in setting up the explosive sites; and Mr. R. F. Gunst and Mr. A. Coindreau for their contribution in the data reduction. The cooperation of these individuals and others is greatly appreciated.

LIST OF ILLUSTRATIONS

LIST OF ILLUSTRATIONS (Cont'd)

LIST OF ILLUSTRATIONS (Cont'd)

LIST OF ILLUSTRATIONS (Cont'd)

LIST OF TABLES

LIST OF SYMBOLS

a_o - Sound velocity (ft/s)
D - Detonation velocity (ft/s)
d - Explosive charge diameter (ft)
H - Scaled height $\frac{h}{W^{1/3}}$ ($ft/lb^{1/3}$)
h - Height from the ground (ft)
I - Impulse (psi-ms)
L - Scaled barricade depth ($ft/lb^{1/3}$)
ℓ - Barricade depth (ft)
N_τ - Number of scaled time interval measurements
N_I - Number of impulse measurements.
N_p - Number of peak pressure measurements
P - Peak overpressure (psi).
p(T) - Time-varying overpressure (psi).
P_o - Ambient pressure (psi).
R - Distance from center of explosive source (ft).
r_i - Shape of source.
T_A - Shock wave time of arrival (ms).
$\bar{T}_A$ - Scaled shock wave time of arrival $\frac{T_A}{W^{1/3}}$ ($ms/lb^{1/3}$)
ΔT - Overpressure pulse duration (ms).
W - Weight of explosive (lb).
x - Barricade width at the top (ft).
Z - Scaled distance $\frac{R}{W^{1/3}}$ ($ft/lb^{1/3}$)

$\Delta\tau$ - Time interval of incident and reflected wave (ms)
ζ - Scaled impulse $\frac{I}{W^{1/3}}$ ($psi\text{-}ms/lb^{1/3}$)
λ - Scale factor
ρ_E - Density of source (lb/ft^3)
σ_I - Standard deviation of impulse measurements
σ_p - Standard deviation of peak pressure measurements
$\sigma_{\Delta T}$ - Standard deviation of shock overpressure measurements
σ_{T_A} - Standard deviation of time of arrival

I. INTRODUCTION

This report describes an experimental program conducted at Southwest Research Institute for the Research Triangle Institute, under Subcontract No. 1-OU-431, Prime Contract DAHCOO4-69-C-0028. The objective of the test program was as follows:

> Conduct scaled experiments to measure air blast parameters from barricaded and unbarricaded high explosive charges, and compare the results with the Research Triangle Institute's analytical program.

One hundred and five shots were fired during the course of this investigation. The conditions considered in this experiment simulated explosive weights of 8000 and 64, 000 lb of explosive with 10- and 20-ft barricade heights. The experiments conducted measured the blast parameters in the free field (no barricade present), the near field (barricade located near the explosive charge), and the far field (barricade located at a considerable distance away from the explosive charge). The experiments utilized 1-lb and 64-lb spherical Pentolite charges. Eighty tests were conducted utilizing the 1-lb charges and 25 tests were conducted utilizing the 64-lb charges. The two charge sizes were selected to verify the scaling laws. The results obtained in the free field condition are compared with results published in the literature.

Two different barricade cross sections were used for the barricade tests, single-revetted and mound. These tests simulated barricaded storage facilities and objects barricaded for protection. Eighty-seven experiments were conducted utilizing at least eight barricade conditions (two cross sections $\times$ two charge sizes $\times$ two barricade spacings).

All blast parameters were measured to an accuracy of $\pm$ 10 percent or better. Measurements were made up to distances corresponding to peak overpressures of 0. 5 psi for the free field condition.

In the report that follows, technical discussion is given covering background information, blast wave scaling, and data acquisition techniques. The experimental program outlines the experimental approach and the experimental setup. The results and analyses are presented in the form of graphs and illustrations. Conclusions and recommendations are made, and two tables of the complete test data are included as Appendix A of the main report.

II. TECHNICAL DISCUSSION

A. Background Information

The present American practice is to assume that barricades reduce the risk of damage from mass-detonating explosives at a given distance. The quantity-distance tables assume that barricades furnish protection over a wide range of distances, over a wide range in weight of explosives, and against a wide variety of damage mechanisms. The tables provide for incremental increases in distances with increasing amounts of explosives and cover amounts up to 500,000 lb net, which is sufficient for most commercial purposes in this country. On the basis of data obtained by the analysis of explosions over a period of 50 yr, the tables were published with the requirement that barricaded distances be approximately one-half the unbarricaded distances, on the theory that barricades and distance were required for protection and that the increased distance specified for unbarricaded explosions was, in reality, a penalty assessed for not providing the barricade. Quantity-distance protection is the stipulation of appropriate distances from a potential source of hazard that would be sufficient to provide the desired degree of protection to whatever target is under consideration. They are "relatively risky" or "relatively safe" distances rather than "absolutely safe" distances.

Broadly categorizing, the distances are generally grouped as follows:

- Magazine distance--sufficient to prevent communication between adjacent stores of material.
- Interline distance--sufficient to limit communication and reduce deaths and injuries upon personnel who are exposed to hazards within manufacturing plants.
- Inhabited building distance--sufficient to protect personnel from risk to life and limb as a result of building collapse, flying debris, blast, and fire.

At the inhabited building distance, most damage is the result of blast pressures of low intensity. The tables specify a different inhabited building distance for barricaded and unbarricaded facilities. There is little discussion, in the present manuals, of methods for designing structures or barricades to better resist the effects of an explosion in cases where a greater level of protection is essential at a given distance than that provided by the quantity-distance tables, or where a structure must be located closer to the potential source of explosion than the barricaded distance. Since barricade-distance tables permit using half as great a distance as unbarricaded-distance tables, they lead to the assumption that the damage would be no greater at

the barricaded distance than that at the unbarricaded distance. Therefore, the tables imply that barricades make a great change in low level air blast pressures.

At interline and intermagazine distances for a mass-detonating explosive, a similar halving of unbarricaded distance for a barricaded condition is allowed for a certain level of damage. But, at higher blast pressures, damage level often related more to blast impulse than to pressure. Since the tables are based on pressures, they may not apply for these conditions. Also, for these interline and intermagazine categories, one could assume from the tables that a reduction in the probability of fragment and debris strikes is made in proportion to the reduction in air blast values. The tables do not, in fact, consider these mechanisms to scale in the same way as the air blast since, in the description of damage at inhabited building distances, it is mentioned that damage from fragments will be negligible except at distances appropriate to small quantities of explosives where blast damage is predicted to be uniformly minor. Discussions in the manual relating to the construction of the barricade and the manner in which it is assumed to furnish protection do not change in accordance with explosive weight, actual or scaled distance, or damage mechanisms.

As a result of our investigations and other investigations, it is currently felt that many of the quantity-distance relations may be improved. Generally, the net result of the use of the present DOD instructions is a loss of economy because: (1) more land may be utilized than necessary to store a quantity of explosives, and (2) structures which may not afford the intended protection for a given damage level may be constructed. A lack of knowledge of effects of barricades on the blast parameters may result in a less than desired degree of safety.

The data reported in Section IV of this report provide additional information to evaluate the effectiveness of barricades, and furnish a foundation for reassessing current barricade procedures.

B. Scaling of Blast Parameters

Experimental studies of blast wave phenomena are often quite difficult and expensive, particularly when conducted on a large scale. Methods of computation of blast wave characteristics are often so involved that one cannot economically repeat these computations while varying, in a systematic manner, all of the physical parameters which may affect the blast wave. So, almost from the outset of scientific and engineering studies of air blast, various investigators have attempted to generate model or scaling laws which would widen the applicability of their experiments or analyses.

The most common form of scaling, familiar to anyone who has had even a rudimentary introduction to blast studies, is Hopkinson or "cube-root,"

scaling. This law was first formulated by B. Hopkinson[1]*, and it states that self-similar blast waves are produced at identical scaled distances from two explosive charges of similar geometry and identical explosive material, but of different size, which are detonated in the same atmosphere. Scaled distance is a nondimensional parameter (or, rather, uniquely determines a nondimensional parameter) defined as

$$Z = R/W^{1/3} \tag{1}$$

where R is distance from center of explosive source and W is weight of explosive.

The implications of Hopkinson scaling can perhaps be best described by the example illustrated in Figure 1. An observer located a distance R from the center of an explosive source of characteristic dimension d will be subjected to a blast wave with amplitude (peak overpressure) P, duration ΔT, and a characteristic time history. The positive impulse I of the blast wave, defined by

$$I = \int_{T_A}^{T_A + \Delta T} p(T)dT \tag{2}$$

where T_A is arrival time of the shock front and p(T) is the wave form of the time-varying overpressure, is also often used to characterize the blast wave. The Hopkinson scaling law then states that an observer stationed a distance λR from the center of a similar explosive source of characteristic dimension λd detonated in the same atmosphere will feel a blast wave of similar wave form, identical amplitude P, duration $\lambda\Delta T$, and impulse λI. All characteristic times such as arrival time T_A are scaled by the same factor as the length scale factor λ. In such scaling, both pressures and velocities are unchanged at homologous times.

Hopkinson scaling has been shown by many investigators to apply over a very wide range of distances and explosive source energies. An example of early published work is that of Stoner and Bleakney[2] which showed that such scaling would apply for a limited range of distances and source energies. The list of other investigations corroborating this law is too numerous to include here, but a recent report by Kingery, et al[3] showing very good agreement between blast data obtained during a field test with a 100-ton TNT detonation and predicted values scaled from experiments with 1- to 8-lb charges, will serve to indicate the usefulness of this ubiquitous law. It has, in fact, become so universally used that blast data are almost always presented in terms of the Hopkinson-scaled parameters:

*Superscript numbers in parentheses refer to references listed in Section VI of this report.

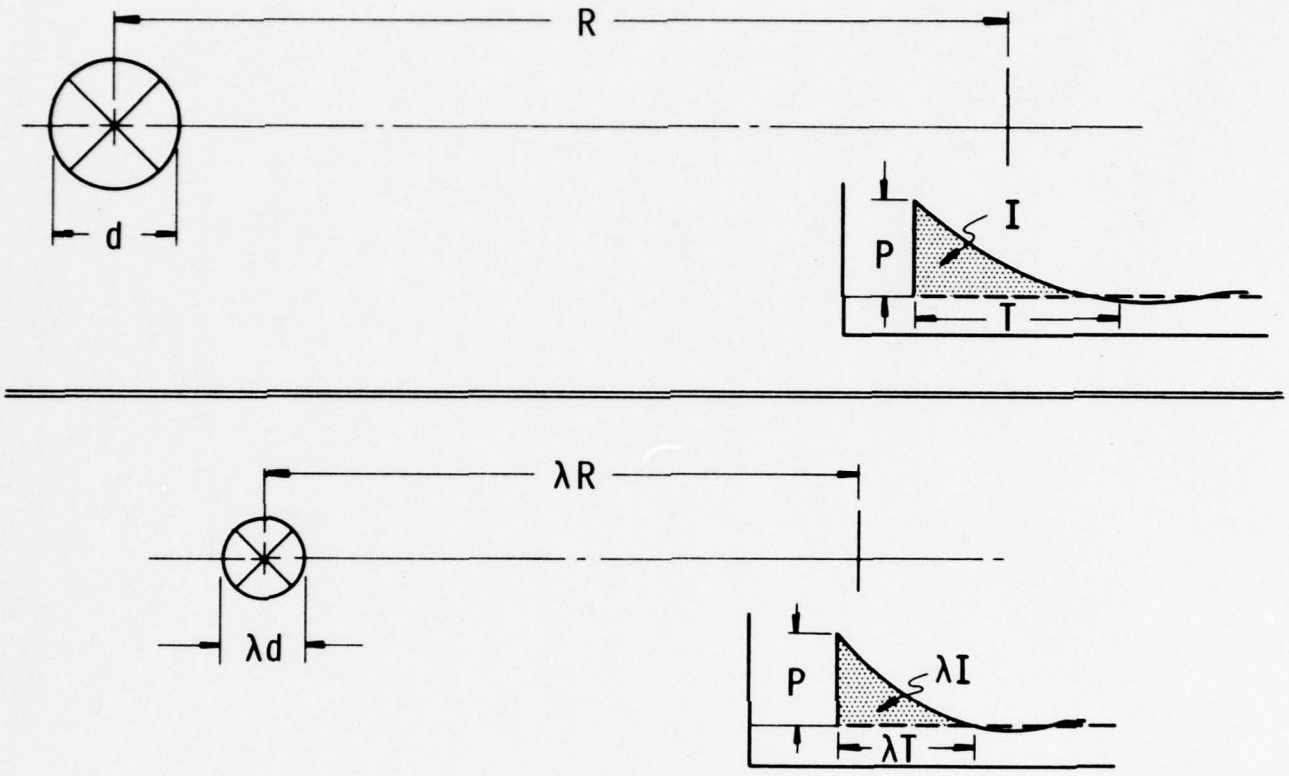

2474

FIGURE 1. HOPKINSON BLAST WAVE SCALING

$$Z = R/W^{1/3} \text{ (scaled distance)}$$

$$T = T/W^{1/3} \text{ (scaled time)} \qquad (3)$$

$$\zeta = I/W^{1/3} \text{ (scaled impulse)}$$

This law implies that all quantities with dimension of pressure and velocity are unchanged in the scaling. Thus, side-on pressure, dynamic pressure, and reflected pressure all remain identical at homologous times; and both shock velocity U and time histories of particle velocity u are unchanged. The law can be stated in another way:

$$P = P(Z)$$

$$T = T(Z) \qquad (4a)$$

$$V = V(Z)$$

$$\zeta = \zeta(Z)$$

i.e., each specific pressure, scaled time, velocity or scaled impulse is given by a unique function of scaled distance Z.

It is not immediately apparent that Hopkinson scaling is indeed true dimensionless modeling, because the parameters shown in Equation (3) are not dimensionless. But, a brief model analysis will show that the parameters there are indeed uniquely defined by dimensionless groups. Let us first list a possible set of physical parameters which should govern blast waves in air under any given ambient conditions, together with their dimensions in a force-length-time (FLT) system.

Symbol	Description	Units
E	Total energy in blast source	FL
d	Size of source	L
r_i	Shape of source	-
R	Distance from source	L
D	Detonation velocity of source (or other characteristic velocity)	L/T
ρ_E	Density of source	FT^2/L^4

Since there are six physical parameters and three fundamental dimensions, then there will be 6 - 3 = 3 dimensionless groups which describe the model law. These π terms, found in the usual manner of dimensional analysis, are:

$$\pi_1 = r_i/d$$

$$\pi_2 = R/d \tag{4b}$$

$$\pi_3 = E/\rho_E D^2 d^3$$

The first term states that ratios of all source dimensions to some characteristic length d must be identical between model and prototype. The second term states that the distances at which various blast wave properties are observed must scale in the same geometrical manner as the sources. The third defines the characteristic length d in terms of known characteristics of conventional chemical explosives. An alternative definition of this last term could be employed for other sources by redefinition. For example, for a compressed gas source, D could be defined as sound velocity in the source, while ρ_E still represented its density. For a nuclear explosive source, fictitious values for ρ_E and D might be required to properly simulate the very high energy densities. This law is the Hopkinson law, slightly generalized to allow some freedom in variation of blast energy source, and the same inferences can be drawn as before.

Hopkinson scaling assumes that heat conduction and viscosity may be neglected. In addition, gravitational effects are assumed minimal. In an attempt to account for the effects of altitude ambient conditions on air blast waves, Sachs[4] proposed a more general blast scaling law than that of Hopkinson. Sachs' scaling law states that dimensionless groups can be formed which involve pressure, time, impulse, and certain parameters for the ambient air, and that these groups are unique functions of a dimensionless distance parameter. Specifically, the groups

$$P/P_o,\ Ia_o/W^{1/3}p_o^{2/3},\ Ta_o p_o^{1/3}/W^{1/3}) \tag{5}$$

are stated to be unique functions of $(R\ p_o^{1/3}/W^{1/3})$. In these relationships, P_o and a_o are ambient pressure and sound velocity respectively.

Sperrazza[5] has presented a careful derivation of Sachs' scaling law, using dimensional analysis techniques. The effects of altitude conditions were not investigated in this program (since it was performed at ground level) and, therefore, discussion of Sachs' scaling laws is not apropos to this report. Scaling of blast parameters where structures such as barricades are present is done by following Hopkinson's scaling laws and applying geometric similarity. Basically, we scaled the entire experiment geometrically, as shown in Figure 2, by a scale factor λ, making the energy source of characteristic dimension λd and locating the barricade of characteristic

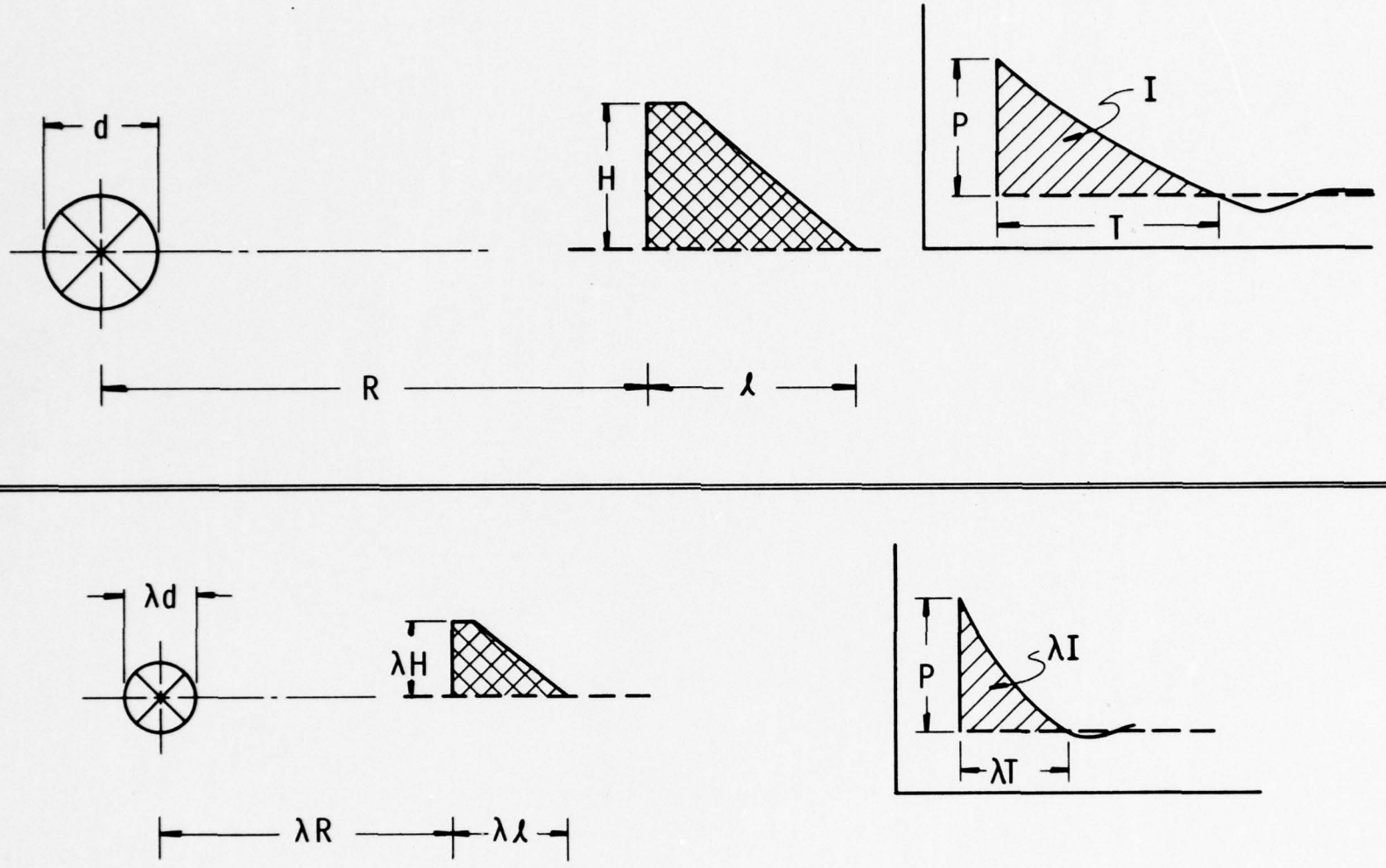

2475

FIGURE 2. GEOMETRICAL SCALING OF BLAST PARAMETERS WITH BARRICADES PRESENT

dimensions λH and at a distance λR from the source. This scaling predicts that the pressures in front and behind the barricade will have similar waveforms to that obtained in the full-scale experiments with amplitude P and duration λT. Therefore, the Hopkinson-scaled parameters for the geometrical scaling of the barricade are given by Equation (6):

$$H = \frac{h}{W^{1/3}}$$

$$L = \frac{\ell}{W^{1/3}} \qquad (6)$$

C. Techniques of Data Acquisition

The configuration and specifications of our experimental apparatus were such that we could measure fourteen channels of pressure-time histories of the blast waves emanating from the detonation of a spherical Pentolite charge at various scaled distances from ground zero. Our apparatus was designed to measure peak pressures from 0.05 to 100 psi with rise times of 1.8 ms or more and pulse lengths of 30 ms with distortion of 5 percent or less. The fourteen channels of pressure-time history were recorded at 60 in. per s (ips) on magnetic tape and replayed at 1-7/8 ips, seven channels at a time, through a recording oscillograph. The resultant pressure-time history records were analyzed for peak pressure, impulse, time of arrival, pulse length, and wave form.

The gages used for the experimental data taken at all locations except those on the surfaces of the barricades were Atlantic Research LC-33 pencil blast gages. These gages have a sensitivity of approximately 3×10^3 picocoulombs/psi (pC/psi), an internal capacitance of 4.5×10^3 pF, and nearly an infinite resistance. Their rise time is 10 μs. The physical appearance of these gages can be seen in Figure 3. The piezoelectric sensitive area of the gage is under the black strip appearing 3 in. from the point of the gage.

Data obtained by mounting a transducer on the barricade or on a plate on the ground behind the barricade were taken with Susquehanna ST-4 transducers. These transducers have a sensitivity of approximately 0.128 pC/psi or considerably iess than that of the pencil blast gages. Their capacitance is approximately 14 pF and internal resistance is above 10^7 Ω. The physical appearance of these transducers can be seen in Figure 3. The piezoelectric sensitive area of the transducer is on the cylinder end.

The nature of this experiment necessitated that the location of personnel and recording apparatus be at safe separation distances of up to 500 ft from the energy source. This meant that cable lengths ranging from 133 to 500 ft were necessary to reach the pencil blast gages and ST-4 transducers in the field from the instrumentation and personnel location. The cable used

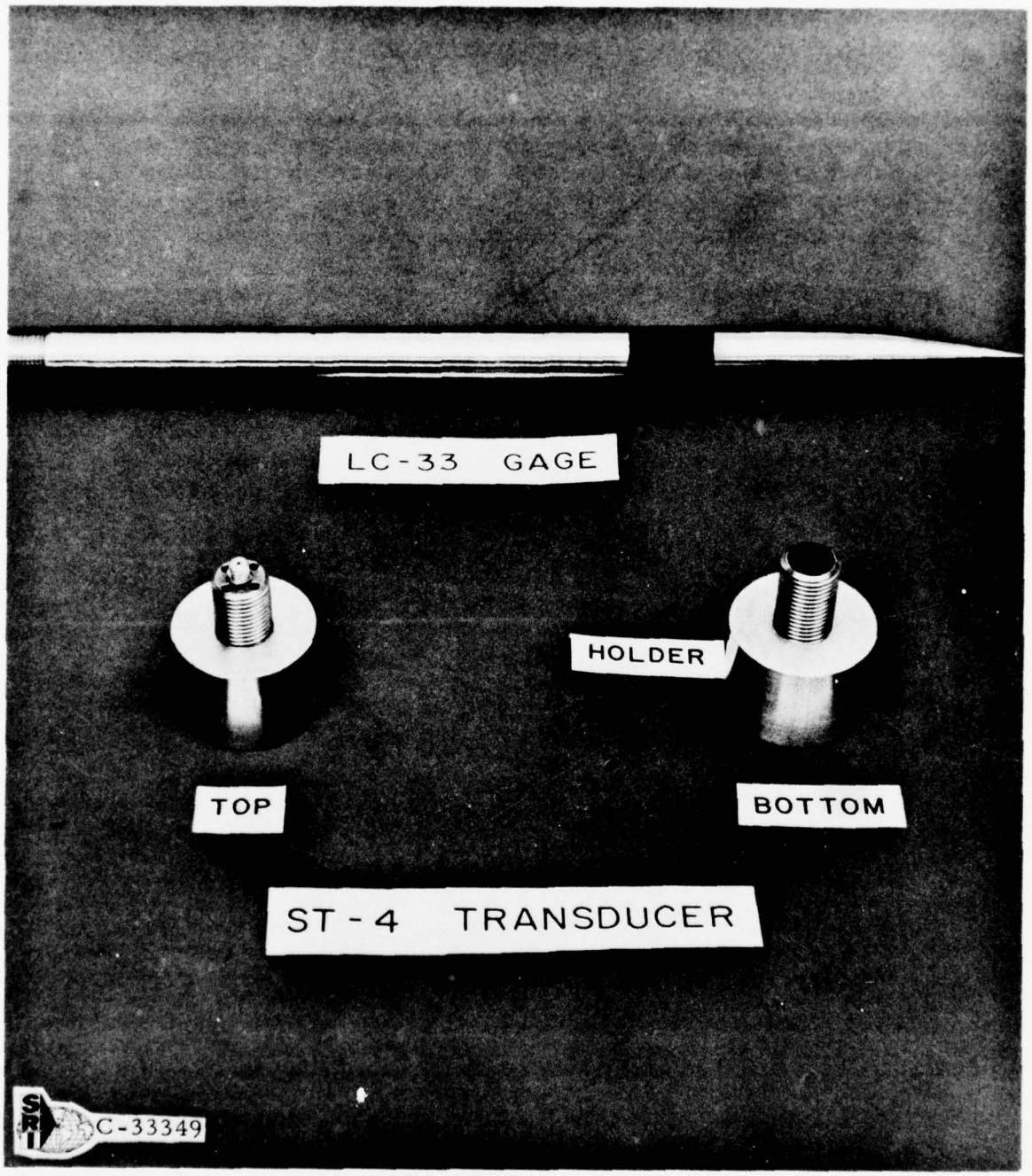

FIGURE 3. TYPICAL PRESSURE TRANSDUCERS

was RG-62U, a coaxial cable whose physical characteristics make it most suitable for blast work. The capacitance of this cable is 14.5 pF/ft; our cable lengths had total capacitances ranging from 1.85 nF to 6.10 nF.

Obviously, cables with such a range of capacitances could affect the calibration of a data channel if calibration and data for a given channel were not both taken with the same cable and transducer on that channel. Gages, cables, and recording channels were never interchanged without recalibration.

Cables from the LC-33 pencil blast gages and ST-4 transducers were connected to the inputs of two 8-channel impedance matching amplifiers designed and built at SwRI. These amplifiers have a voltage amplification factor of ten and serve to prevent loss of low-frequency response of the measuring system due to the high impedance of the gages and cables compared to the low (approximately $20 \times 10^3 \Omega$) input impedance of the tape recorder system. The input capacitance of these amplifiers is variable in steps from 0.01 μf to 1.0 μf, thus allowing some adjustment of the total capacitance seen by the LC-33 and ST-4 gages. Since these gages produce charge proportional to the applied pressure, varying the total capacitance that a gage may see effectively varies the voltage per unit pressure sensitivity factor at the amplifier inputs for that channel. Consequently, the voltage per unit pressure sensitivity of the gages, cables, and amplifier channels taken together could be adjusted channel by channel to give approximately the same total voltage out of each amplifier channel even though one channel might be sensing a 50 psi peak pressure event while another was sensing a 0.5 psi peak pressure event. This characteristic of our impedance matching amplifier allowed us to use a tape recorder without overextending the voltage range (1) within which the recorder was linear, (2) within which the recorder had a high signal to noise ratio, and (3) within which the recorder could be adjusted to maximize the linear displacement of the galvanometers in our recording oscillograph for the peak voltage it was expected that channel would sense.

The output of each impedance matching amplifier channel was connected to the input of one of the fourteen channels of our Ampex FR-1800-L tape recorder with ES-100 FM Signal Electronics. The signal electronics (Figure 4) consists of fourteen FM record and replay amplifiers with a high-frequency response of 2×10^4 Hz at a record speed of 60 ips. The low-frequency response of the signal electronics is DC. All data were recorded at 60 ips and replayed at 1-7/8 ips. This allowed us to record the data with a relatively high frequency response and yet replay it into a recording oscillograph whose galvanometers had much lower maximum frequency response without distorting the data. The tape recorder FM electronics, however, established the high-frequency limit of our measuring system at 2×10^4 Hz.

Data taken at 60 ips replayed at 1-7/8 ips expanded our time scale by a factor of 32. This time scale was further affected by our recording oscillograph. The output of the tape recorder channels was fed through a switch

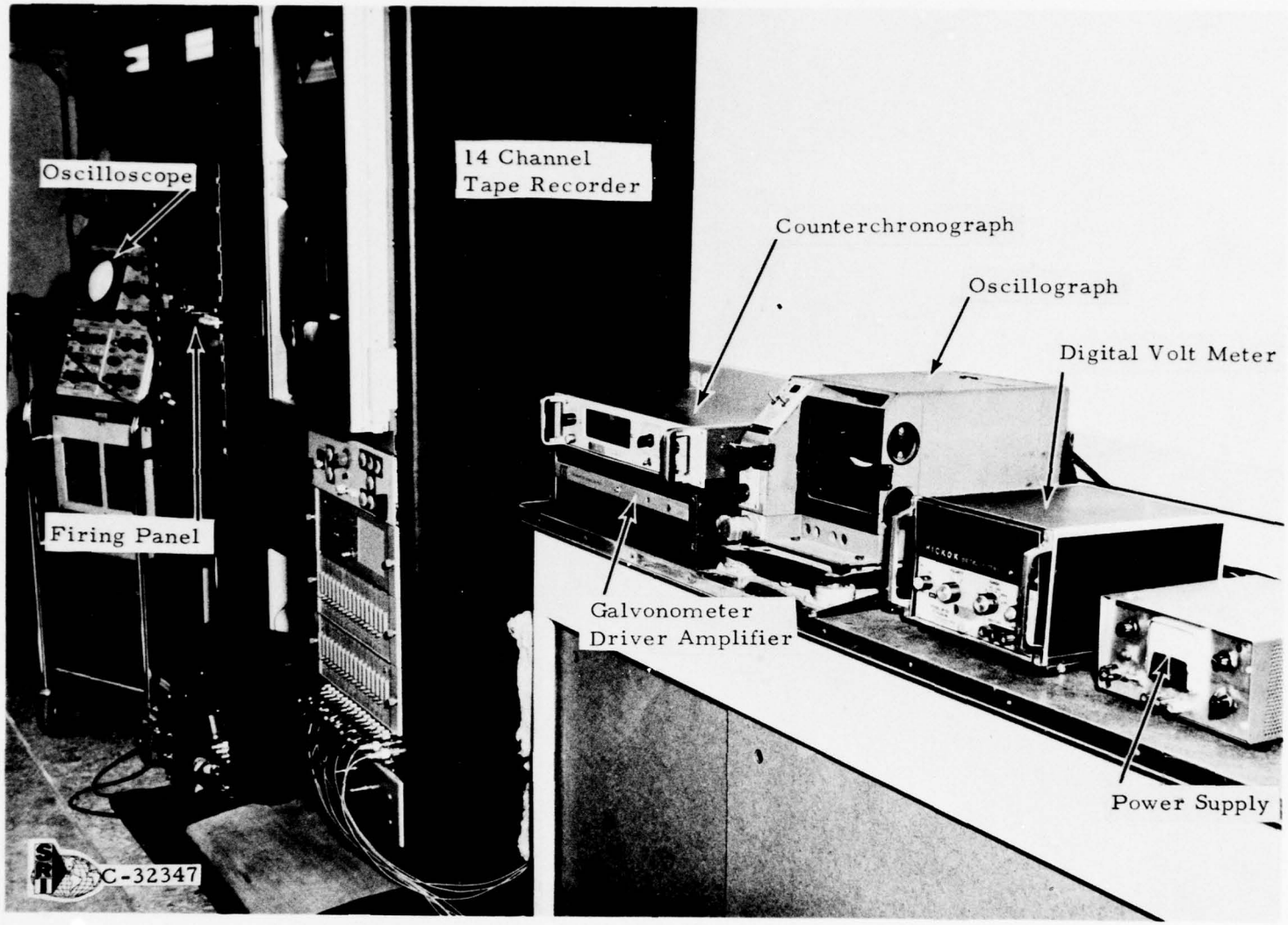

FIGURE 4. RECORDING EQUIPMENT

box, seven channels at a time, into a seven-channel recording oscillograph. The frequency response of the recording oscillograph was from DC to 5×10^3 Hz. A maximum linear deflection of 1.0 in. was possible for each channel of this recording device. The paper speed was either 16 or 32 ips with timing marks at every 10^{-2} second. We relied on these timing marks to determine our pulse arrival times and pulse lengths, eliminating variation in paper speed as a source of error, as described in more detail in the calibration discussion in Section III.

Data obtained from the output of the impedance matching amplifier channels to which ST-4 transducers were connected were recorded directly by an oscilloscope.

As an origin to our time scale, it was necessary to devise a means of superimposing a mark on our data which would occur at the precise moment of a charge detonation. This was accomplished with the use of two operational amplifiers used as summing circuits of amplification factor one. A pulse at $t = 0$ or the instant of charge detonation was obtained by the use of a break wire circuit with the break wire in direct contact with the explosive. At the moment discontinuity was obtained in the break wire the voltage drop across a resistor was recorded on two channels of the tape recorder through the summing circuits. The "start" pulse or $t = 0$ pulse thus recorded could be related to all other record channels with microsecond resolution. Rise time of this "start" pulse was on the order of microseconds. A block diagram of the experimental apparatus may be seen in Figure 5.

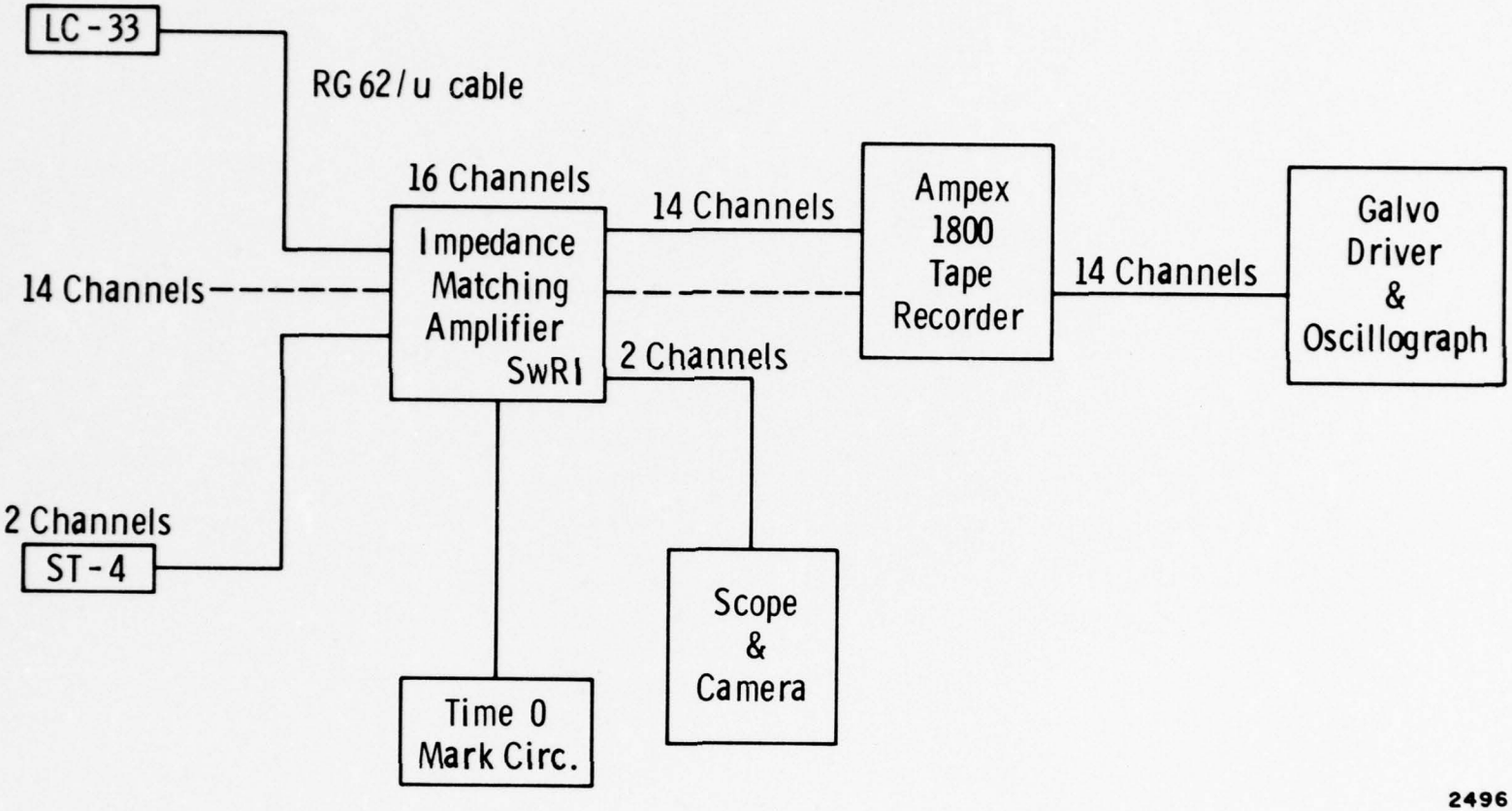

FIGURE 5. BLOCK DIAGRAM OF EXPERIMENTAL APPARATUS

III. EXPERIMENTAL PROGRAM

A. Experimental Approach

A total of 105 scaled experiments were conducted with the objective of measuring air blast parameters from barricaded and unbarricaded high explosive charges.

The experimental program was designed by applying the Hopkinson scaling laws described in Section II of this report to the following full-scale conditions:

- Explosive limits--8000 and 64,000 lb of TNT
- Barricade shapes--single-revetted and mound
- Barricade dimensions--10 ft and 20 ft high; slope 2.5:1
- Location of barricade relative to explosive charge--scaled distance ($Z = R/W^{1/3}$) = 1 and 40.

The scaled models generated from the above conditions were as follows:

- Explosive--Pentolite spheres
- Explosive weights--1 and 64 lb
- Barricade shapes--single-revetted and mound
- Barricade dimensions--6, 12, and 24 in. high; slope 2.5:1
- Location of barricades relative to explosive charge--scaled distance ($Z = R/W^{1/3}$) = 1 and 40
- Height of the explosive charge above the ground--4 in. to the center of the 1-lb charge and 16 in. to the center of the 64-lb charge.

The relationship of scaling equivalents between explosive weights and barricade dimensions is shown in Table I.

TABLE I. RELATION OF SCALED EQUIVALENCY

Model Scale		Full-Scale	
Explosive Weight (lb)	Barricade Height (in.)	Explosive Weight (lb)	Barricade Height (ft)
1	6	64,000	20
64	24	64,000	20
1	12	8,000	20
1	6	8,000	10
64	12	64,000	10

The following three major configurations were used for measuring the air blast parameters from barricaded and unbarricaded high explosive charges:

- Free Field--measurement of blast parameters without the presence of any barricade
- Near Field--measurements of air blast parameters made with a barricade located at a scaled distance of $Z \approx 1$ from the explosive source
- Far Field--measurement of blast parameters with the barricade located at a scaled distance of $Z = 40$ from the explosive source.

Mound and single-revetted barricades were used in this investigation. The definitions of these types of barricades are given below[6]:

> Mound. An elevation of earth having a crest at least 3 ft wide, with the earth at the natural slope on each side and with such elevation that any straight line drawn from the top of the side wall of a magazine or operating building or the top of a stack containing explosives to any part of a magazine, operating building, or stack to be protected will pass through the mound. The toe of the mound shall be located as near the magazine, operating building, or stack as practicable.
>
> Single-Revetted Barricade. A mound which has been modified by a retaining wall, preferably of concrete, of such slope and thickness as to hold firmly in place the 3-ft width of earth required for the top, with the earth at the natural angle on one side. All other requirements of a mound shall be applicable to the single-revetted barricade.

The barricade shapes and their location relative to the source of energy are illustrated in Figure 6. In the case of the far field, the single-revetted barricade was placed with the toe of the barricade facing the explosive source. This simulated the conditions of external blast sources loading

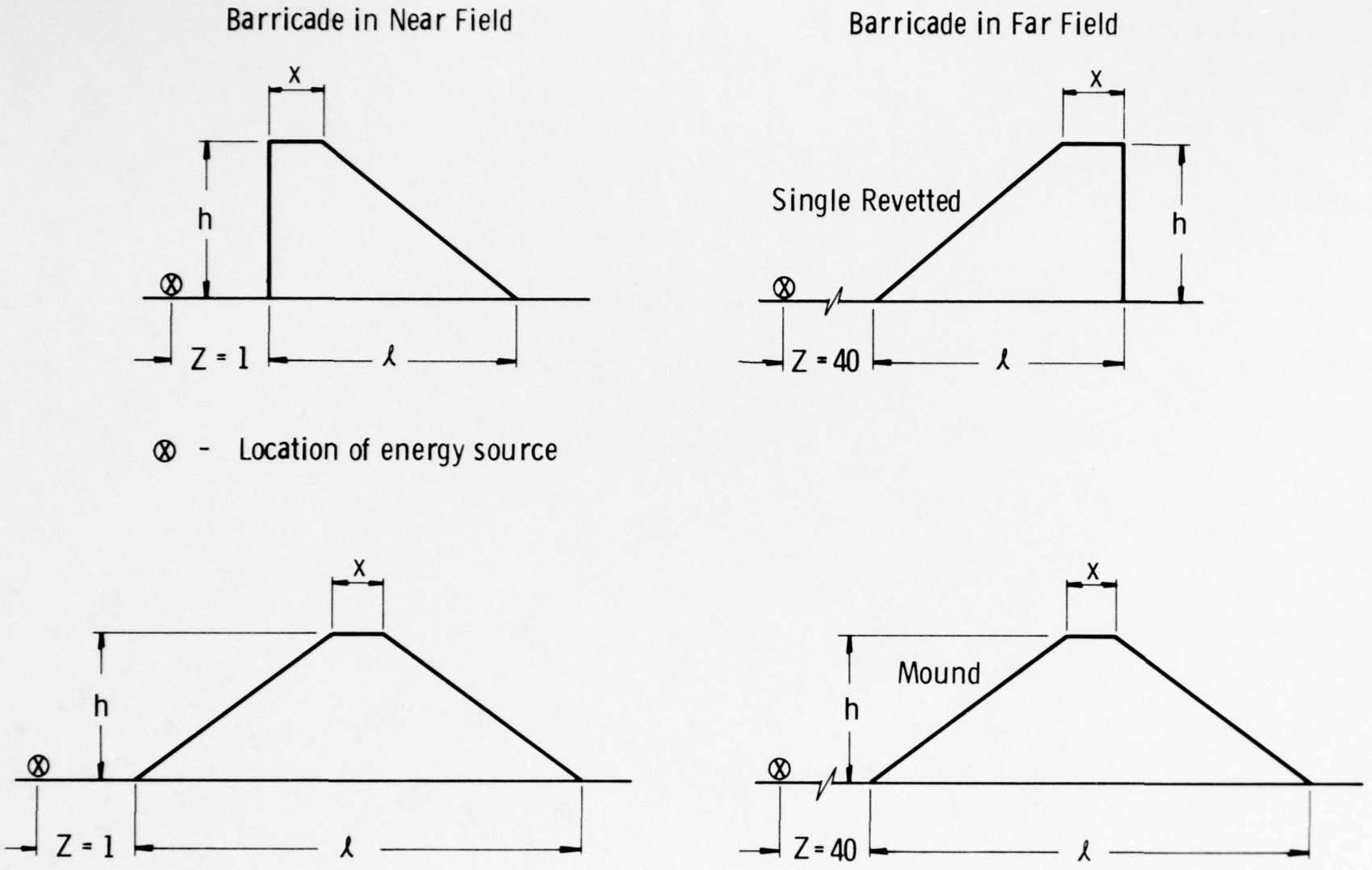

FIGURE 6. BARRICADE CONFIGURATIONS STUDIED

2476

a structure which the barricade was protecting. The location of the gages relative to the explosive charge and their scaled heights from the ground are given in Table II. Note from Table II that, for the near gage locations, the heights of the detectors increased with distance from the barricade. In every case, the scaled heights ($H = \frac{h}{W^{1/3}}, \frac{ft}{lb^{1/3}}$) were preserved for experiments with different charge sizes. The increase in height with scales distance was designed to minimize any ground interference effects. Typical pressure-time history traces obtained during the conduct of our experiments are shown in Figure 7. The upper trace shows a pressure-time history for an unbarricaded condition, illustrating the well-known sharp rise time and exponential decay of the shock wave. The middle trace illustrates the pressure-time history obtained from a gage located behind a single-revetted barricade in the far field case at a scaled distance of Z = 43, and at one barricade height from the ground. The initial rise represents the arrival of the incident wave, and the hump following the initial rise represents the arrival of the reflected wave generated as the shock wave passed over the barricade.* The lower trace represents the typical pressure-time history of a gage located at the same scaled distance as the above trace, but at one-sixth barricade height from the ground. In this particular case, note that the pressure associated with the hump is greater than the pressure associated with the incident wave. This effect was observed by other investigators studying the shapes of air blast waves passing over small-scale obstructions of various shapes.[7-14] The peak pressures reported in Section IV of this report were obtained by measuring the maximum pressure output recorded by the individual gages regardless of whether this maximum was associated with the incident or reflected wave.

The pressure calibration technique used in this program was a quasi-dynamic application of pressure to the sensitive area of the gage. The specific cable, impedance matching amplifier channel, tape recorder channel, and galvanometer channel with which a gage would be used to take data were also used to obtain the calibration record for the gage. The sensitive areas of the LC-33 pencil blast gages were inserted in a specially made chamber that could be pressurized up to 50 psi. This chamber was "O" ring leakproof and its physical appearance can be seen in Figure 8. Preceding this chamber was a solenoid valve which could be actuated to allow influx into the chamber of compressed air from a reservoir. The volume of the chamber surrounding the gage element was insignificant in comparison to that of the reservoir. Pressures were measured at the reservoir with a calibrated bourdon gage or a mercury or water manometer. The bourdon gage was used to measure pressures above 20 psi and was dead-weight tested for calibration. The mer-

*The probable reason for lack of a sharp rise in the reflected wave is that this wave has been modified by interaction with an expansion fan which follows the incident wave in diffracting over the corner of the barricade.

TABLE II. LOCATION OF GAGES

Location From HE $Z = R/W^{1/3}$ (ft/lb$^{1/3}$)	Free Field	Height of Gage $h/W^{1/3}$ (ft/lb$^{1/3}$)
5		0.75
7		1.00
12		1.50
25		2.00
45		3.00
58		3.00
80		3.00
	Near Field	
3		0.5*
4		0.17*
5		0.75
7		1.00
12		1.50
25		2.00
45		3.00
45		0.75†
58		3.00
80		3.00
	Far Field	
12		1.50
25		2.00
43		0.17
43		0.50
43		1.00
43		3.00
45		3.00*
58		2.00‡
58		3.00
80		3.00

*Stations located only in the 64-lb case.
†Used in 64-lb mound case only.
‡1-lb case only.

Free Field Condition

Far Field, Single Revetted Barricade
Sensor At One Barricade Height From Ground, Z = 43

Far Field, Single Revetted Barricade
Sensor At One-Sixth Barricade Height From Ground, Z = 43

2477

FIGURE 7. TYPICAL PRESSURE-TIME HISTORY

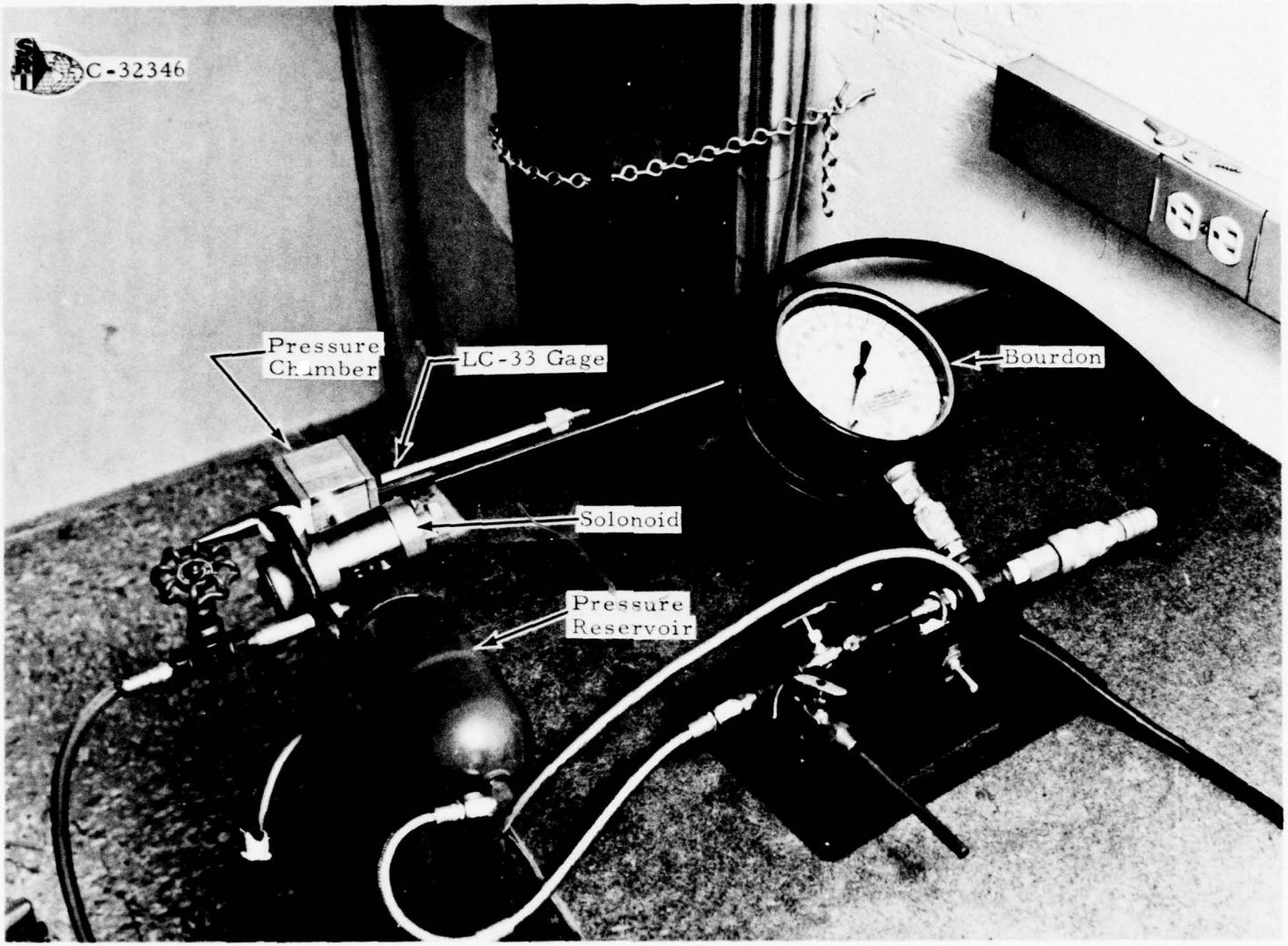

FIGURE 8. PRESSURE TRANSDUCER CALIBRATION APPARATUS

mercury and water manometers were used to measure pressures in the 2.0 to 1.0 psi and 1.0 to 0.2 psi ranges, respectively. The air in the reservoir was obtained from a compressed air cylinder and was regulated by a 0- to 50-psi regulator. Operation of the solenoid valve could bring the pressure in the chamber surrounding the gage element from 0- to 50-psi in 10 ms or less. This "rise" time to peak pressure was a function of air inertia and the time-dependent opening characteristics of the solenoid valve, but was considerably less than one-tenth the RC constant of the system. The limiting RC constant of the system was determined by the RC coupling of the impedance matching amplifier to the tape recorder input (RC = 300 ms). The pressure applied (i.e., the pressure in the reservoir at the time of calibration) divided by the peak of the deflection of the trace obtained in the oscillograph in inches gives the calibration for that gage, amplifier channel, tape recorder channel, and oscillograph channel. We will henceforth refer to this combination as "a" channel. For any individual change in a component of a channel, the channel was recalibrated.

The Susquehanna ST-4 transducers and channels in which they were used were calibrated by the previous method with the exception that the output of the impedance matching amplifier was displayed directly on an oscilloscope. The RC coupling between these components gave a constant of RC = 15s, and between the transducers and line and the impedance matching amplifier input gave a constant of RC = 10^4s, resulting in a very low frequency response characteristic for this system. Furthermore, the rise-time capabilities for this system were improved by the use of the scope. The high-frequency response of the amplifier and scope was on the order of megahertz; therefore, the rise time for this system was limited by the gage to a few μs or less. Scope traces of the pressure calibration signal from the quasi-dynamic calibration device were used to calibrate two channels using ST-4's in terms of psi/volt.

Time scale calibration for channels using the tape recorder and oscillograph was obtained by aligning the tape recorder according to its specifications and reducing the real time scale of events by a factor of 32 to allow for the tape slowdown from 64 ips to 1-7/8 ips on replay. The oscillograph contains a 10^{-2}-s interval marker which was used to measure the expanded time scale from the tape recorder. In general, the oscillograph was run at 32 ips giving an approximate real time scale of $(1/32) \cdot (1/32) \simeq 1.0$ ms/in. of chart. For pressure calibrations, the oscilloscope was run at 1/4 ips giving an approximate real time scale of 130 ms/in. of chart. Accurate measurements of time of arrival and pulse lengths for each individual record were accomplished, however, by counting the 10^{-2}-s time interval marks on the oscillograph record and dividing by 32 to allow for the time scale expansion by the tape recorder. Error of about 3 percent in the action of the 10^{-2}-s time interval marker which occurred in the field when our power source was a generator (as it was in the case of the 64-lb experiments) rather than the city-supplied line voltage (as it was in the case of the 1-lb experiments) was taken into account and all events under these conditions were corrected in relation to their time scales.

B. Experimental Setup

The experimental program was conducted at the SwRI explosive facilities for the 1-lb experiments, and, with the permission of the Army, at Camp Bullis, Texas, 30 miles from SwRI, for the 64-lb experiments. All tests were remotely fired from a fully instrumented control trailer located at the experimental sites. Both explosive facilities met all the safety requirements imposed by the Federal and State governments

1. 1-Lb Experiments

The blast field established for the 1-lb experiments is shown in Figure 9. In addition to the instrumentation described earlier to measure the blast parameters, an anemometer, barometer, relative humidity indicator, and thermometer were present at the time of experimental operations to measure ambient conditions for each event. Generally, the wind velocity was immeasurably low (approximately 3 mph), the humidity was of the order of 50 percent, and the temperature was 90°F or less during the course of the experiments.

The site was laid out such that the trailer was approximately 130 ft from the explosive source and the farthest gage was located at a scaled distance of $Z = 80$. Ground zero was established by mounting a steel plate of dimensions $36 \times 36 \times 2$ in. in the ground with its upper surface level with the ground. On the center of this plate the explosive charge was mounted on a cardboard holder such that the charge center (the charge was a sphere) was 4 in. above the plate's surface, as illustrated in Figure 10. For the 1-lb experiments, there were three cases studied: (1) free field, (2) near field, and (3) far field.

For the free field case LC-33 gages were located at scaled distances ranging from $Z = 5$ to $Z = 80$, and scaled heights ranging from $H = 0.17$ to $H = 3$, as described in Table II and illustrated in Figure 9. There were a minimum of seven stations and each station consisted of two channels. Each channel consisted of a gage mounted at the end of a 3-ft pipe, as illustrated in Figure 11. The sensitive area of the gage protruded 1 or 2 in. in front of a streamlined adapter mounted in the pipe. Cable connections were contained within the pipe. This meant that no significant shock effects were felt by the cable until the blast wave had passed over the gage and 3 ft farther where the cable emerged from the pipe. Gages and pipes were mounted on pipe T's such that two gage elements would be nearly 10 in. apart at the same scaled distance and scaled heights. For the near stations, the gages pointed directly at the charge center, while for the far stations, the gages were mounted perpendicular to the ground at a scaled height well within the Mach stem of the shock front. The exact locations of all pressure transducers for all channels are given in Table II.

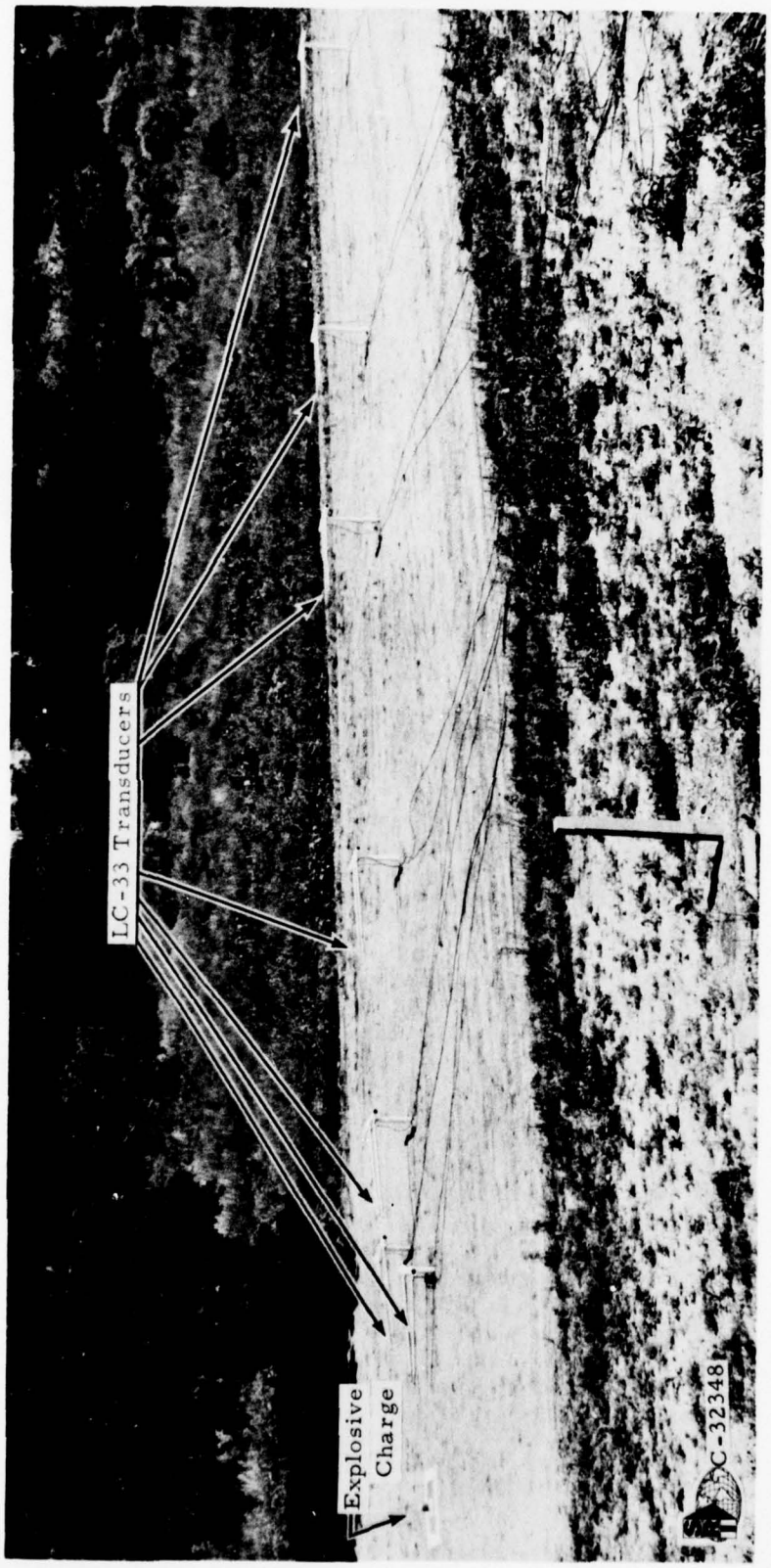

FIGURE 9. FREE FIELD SETUP FOR 1-LB EXPERIMENTS

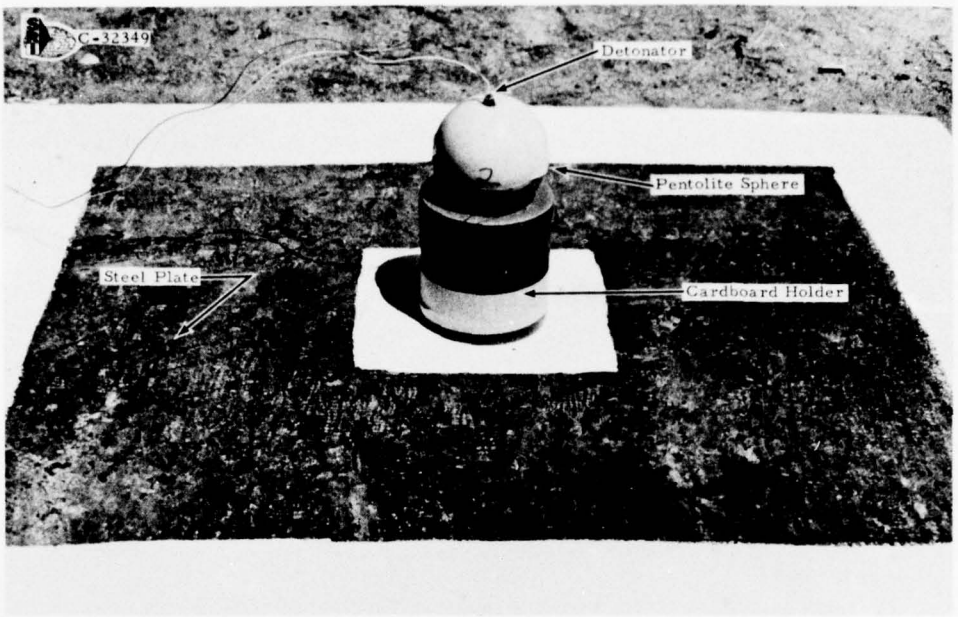

FIGURE 10. CLOSEUP OF 1-LB EXPLOSIVE CHARGE

FIGURE 11. CLOSEUP OF LC-33 GAGE MOUNTS

For the near field case, four barricade configurations were studied. They were the single-revetted and mound, 6-in. barricade, and single-revetted and mound, 12-in. barricade.* The locations of the barricade relative to the energy source are illustrated in Figures 12 through 15. Single-revetted and mound barricades were made of concrete and reinforcing steel and were 16 ft in total length, as shown in Figures 12 and 13. The length of these barricades was selected to insure that no diffracted waves from the corners of the barricade impinged on the transducer during the passage of the incident wave over the blast gages, and also, to simulate, at least approximately, the conditions for which the analytical model was being developed.

The exact location of the gages relative to the energy source for the near field case is given in Table II. Of special interest for this case, ST-4 transducer channels were mounted on top of the barricade, halfway down the slope of the single-revetted and mound barricade, and in a steel plate level with the ground immediately behind the barricade. The transducers were mounted flush with the barricade surface and all cables were run through the beneath the barricade and underground for some distance.

For the far field case, the same four barricade configurations were also studied. Exact gage locations are given in Table I. Of special interest were gages mounted at the scaled distance of $Z = 43$ with the transducer elements varying in height from the ground for scaled heights of $H = 0.17$ to $H = 3.0$ as illustrated in Figure 16 and 17.

Eighty experiments were conducted for all field cases and barricade configurations, using the 1-lb charges at the SwRI explosive facilities.

2. 64-lb Experiments

To check validity of scaling of the results obtained from the 1-lb experiments as well as to obtain additional data not corresponding to scaled 1-lb experiments, 64-lb experiments were conducted at the Camp Bullis test site.

The setup of the blast field with a barricade is illustrated in Figure 18. Power to the instrumentation trailer was obtained by the use of a 15-kw generator driven by an internal combustion engine. A check on line voltage fluctuations indicated that all equipment could function normally within the limits of these fluctuations and that the voltage level was adequate (115 to 120 volts AC).

*Throughout this report, a single dimension associated with a barricade indicates its height.

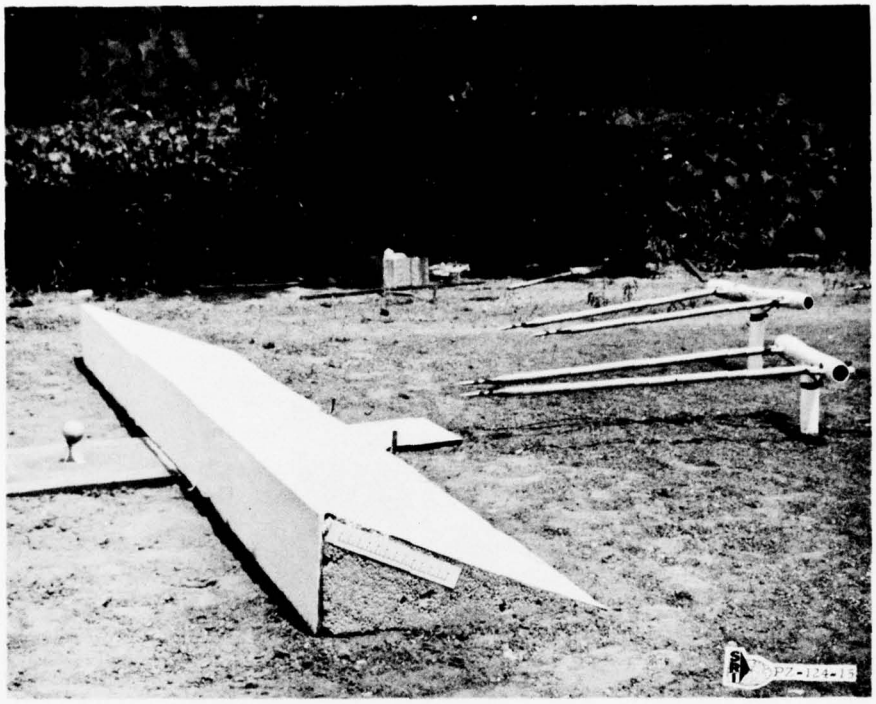

FIGURE 12. SINGLE-REVETTED, 12-IN. BARRICADE SETUP NEAR FIELD, 1-LB EXPERIMENTS

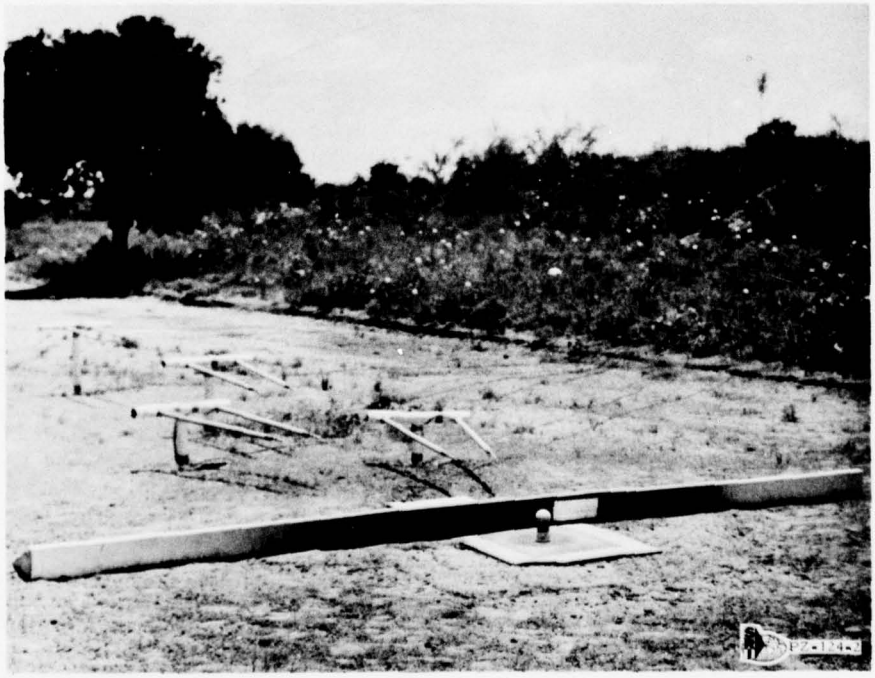

FIGURE 13. SINGLE-REVETTED, 6-IN. BARRICADE SETUP NEAR FIELD, 1-LB EXPERIMENTS

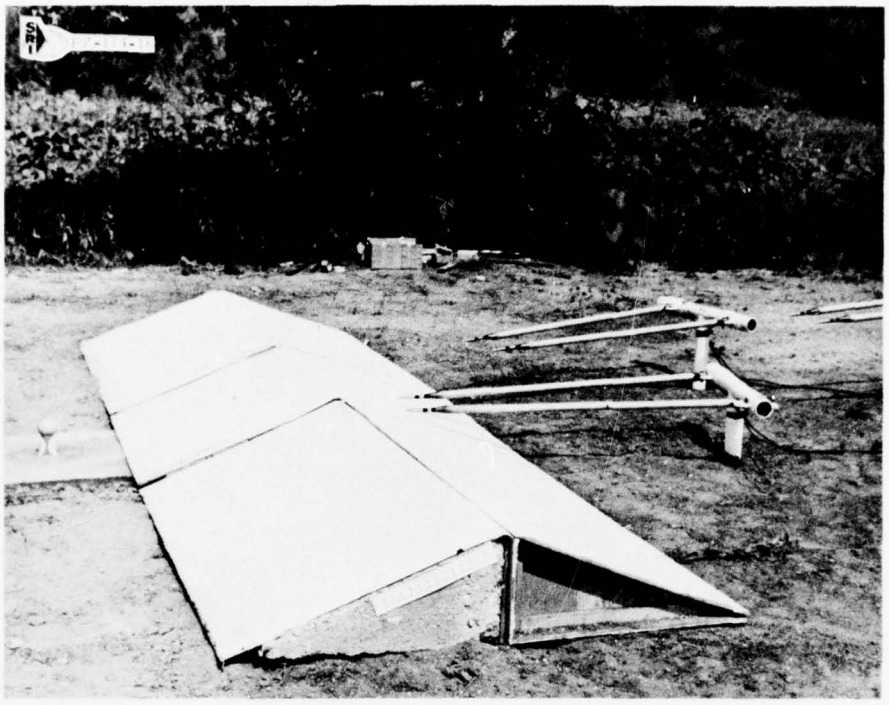

FIGURE 14. MOUND, 12-IN. BARRICADE SETUP
NEAR FIELD, 1-LB EXPERIMENTS

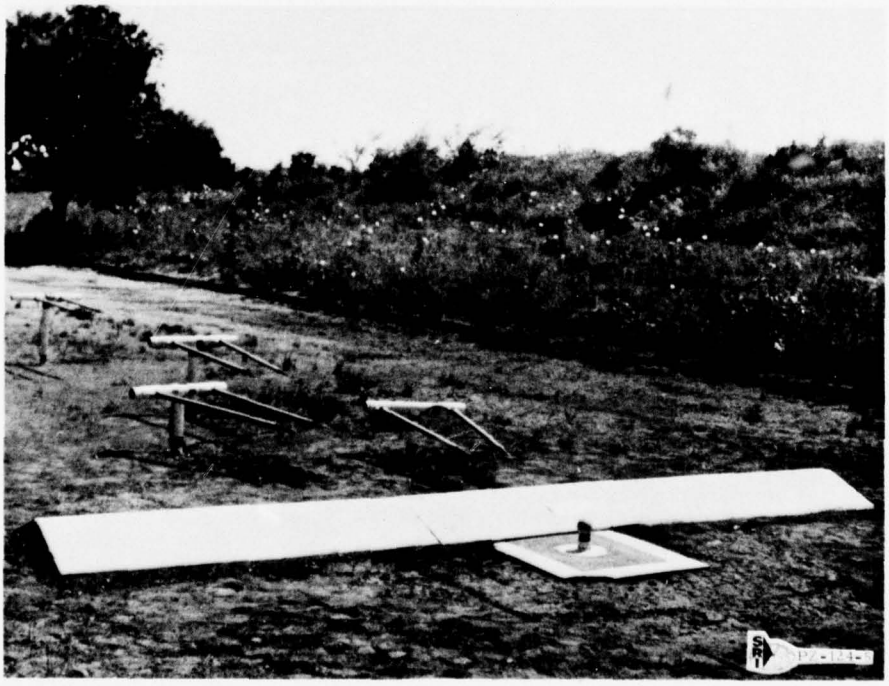

FIGURE 15. MOUND, 6-IN. BARRICADE SETUP
NEAR FIELD, 1-LB EXPERIMENTS

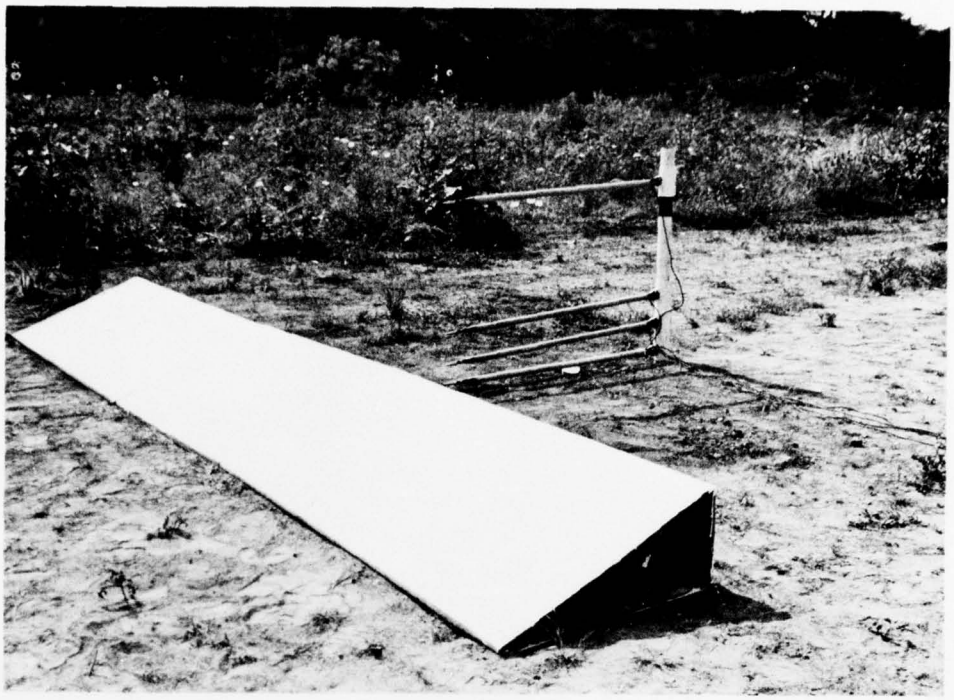

FIGURE 16. SINGLE-REVETTED, 12-IN. BARRICADE
FAR FIELD, 1-LB EXPERIMENTS

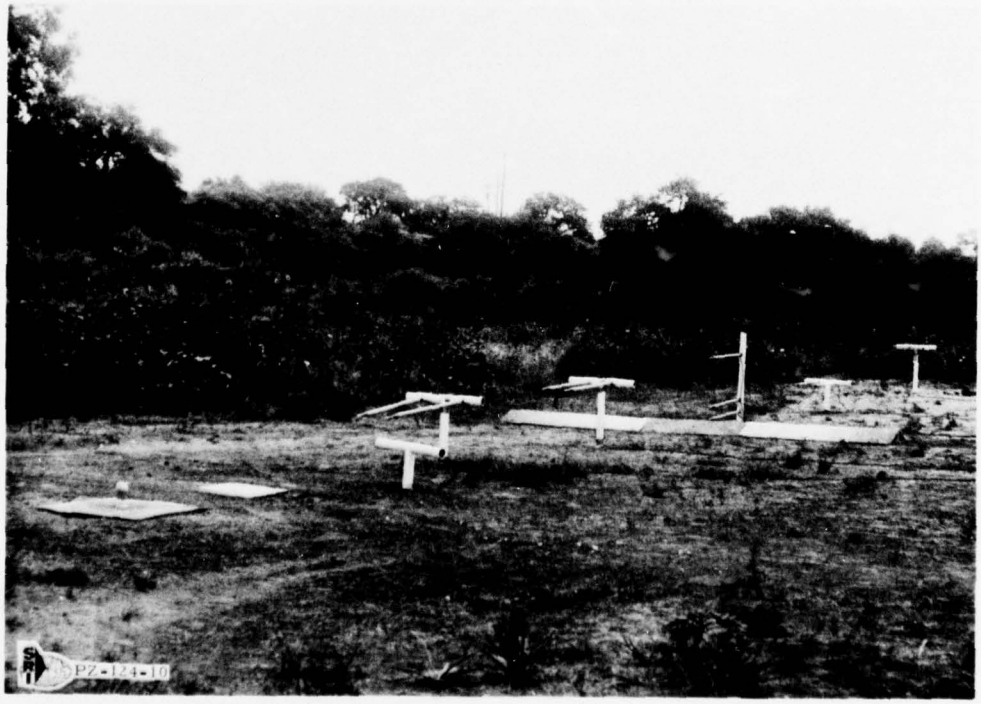

FIGURE 17. MOUND, 6-IN. BARRICADE
FAR FIELD, 1-LB EXPERIMENTS

The Camp Bullis site consisted of a level-graded and dragged field of about 75 by 250 yards. The instrumentation trailer was located behind a clump of trees at 500 ft from ground zero. Ground zero consisted of a steel plate of 8 × 8 × 1/2-ft mounted on the ground and supported by reinforced concrete to a depth of 3 ft, with the surface of the steel plate at ground level. The 64-lb charges were mounted on a light plywood piece with a cutout which was supported by a cardboard box such that the charge centers were 16 in. from the steel plate.

The same three field cases were studied for the 64-lb experiments as were studied for the 1-lb tests. Gage mountings were generally the same as for the 1-lb event except that their locations from ground zero and their heights from the ground were scaled by a factor of 4.

The test setup for the free field case was a scaled duplicate of the 1-lb experiments. The setup for the near field gages was also scaled to the 1-lb case except that two additional stations were added at scaled distances of Z = 3 and Z = 4. Barricades used for the near field case were single-revetted and mound barricades, 64 ft long and 2 ft high with a section consisting of a steel shell filled with reinforced concrete 18 ft in length placed in the center, and a steel-faced, earth-filled section on the ends, as shown in Figures 18 through 21. The steel and concrete sections of the barricades were "pegged" into the ground with 1-in.-diameter steel drill rod to prevent movement of the barricade. The gage locations and their heights for the near field case are given in Table II.

In the far field case, four barricade configurations were studied: (1) single-revetted and mound, 24-in. barricade; (2) single-revetted and mound, 12-in. barricade. The 24-in. barricade configurations are direct scale models of the 6-in. barricades utilized in the 1-lb experiments. The 12-in. barricade configurations represent new data and their scaled equivalency is given in Table I. The physical locations of the gages were directly scaled from the 1-lb experiments except for the addition of one station at Z = 45. The exact gage locations are given in Table II.

Twenty-five 64-lb experiments were studied at the Camp Bullis location. Regarding special problems involved for these tests, long cables necessitated by locating the trailer 500 ft from ground zero did not significantly affect our data signal-to-noise ratio through antenna "pickup," although there was a slight increase in the discernible RF noise level. The ambient conditions at Camp Bullis were approximately the same as for the study of 1-lb experiments with the possible exception of temperature which ranged in the high 90's and low 100's. Certain other ambient effects worked detrimentally on our experiments (namely, animal life feeding on our cables) and necessitated that all cables be buried or otherwise protected in the field. All cables above ground were protected by steel conduit.

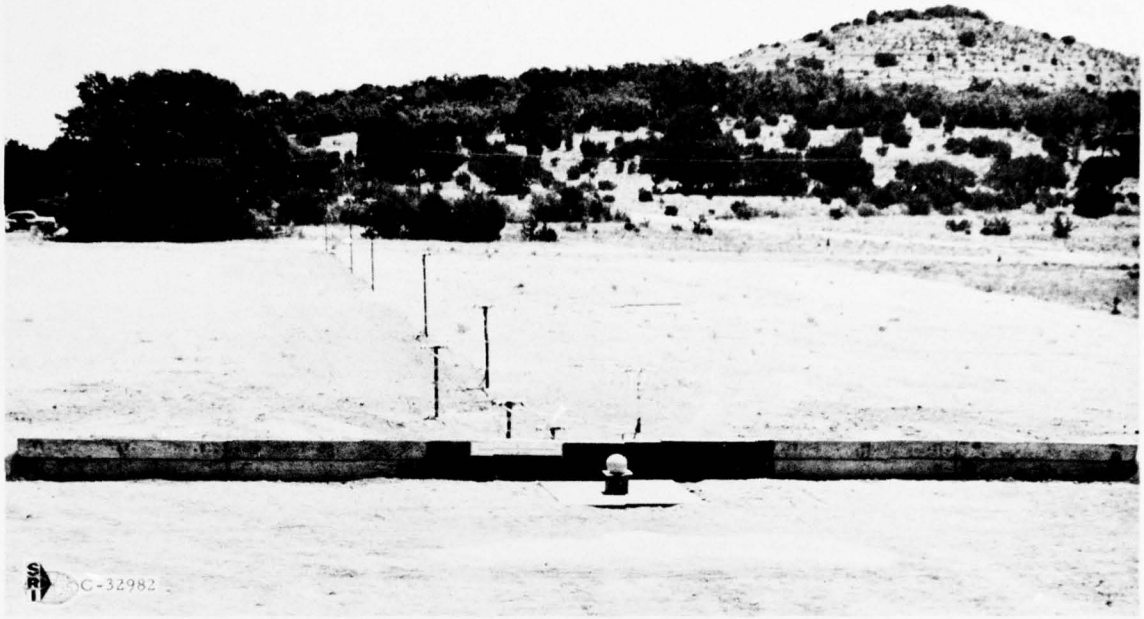

FIGURE 18. TYPICAL SETUP OF THE BLAST FIELD WITH A BARRICADE FOR THE 64-LB EXPERIMENTS

FIGURE 19. SINGLE-REVETTED, 24-IN. BARRICADE NEAR FIELD, 64-LB EXPERIMENTS

FIGURE 20. MOUND, 24-IN. BARRICADE
NEAR FIELD, 64-LB EXPERIMENTS

FIGURE 21. MOUND, 24-IN. BARRICADE
FAR FIELD, 64-LB EXPERIMENTS

IV. RESULTS AND ANALYSIS

The data obtained in the experimental program described in Section III include measurements of peak pressure, impulse, time of shock arrival, and positive overpressure durations. As stated before, measurement were made in the free field, near field, and far field cases. All the data obtained have been tabulated and included in Appendix A to this report. The data given in that appendix include tables describing the barricade configuration, the scaled distance, the total number of peak pressure measurements made, the peak pressure, the standard deviation for peak pressure, the number of impulse measurements made, the scaled impulse, the standard deviation on the scaled impulse, the scaled times of arrival, the standard deviations of the measurements on times of arrival, the scaled overpressure durations, and the standard deviations of the overpressure durations. For the 64-lb data, there were not sufficient experiments conducted to be able to calculate meaningful standard deviations; therefore, an absolute average was reported for each data point.

The results that follow are evaluations of the blast parameters in terms of the unbarricaded and barricaded conditions, and in each condition, the results are compared to either a standard generated by other investigators or the measurements are compared to the free field cases measured in our experiments.

A. Free Field Case

The objectives of the free field experiments were to verify the scaling laws and to generate data that could be compared with results of other investigators for the purpose of establishing confidence in our measuring system. A total of fifteen 1-lb and three 64-lb experiments were conducted in the free field case. The first five tests utilizing the 1-lb charges were fired to check out the overall system; therefore, the data obtained from these tests are not reported. Results of the subsequent experiments dealing with measurements of the blast parameters in the free field case are shown in Figures 22 through 25 as a function of scaled distance. These measurements are compared with the standard Ballistics Research Laboratories (BRL) free field data generated for large TNT explosions[15] for the parameters peak pressure and impulse. The measurements of time of shock arrival are compared with the BRL compiled free-air blast data[16] by applying a 1.8 reflection factor to account for our explosive proximity to the ground. It is observed that, for the case of the peak pressures, our experimental data fall somewhat above the BRL standard for scaled distances ranging up to $Z = 10$, but they are in general agreement with it and do confirm the scaling laws for this configuration. Note that for the case of the scaled impulse and scaled shock arrival times shown in Figures 23 and 24, our data agree well with the BRL data. A possible explanation for the small discrepancies between our data and the BRL

standard shown in the peak pressure plots (Figure 22) can be attributed to the difference between TNT and Pentolite and the facts that in our experiments the explosives were not in direct contact with the ground as they were in the BRL work[15], and that we employed a rigid reflector plate to prevent cratering. This latter fact is significant because not as much energy is absorbed by the ground in our experiments as compared to the TNT experiments. Figure 25 shows the correlation of the peak pressure with the scaled impulse, which may be of value for vulnerability analysis. This figure gives the relationship between the peak pressure and the impulse at the scaled distances where the measurements were taken.

B. Near Field Case

Following confirmation of the scaling laws and establishing of confidence in our measuring system, two barricade configurations (single-revetted and mound) were located in the near field at a scaled distance of Z = 1. The objectives of the near field experiments were primarily to evaluate the effectiveness of the barricades immediately behind the structure and at the inhabited building scaled distance of Z = 40. In order to properly evaluate the data, reference is made to the table relating scaled equivalency (Table I) and the location of the gages relative to the explosive charge and height from the ground (Table II) given in Section III of this report.

A total of thirty-seven 1-lb and nine 64-lb experiments were conducted in the near field case, and the results of the effectiveness of the barricade on the blast parameters are shown in Figures 26 through 37. Figures 26 through 31 compare the effectiveness of the single-revetted and the mound barricades on the peak pressures and impulses. All the measurements were compared with the free field case as measured in our experiments. For experiments involving the single-revetted configuration, peak pressures and impulses were reduced significantly up to scaled distances of Z = 10. Beyond the scaled distance of Z = 10, the peak pressures tended to approach those of the free field case very rapidly and at the inhabited building distance of Z = 40 the peak pressures were almost the same as that of the unbarricaded conditions. The impulses also tended to approach those of free field case but not as rapidly as the peak pressures; at the inhabited building distance of Z = 40, one still observes some reduction in the scaled impulse. In the case of the mound barricade, the following observations are made:

- An increase in pressure and impulse over the free field case is observed at a scaled height of H = 0.17 at a scaled distance location of Z = 4. However, the pressure and impulse observed at the scaled height of H = 0.5 at Z = 3 are both less than free field values, as shown in Figures 27 and 30.

- There is a variation of the peak pressure and impulse with scaled height for the two gages located at Z = 45 at scaled heights of H = 0.75 and H = 1.50, respectively.

- The effects of decrease in peak pressures and impulses by the mound barricades are not as great as for the single-revetted barricades.

The observations made above suggest that there is a pressure gradient as a function of the location of the gages relative to the ground.

Figures 28 and 31 show a comparison of the peak pressures and scaled impulse for the 12-in, single-revetted and mound barricades. The same observations made for the previous two barricade conditions can be made for these conditions. Note that these figures indicate that, for the mound barricade condition, both pressures and impulses tend to approach those of the free field case at the scaled distance of Z = 10; on the other hand, for the single-revetted case Figures 28 and 31 indicate that there is still some reduction in peak pressures and scaled impulse at scaled distances greater than Z = 10.

Analyzing the shock wave time-of-arrival data, it is observed that, for the single-revetted barricade configuration, the times of arrival at the specific gage locations are greater than those of the free field case for scaled distances up to Z = 15, as seen in Figure 32. At scaled distances greater than Z = 15 they approach rapidly those of the free field case. For the mound barricades configuration, times of arrival were the same as those observed in the free field case for all scaled distances, as seen in Figure 33.

The pulse shape (pressure-time history) observed for the single-revetted barricade condition was the typical triangular shape observed in the free field case, illustrated in Figure 7. This was true for all gage locations. For the mound barricades, the typical triangular shaped pulse was observed for all gage locations except those located at Z = 5. At this location, a double peak was present in every measurement, indicating the presence of the incident wave and a reflected wave. The peak pressure associated with the reflected wave was approximately the same as that of the incident wave.

Field blast measurements were taken with flush-mounted transducers (ST-4 gages) located at the tops of the barricades, halfway down the slope of the barricades, and on a ground plate mounted flush with the ground immediately behind the barricades, as shown in Figure 12. The results of these measurements are given in Table III. Comparing the peak pressure data of these transducers with those of the free field case, the following observations are made:

The gages located on top of the barricade measured peak pressures which were in good agreement with the free field case.

TABLE III. MEASUREMENT OF BLAST PARAMETERS WITH FLUSH MOUNTED TRANSDUCERS ON BARRICADE LOCATED IN THE NEAR FIELD

Barricade Type	Location	Z ($ft/lb^{1/3}$)	Number of Measurements	Average Peak Pressure, P (psi)	Average Scaled Impulse, $I/W^{1/3}$ ($psi\text{-}ms/lb^{1/3}$)	Average $T_A/W^{1/3}$ ($ms/lb^{1/3}$)
6-in, Single-Revetted	Top	1.00	4	821 ±185	18.2 ±*	0.07 ±0.01
	Slope	1.63	7	203 ± 64	12.9 ±6	0.25 ±0.04
	Ground	3.50	4	124 ± 8	10.0 ±3	0.86 ±0.06
6-in., Mound	Top	1.63	5	622 ±160	45.1 ±9	0.14 ±0.01
	Slop	2.34	2	367 ± 47	14.9 ±2	0.25 ±0.01
	Ground	5.00	1	57 ±*	3.5 ±*	1.28 ±0.10
12-in., Single-Revetted	Top	---	-	-- --	-- --	-- --
	Slope	2.25	3	45.6 ±13	-- --	0.34 ±0.10
	Ground	4.25	8	47.2 ±10	11.4 ±2	1.51 ±0.30
12-in., Mound	Top	---	-	-- --	-- --	-- --
	Slope	2.50	8	664.3 ±105	61.8 ±7	0.28 ±0.01
	Ground	---	-	-- --	-- --	-- --

*One measurement taken

- The peak pressures associated with the measurements made with the gages located on the slope of the barricade and on the ground plate were considerably lower than the free field case.

The data on peak pressures vs scaled impulse are given in Figures 35 through 37 and the data shock overpressure durations are given in the tables reported in Appendix A.

C. Far Field Case

The primary objective of the experiments in the far field case was to obtain measurements immediately behind the barricade, when the toe of the barricade was located at the inhabited building scaled distance of Z = 40, as illustrated in Figure 6. Again, in order to properly evaluate the data, the reader is referred to Tables I and II in Section III of this report.

Twenty-eight 1-lb and thirteen 64-lb experiments were conducted in the far field case, and the results of the effectiveness of the barricade on the blast parameters are shown in Figures 38 through 53. Figures 38 through 45 compare the effectiveness of the single-revetted and the mound barricades on the peak pressures and impulses. Again, as in the near field case, all far field measurements were compared with those of the free field case. Both single-revetted and mound barricade configurations caused peak pressures and impulses to be reduced significantly within two barricade heights behind the after toe of the barricade, and these peak pressures and scaled impulses vary as a function of the height of the gage above the ground. It must be noted that the evidence shown in these experiments, combined with the observations made in the near field case, indicate that the peak pressure and impulse vary with gage height at each of the scaled distances. But, due to the nature of our experimental setup, we cannot determine from these measurements the pressure and impulse gradient as a function of height. Careful analysis of the data indicates that the results obtained with the 1-lb and 64-lb explosive charges immediately behind the barricades do not appear to conform to the scaling laws. It is not known if this observation is true or whether it may be attributed to the fact that the angle at which the incident and reflected shock wave fronts impinge on the individual transducer elements was not perpendicular to the axis of the pencil gage. Since these gages are designed to measure plane waves impinging on the transducer perpendicular to the axis of the pencil gage, it is possible that the absolute numbers associated with the peak pressures and impulses measured immediately behind the barricade may be in error. Special attention should be paid to this point in any future experiments.

Comparing the results of the 6-in. and 24-in., single-revetted and mound barricades, it is observed that the peak pressures in the single-revetted configuration never exceeded the pressures measured in the free field case; however, for the mound configuration, an increase of pressure

was observed for the gage located immediately above the barricade (H = 1.0, Z = 43), as shown in Figure 39. The impulse data followed much the same trend as the peak pressure data. These data are shown in Figures 42 through 45. The measurements of times of shock arrival indicate that they were equal to those of the free field case, the same for any given Z, regardless of the barricade conditions.

The pulse shapes (pressure-time histories) observed in single-revetted and mound configurations were the typical triangular shapes observed in the free field case, see Figure 7, for all gage locations except those located immediately behind the barricade. For the gages located at a scaled distance of Z = 43 and scaled heights of H = 0.17 to 3.00, the pulse shapes observed were similar to those illustrated in Figure 7 where the initial rise of the incident wave is followed by a subsequent rise (hump) associated with the arrival of the reflected wave. The peak pressure associated with the reflected wave varied as a function of the location of the gage relative to the ground. In some cases, the pressure of the reflected wave was greater than that of the incident wave for the gages located nearest the ground. As reported earlier, peak pressure was obtained by measuring the maximum pressure output recorded by the individual gages regardless of whether this pressure was associated with the initial or reflected wave. A close analysis of all the pressure-time histories for gages located behind the barricade configurations studied (Z = 43 or greater) reveals the following observations:

- For all 1-lb experiments, the double-pulse shape illustrated in Figure 7 was present for Z = 43 to 58 for all scaled heights measured.

- For the 64-lb experiments, the previous observation held except for the mound configuration. In the mound configuration, the double pulse was present for all scaled heights and distances but Z = 43, H = 0.17, and H = 0.5. At these scaled heights, the triangular shape typical of the free field case was observed.

- The scaled time intervals between the arrival of the incident and reflected waves ($\frac{\Delta\tau}{W^{1/3}}$, as given in Table IV) indicate that scaling held for scaled heights of H = 1.00 to 3.00 (or above the barricade heights). Scaling does not appear to have held for scaled heights of H less than 1.00 immediately behind the barricade for the reasons outlined previously.

Table IV reports the scaled time interval between the arrival of the incident and reflected waves for the barricade condition analyzed as a function of scaled distance and height for the number of measurements made (N_τ).

As in the near field case, the pressure vs scaled impulse in the far field cases are given in Figures 50 through 53 and the shock overpressure duration is reported in the tables given in Appendix A.

TABLE IV. SCALED TIME INTERVAL OF INCIDENT AND REFLECTED WAVE FOR FAR FIELD CASE

Barricade Configuration	Explosive Weight (lb)	Z ($ft/lb^{1/3}$)	H ($ft/lb^{1/3}$)	N_τ	$\Delta\tau/W^{1/3}$ ($ms/lb^{1/3}$)
Single-Revetted	1	43	0.17	2	0.74
		43	0.50	2	0.25
		43	1.00	1	0.93
		43	3.00	2	0.67
		58	3.00	4	0.16
		80	3.00	8	*
Single-Revetted	64	43	0.17	2	0.26
		43	0.50	3	0.09
		43	1.00	2	0.94
		43	3.00	1	0.49
		58	3.00	5	0.12
		80	3.00	4	*
Mound	1	43	0.17	3	0.14
		43	0.50	2	0.45
		43	1.00	2	0.96
		43	3.00	3	0.93
		58	3.00	4	0.16
		80	3.00	6	*
Mound	64	43	0.17	4	--
		43	0.50	4	--
		43	1.00	2	0.93
		43	3.00	1	0.94
		58	3.00	4	0.08
		80	3.00	8	*

*Triangular pulse shape observed.

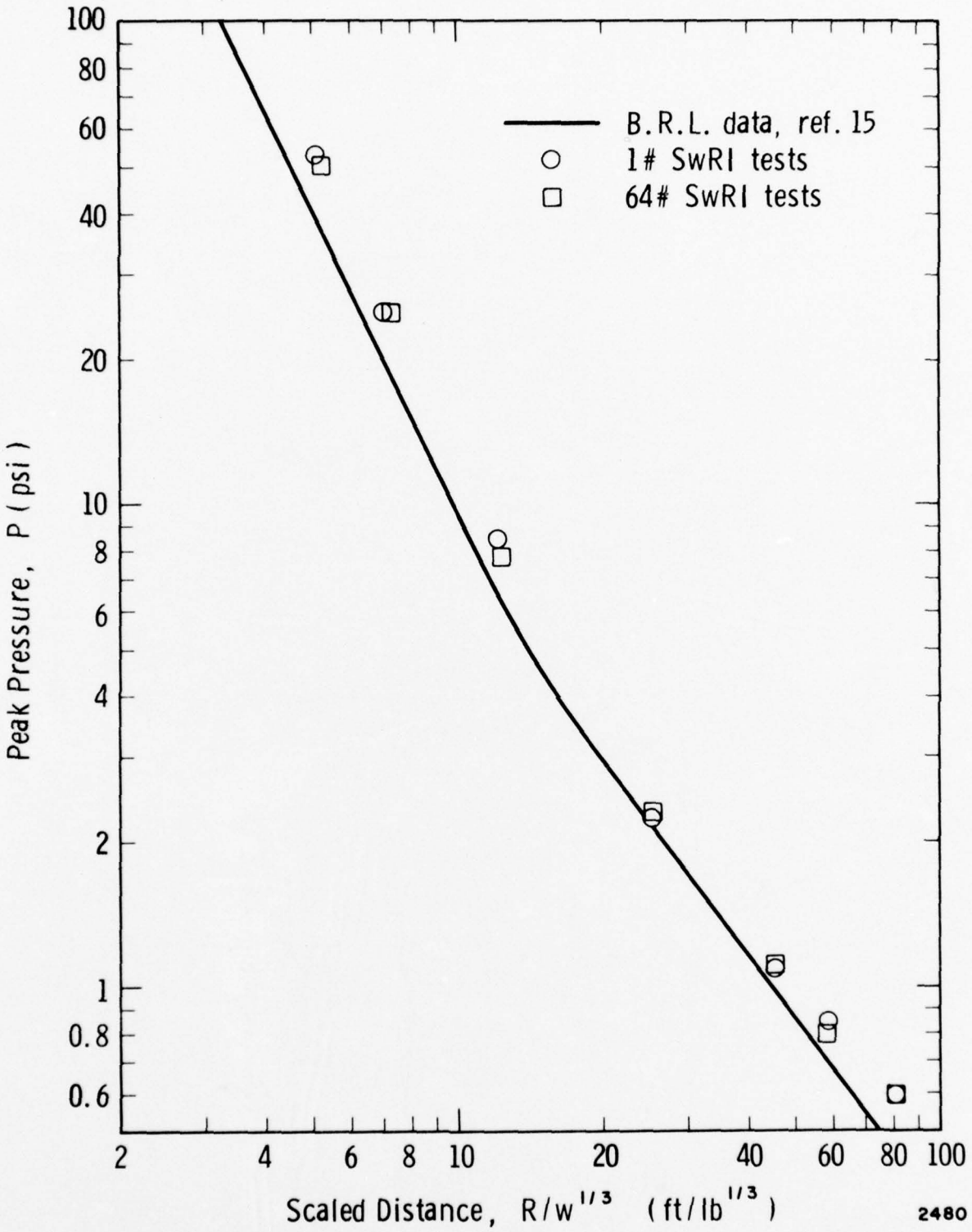

FIGURE 22. PEAK PRESSURE VS SCALED DISTANCE, FREE FIELD

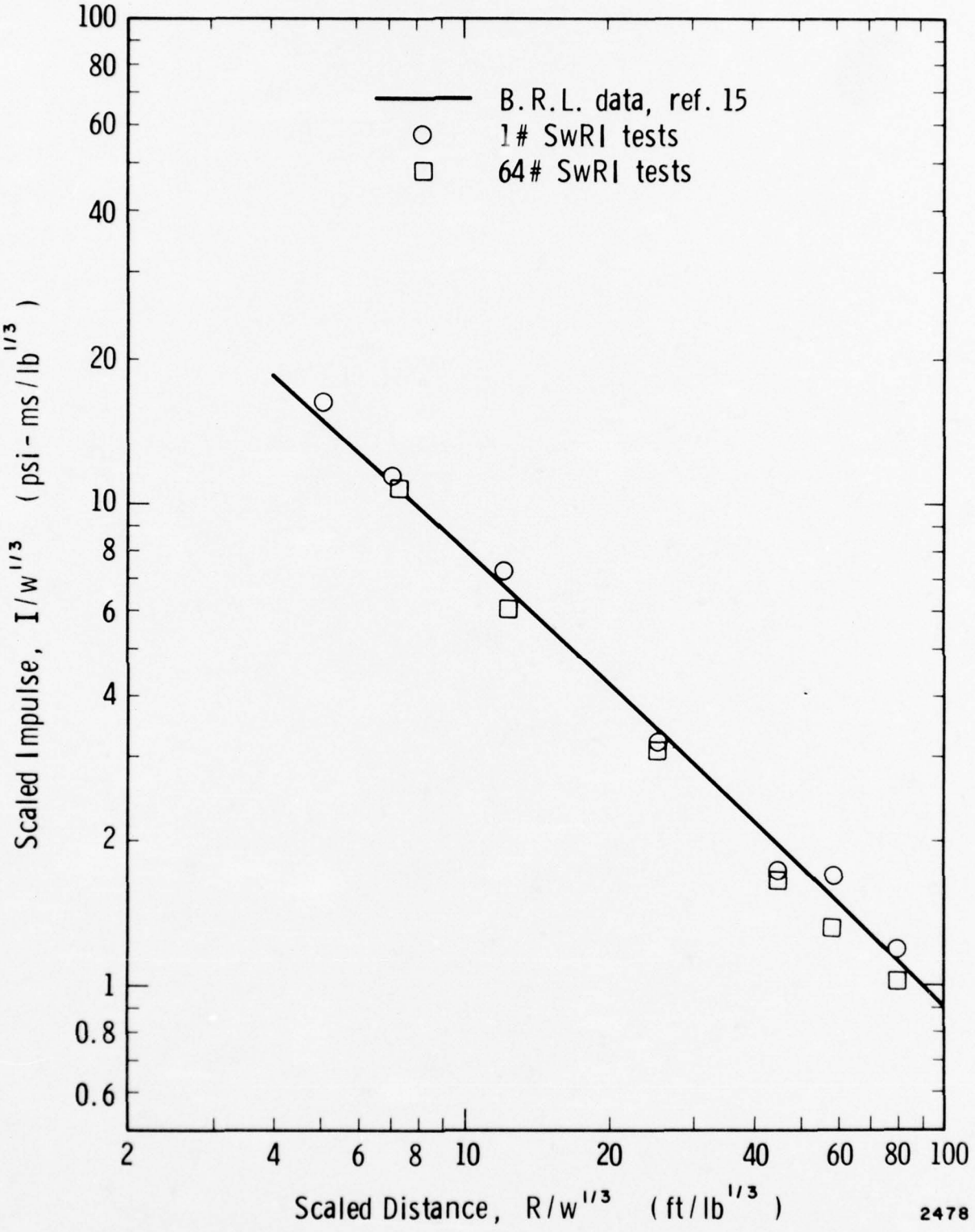

FIGURE 23. SCALED IMPULSE VS SCALED DISTANCE, FREE FIELD

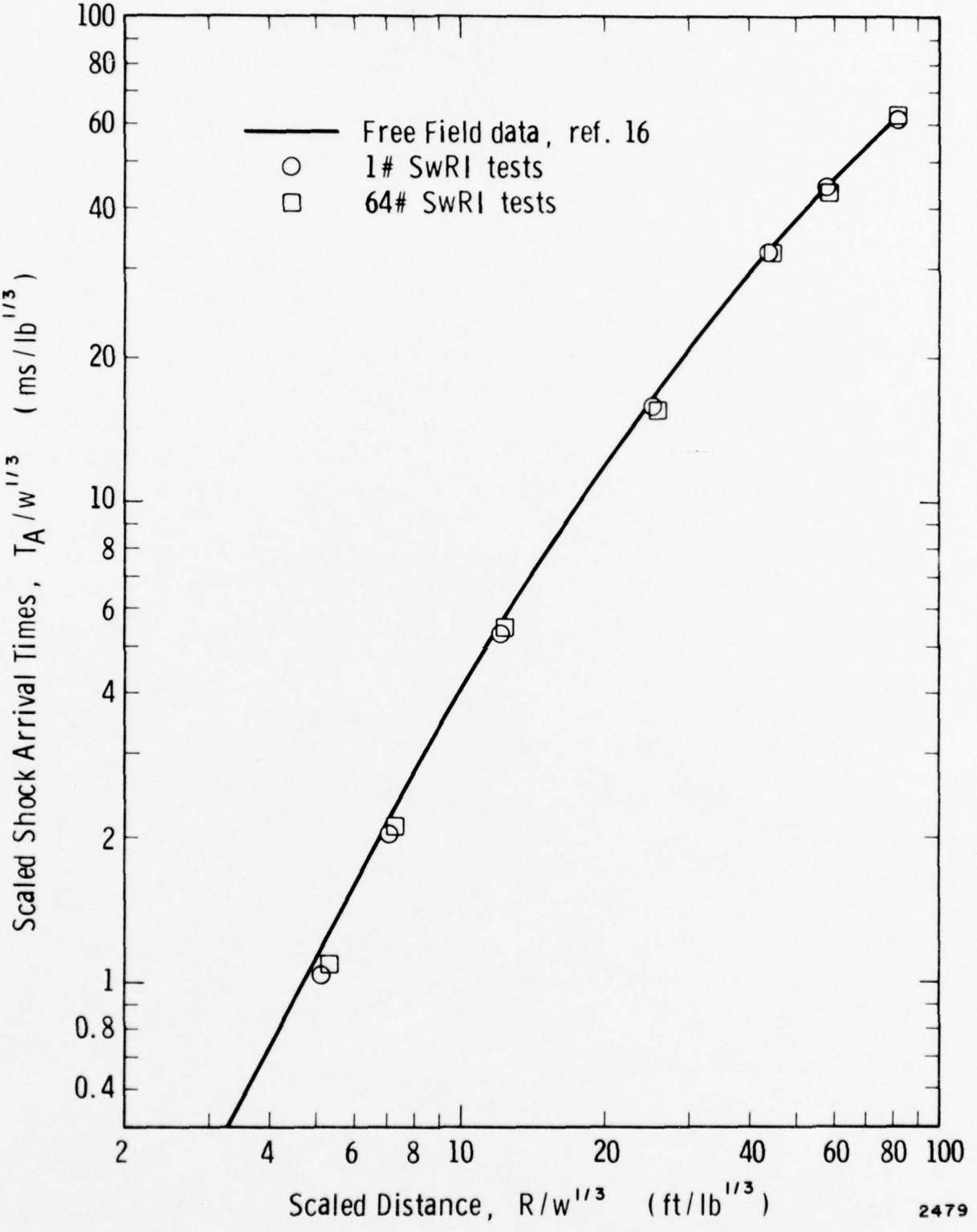

FIGURE 24. SCALED ARRIVAL TIMES VS SCALED DISTANCE, FREE FIELD

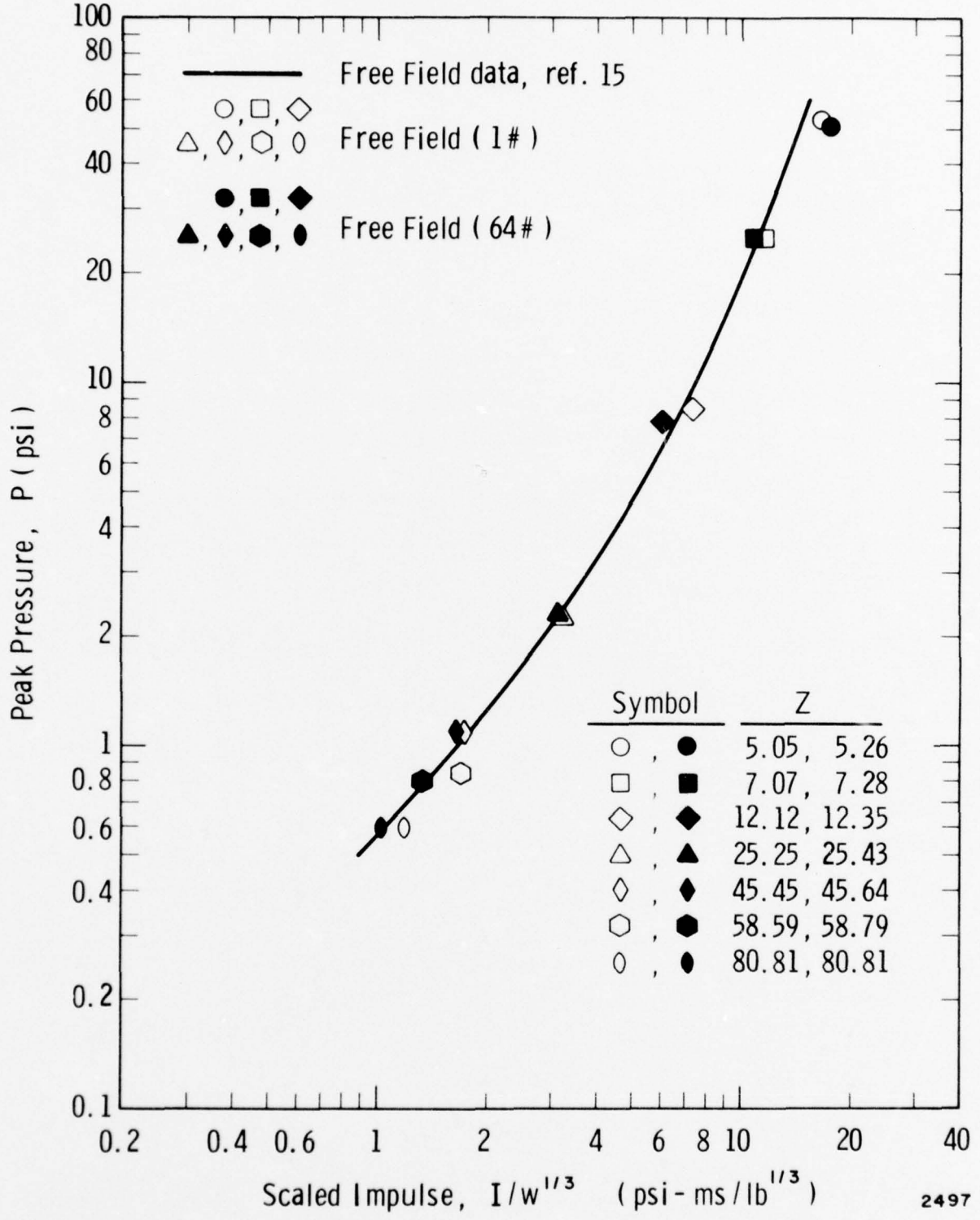

FIGURE 25. PEAK PRESSURE VS SCALED IMPULSE, FREE FIELD

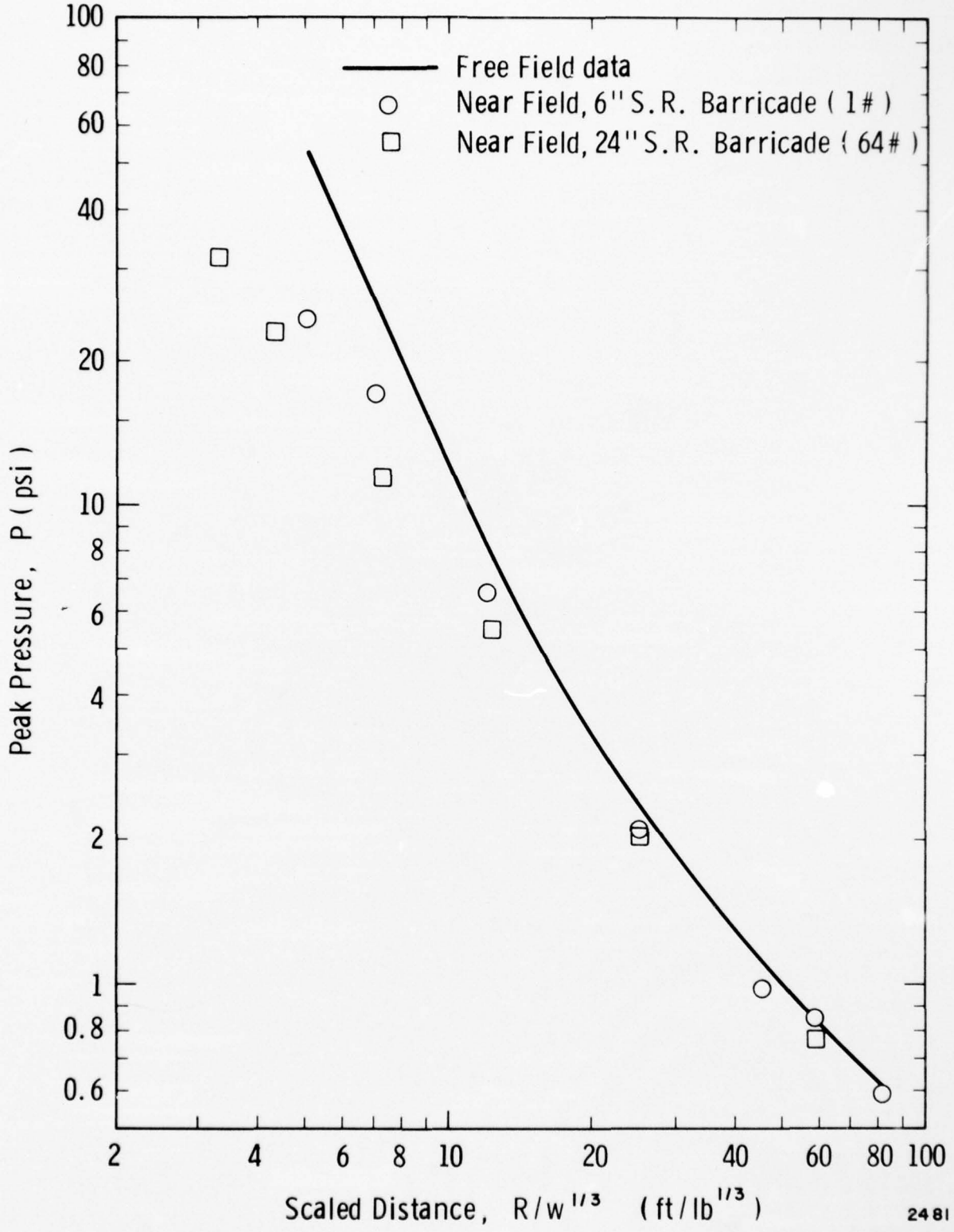

FIGURE 26. PEAK PRESSURE VS SCALED DISTANCE, SINGLE-REVETTED, 6-IN. AND 24-IN. BARRICADES, NEAR FIELD

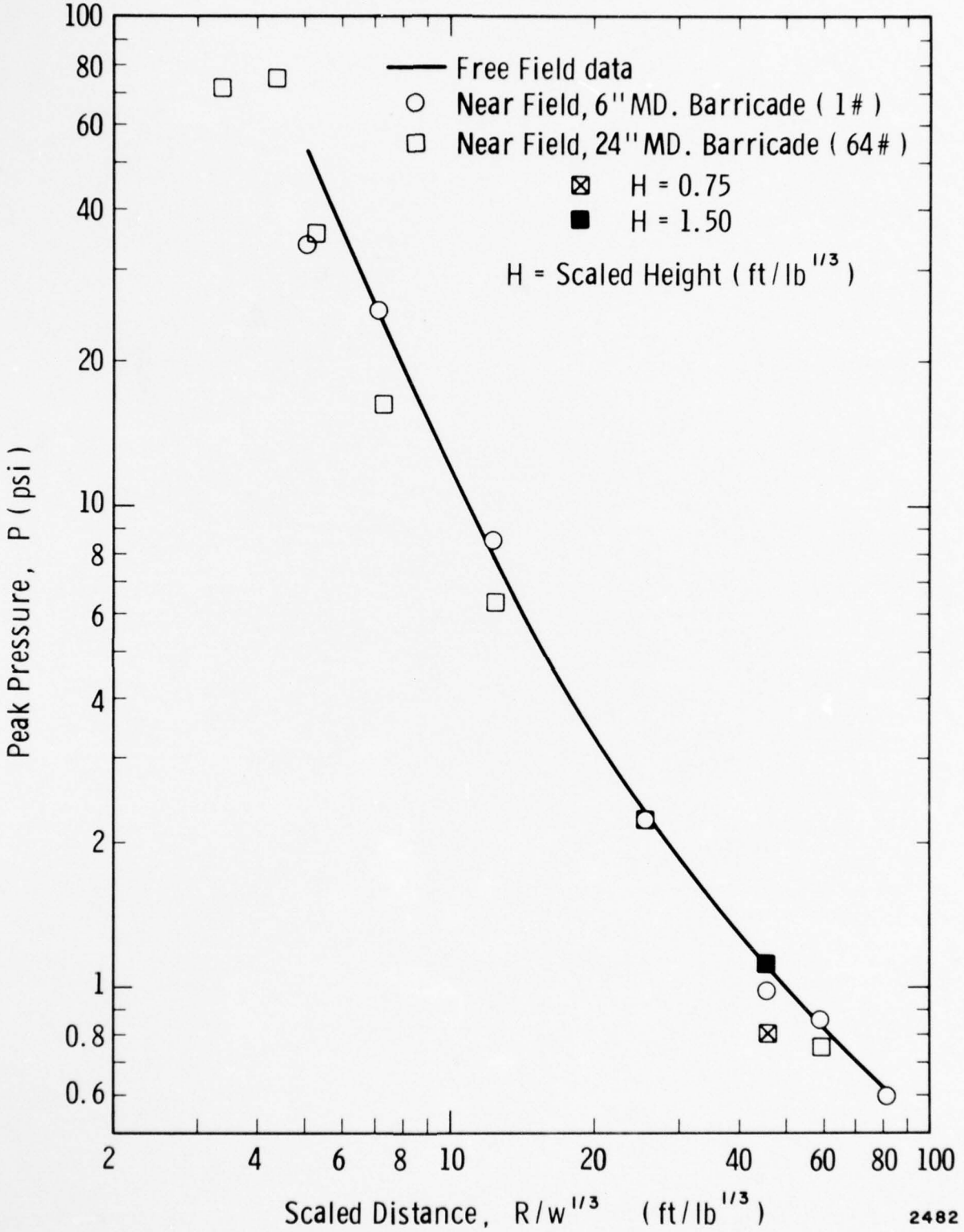

FIGURE 27. PEAK PRESSURE VS SCALED DISTANCE, MOUND, 6-IN. AND 24-IN. BARRICADES, NEAR FIELD

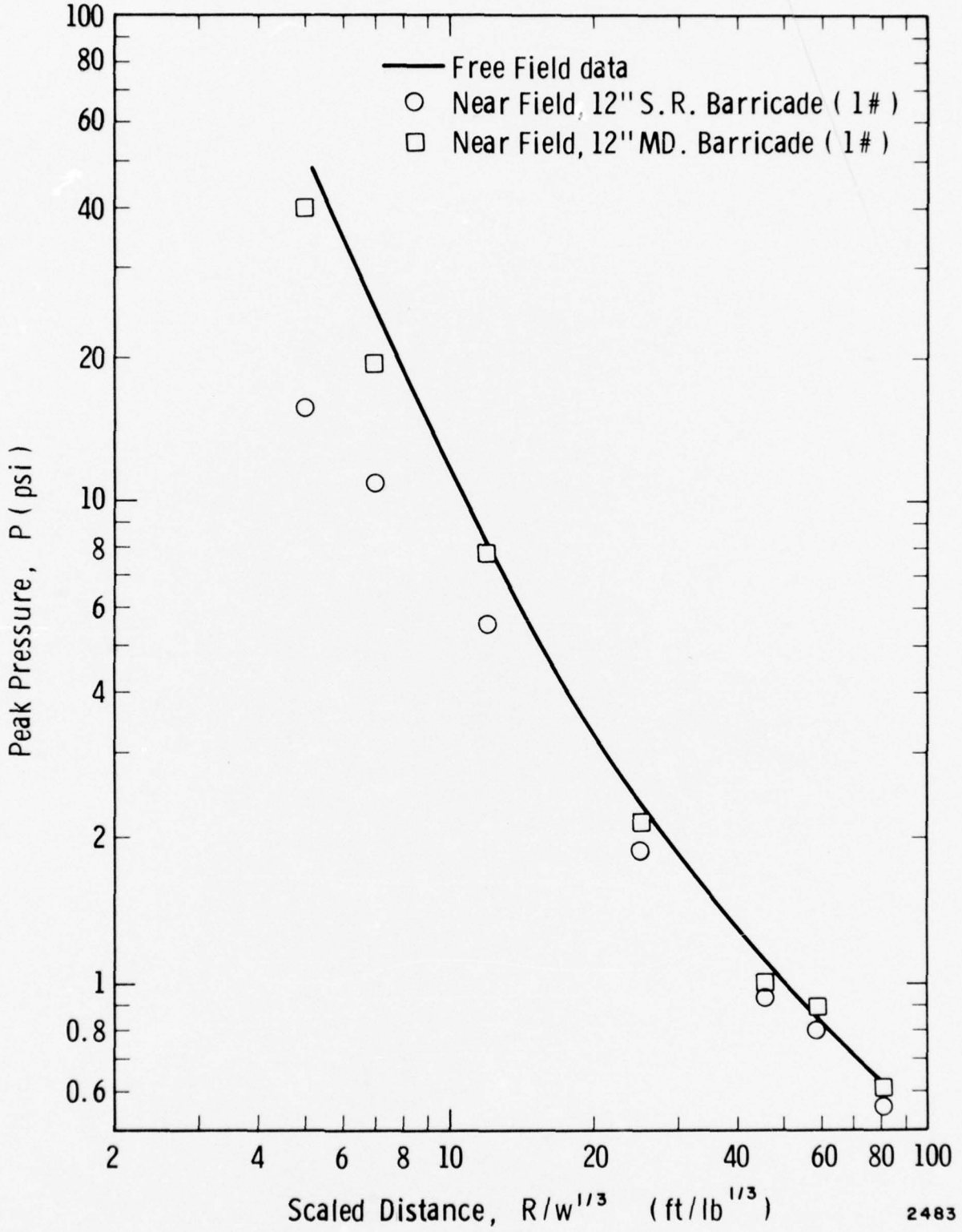

FIGURE 28. PEAK PRESSURE VS SCALED DISTANCE, SINGLE-REVETTED AND MOUND, 12-IN. BARRICADES, NEAR FIELD

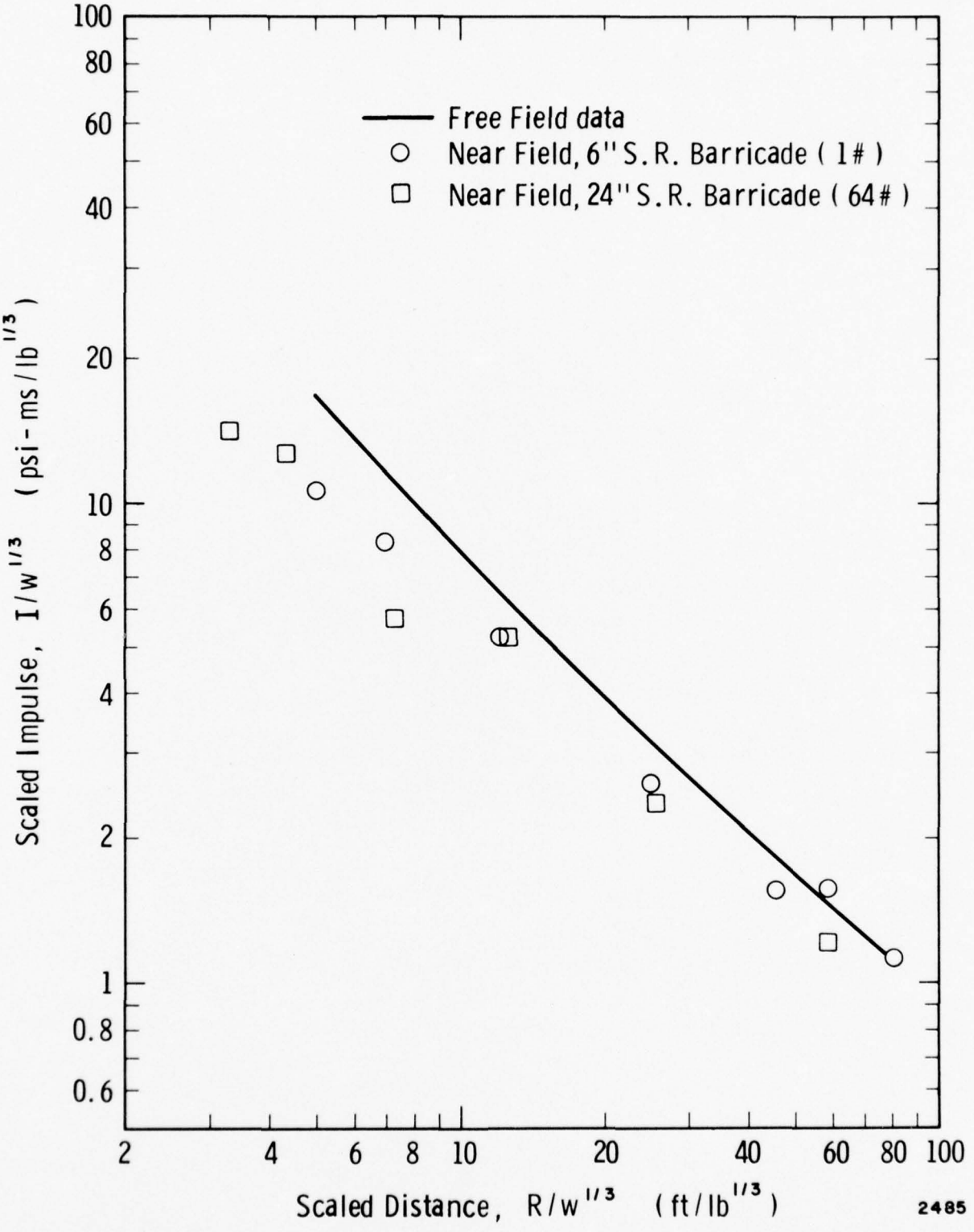

FIGURE 29. SCALED IMPULSE VS SCALED DISTANCE, SINGLE-REVETTED, 6-IN. AND 24-IN. BARRICADES, NEAR FIELD

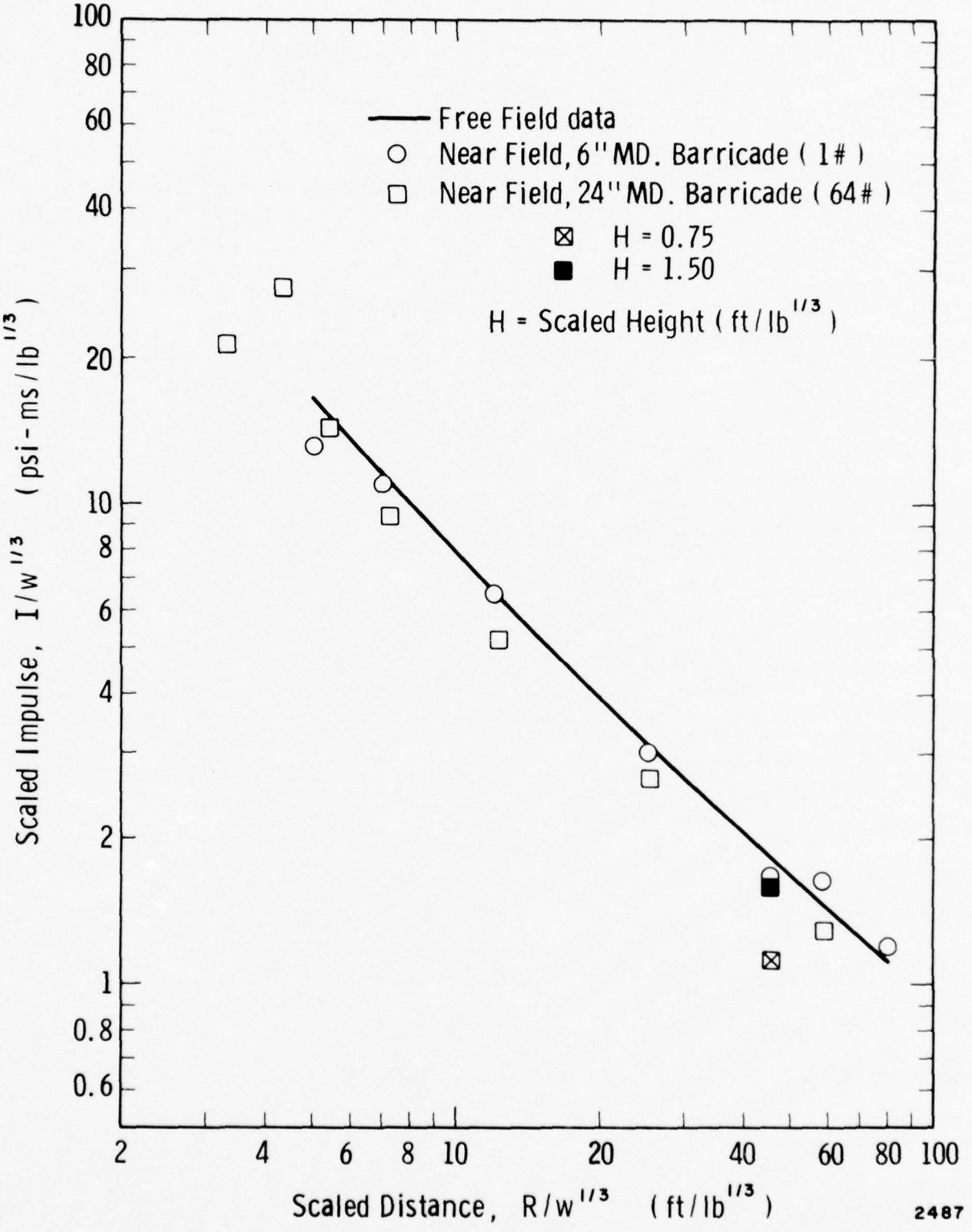

FIGURE 30. SCALED IMPULSE VS SCALED DISTANCE, MOUND, 6-IN. AND 24-IN. BARRICADES, NEAR FIELD

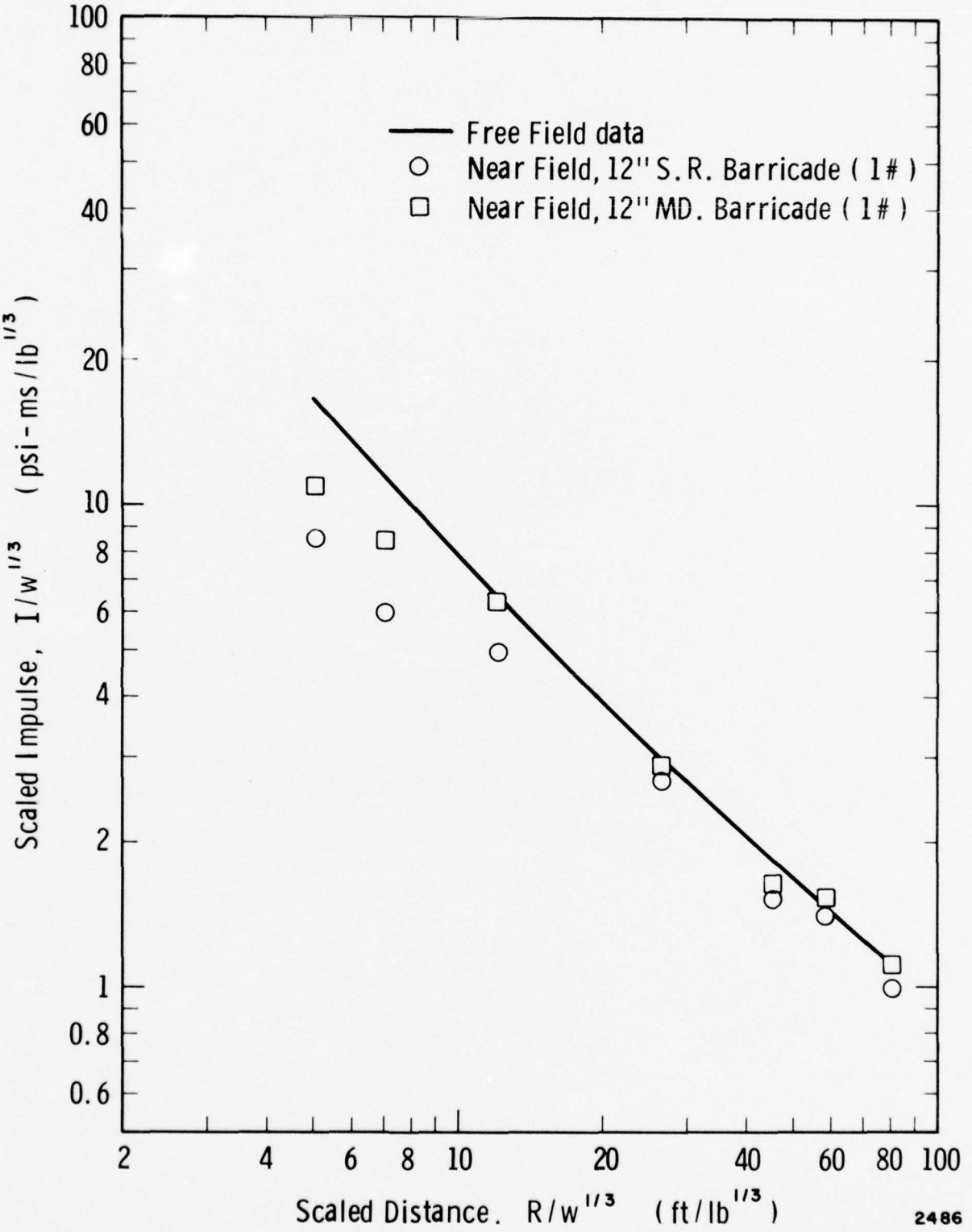

FIGURE 31. SCALED IMPULSE VS SCALED DISTANCE, SINGLE-REVETTED AND MOUND, 12-IN. BARRICADES, NEAR FIELD

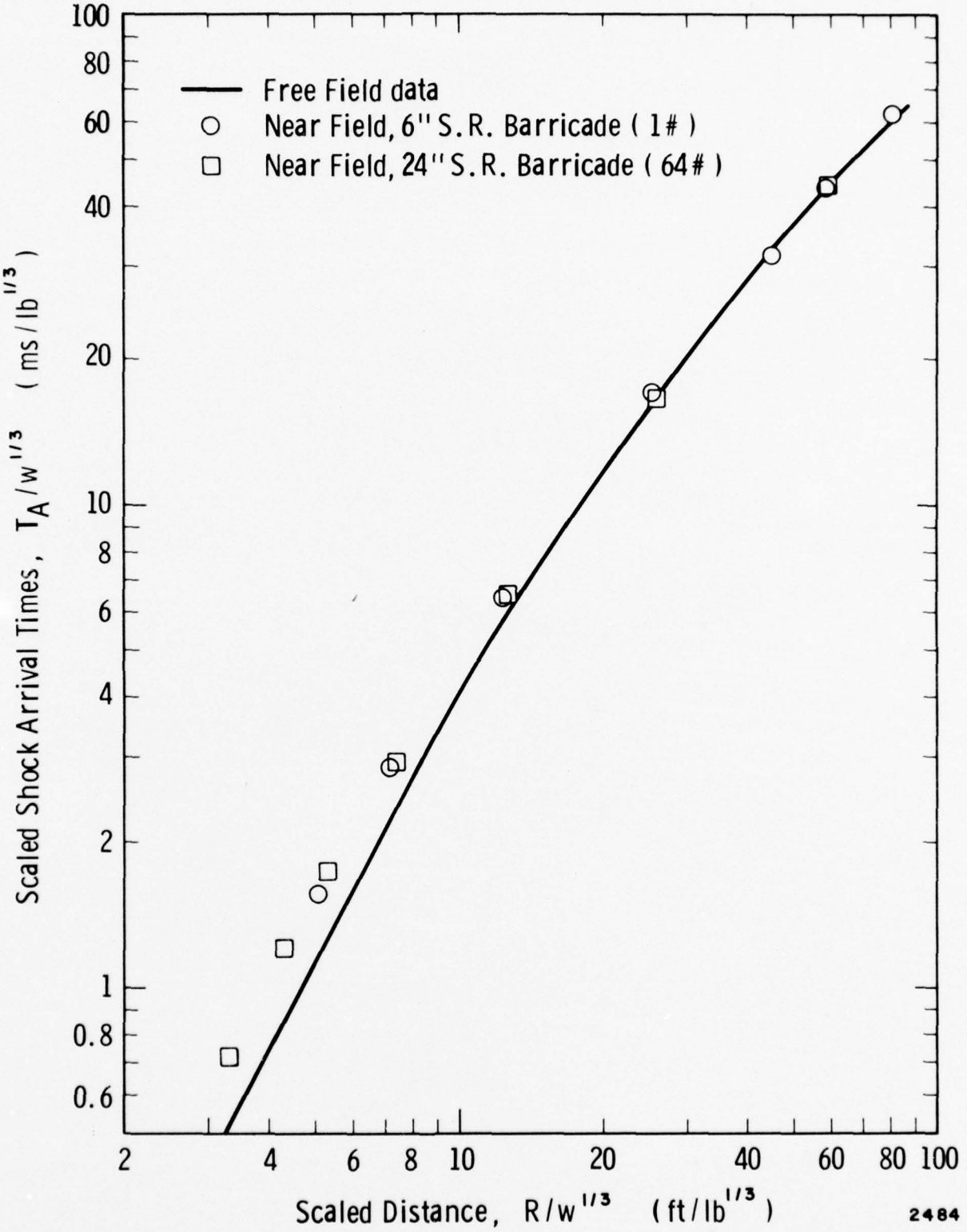

FIGURE 32. SCALED ARRIVAL TIMES VS SCALED DISTANCE, SINGLE-REVETTED, 6-IN. AND 24-IN. BARRICADES, NEAR FIELD

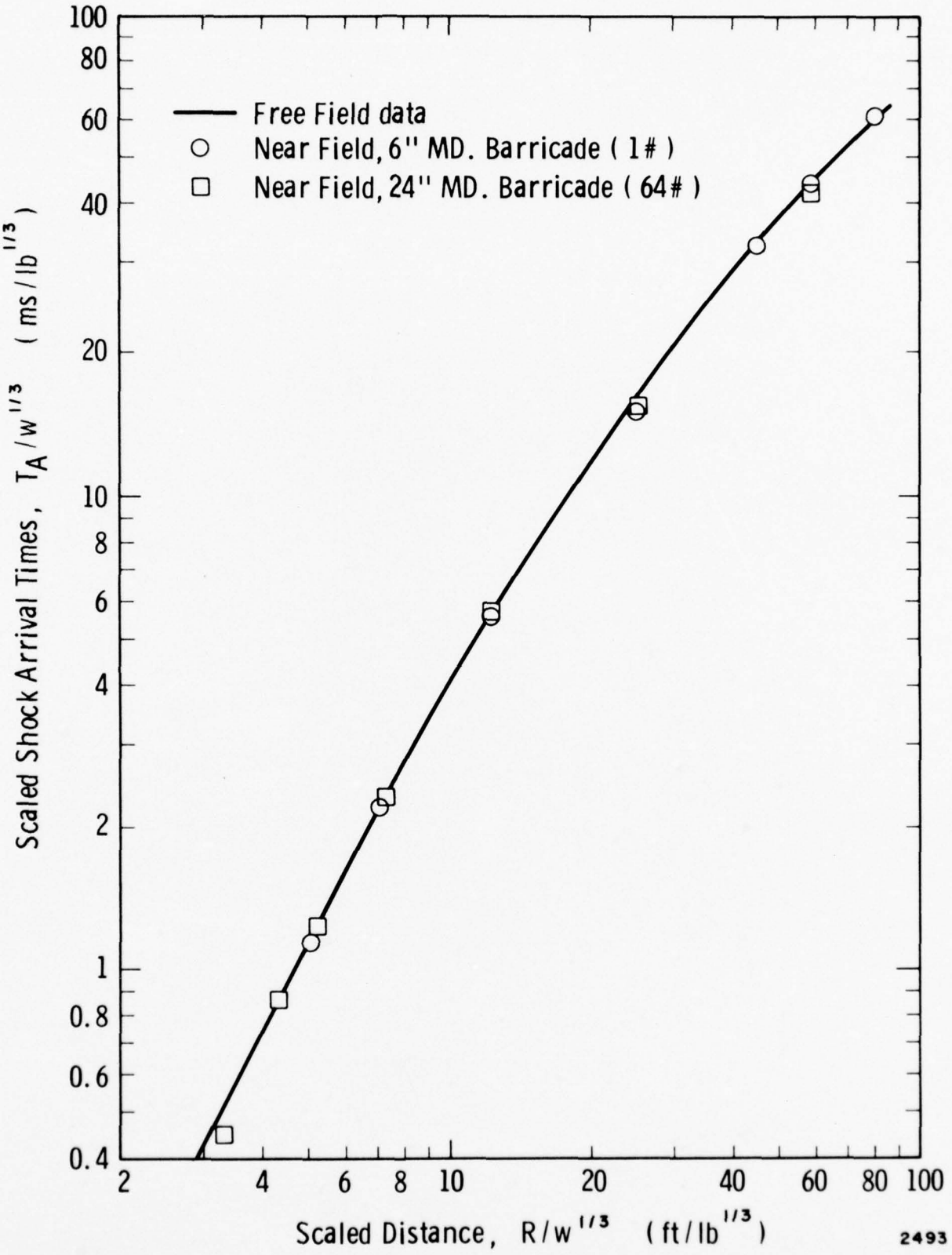

FIGURE 33. SCALED ARRIVAL TIMES VS SCALED DISTANCE, MOUND, 6-IN. AND 24-IN. BARRICADES, NEAR FIELD

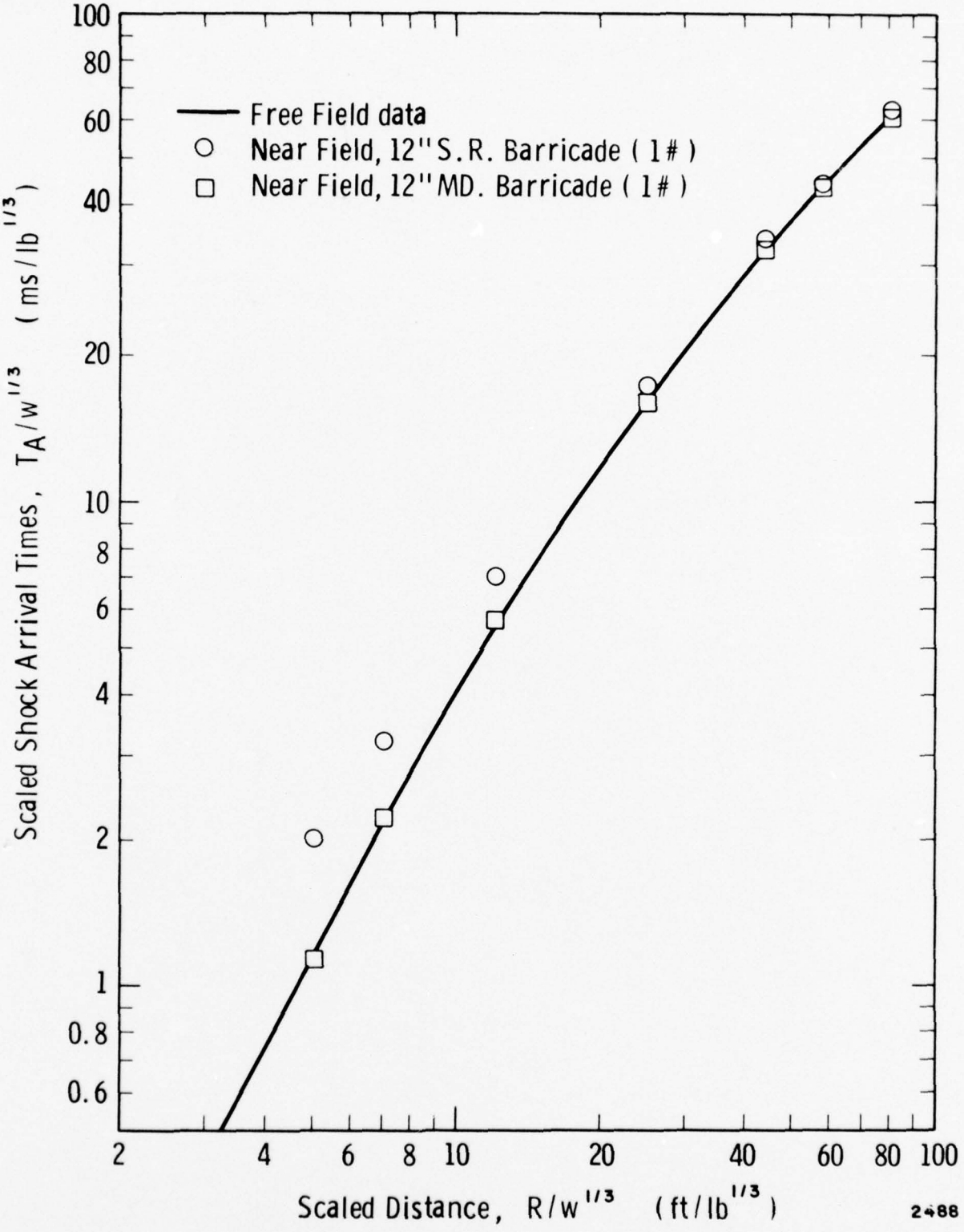

FIGURE 34. SCALED ARRIVAL TIMES VS SCALED DISTANCE, SINGLE-REVETTED AND MOUND, 12-IN. BARRICADES, NEAR FIELD
(1-lb Tests)

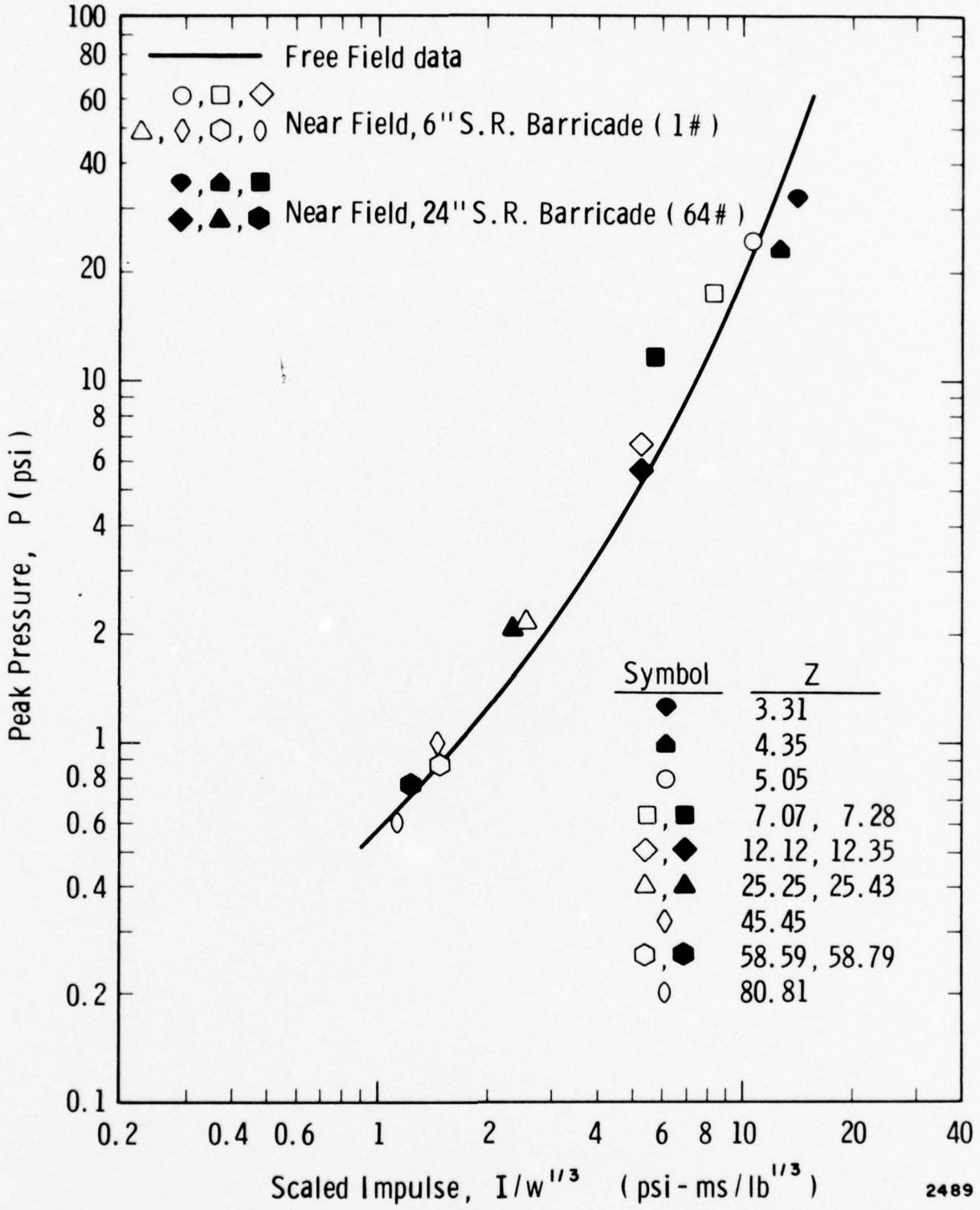

FIGURE 35. PEAK PRESSURE VS SCALED IMPULSE, SINGLE-REVETTED, 6-IN. AND 24-IN. BARRICADES, NEAR FIELD

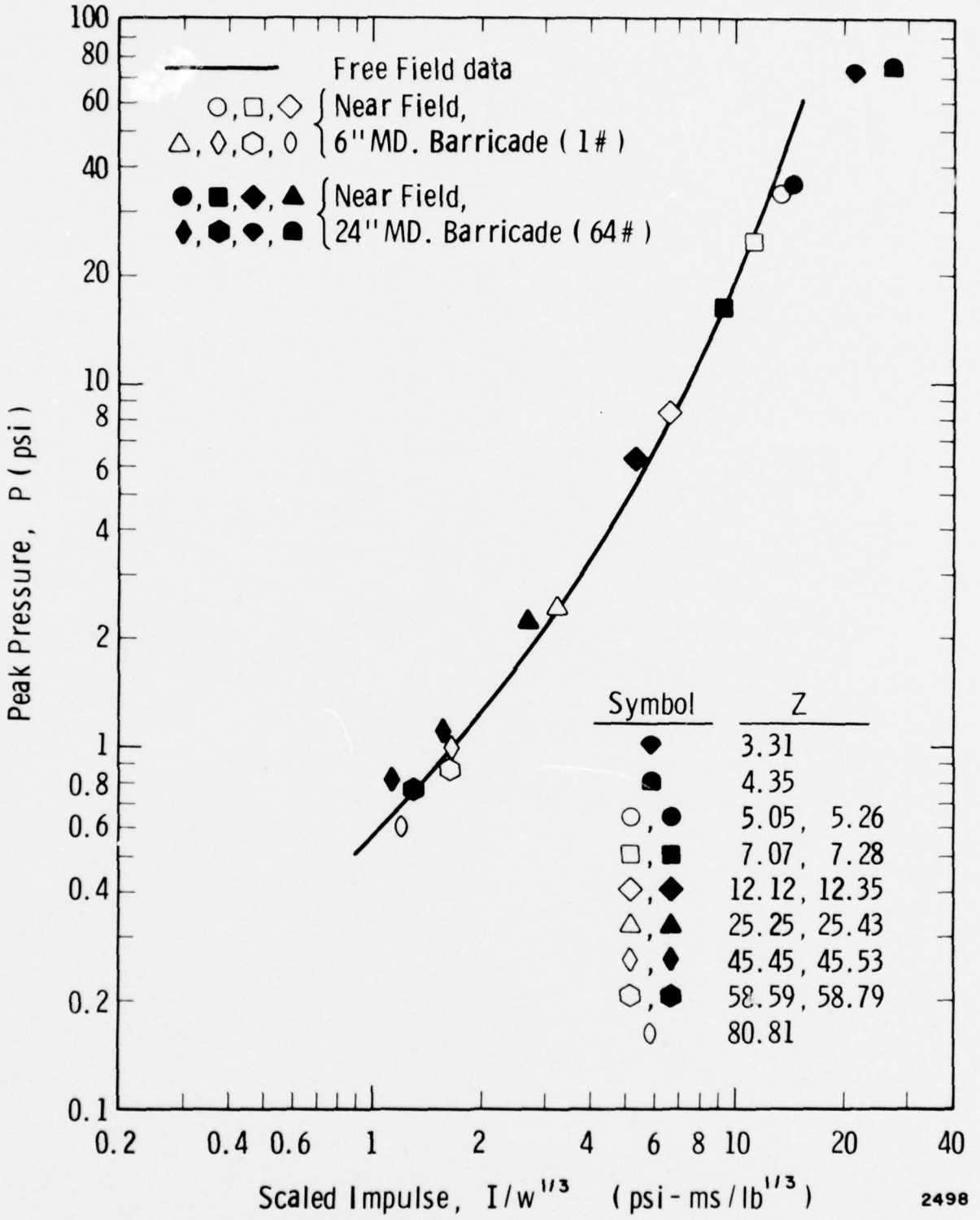

FIGURE 36. PEAK PRESSURE VS SCALED IMPULSE, MOUND, 6-IN. AND 24-IN. BARRICADES, NEAR FIELD

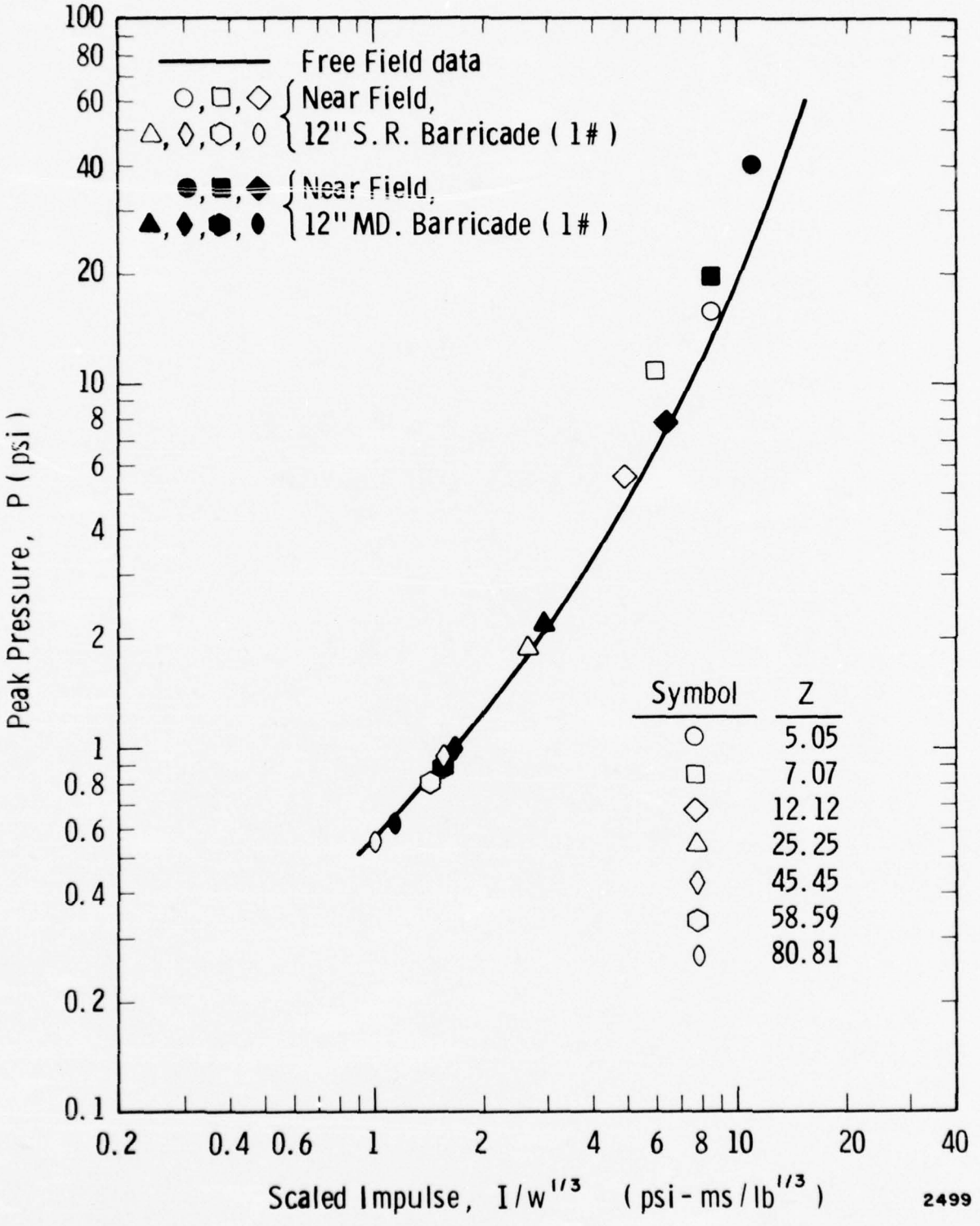

FIGURE 37. PEAK PRESSURE VS SCALED IMPULSE, SINGLE-REVETTED AND MOUND, 12-IN. BARRICADE, NEAR FIELD

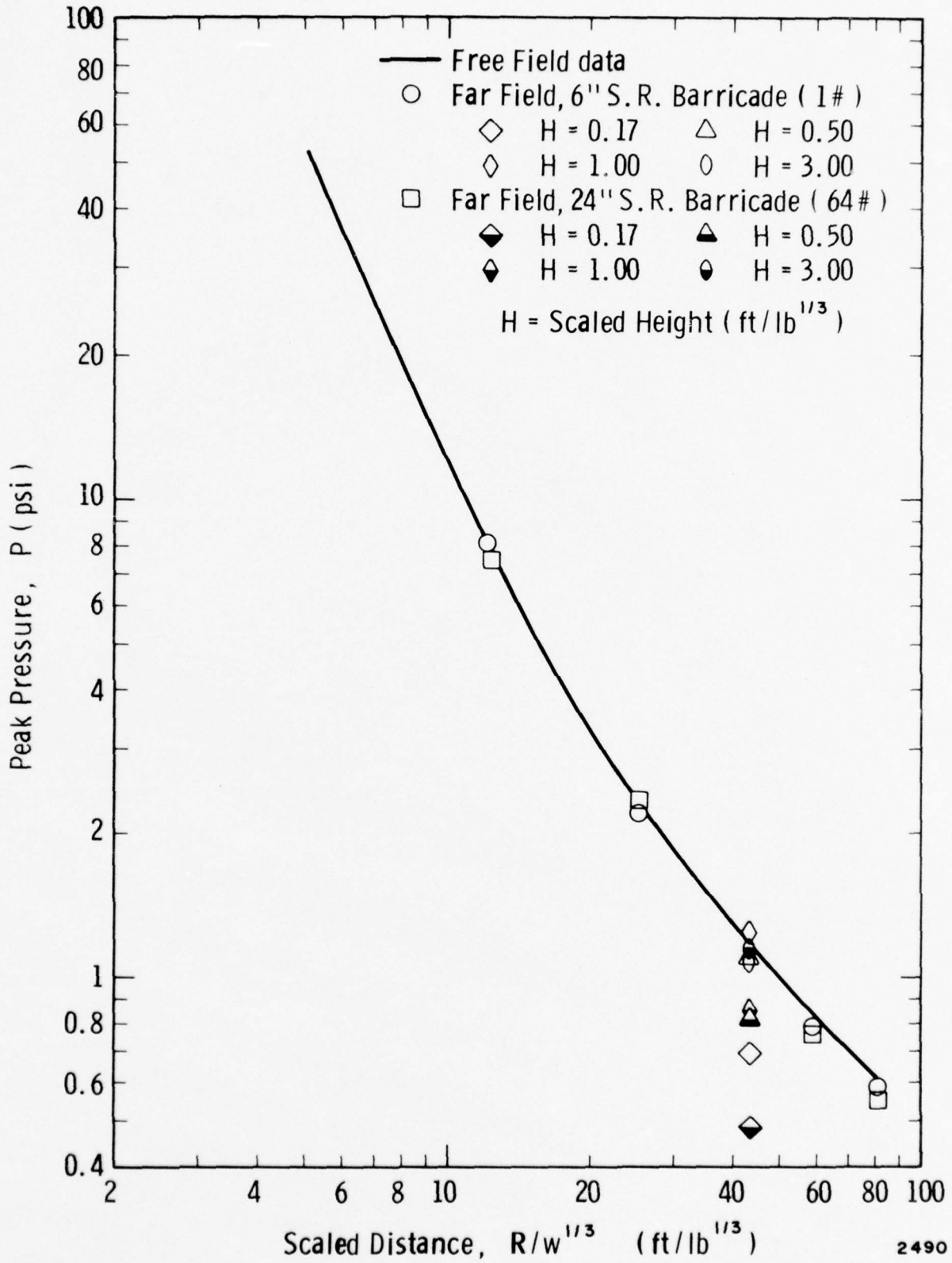

FIGURE 38. PEAK PRESSURE VS SCALED DISTANCE, SINGLE-REVETTED, 6-IN. AND 24-IN. BARRICADES, FAR FIELD

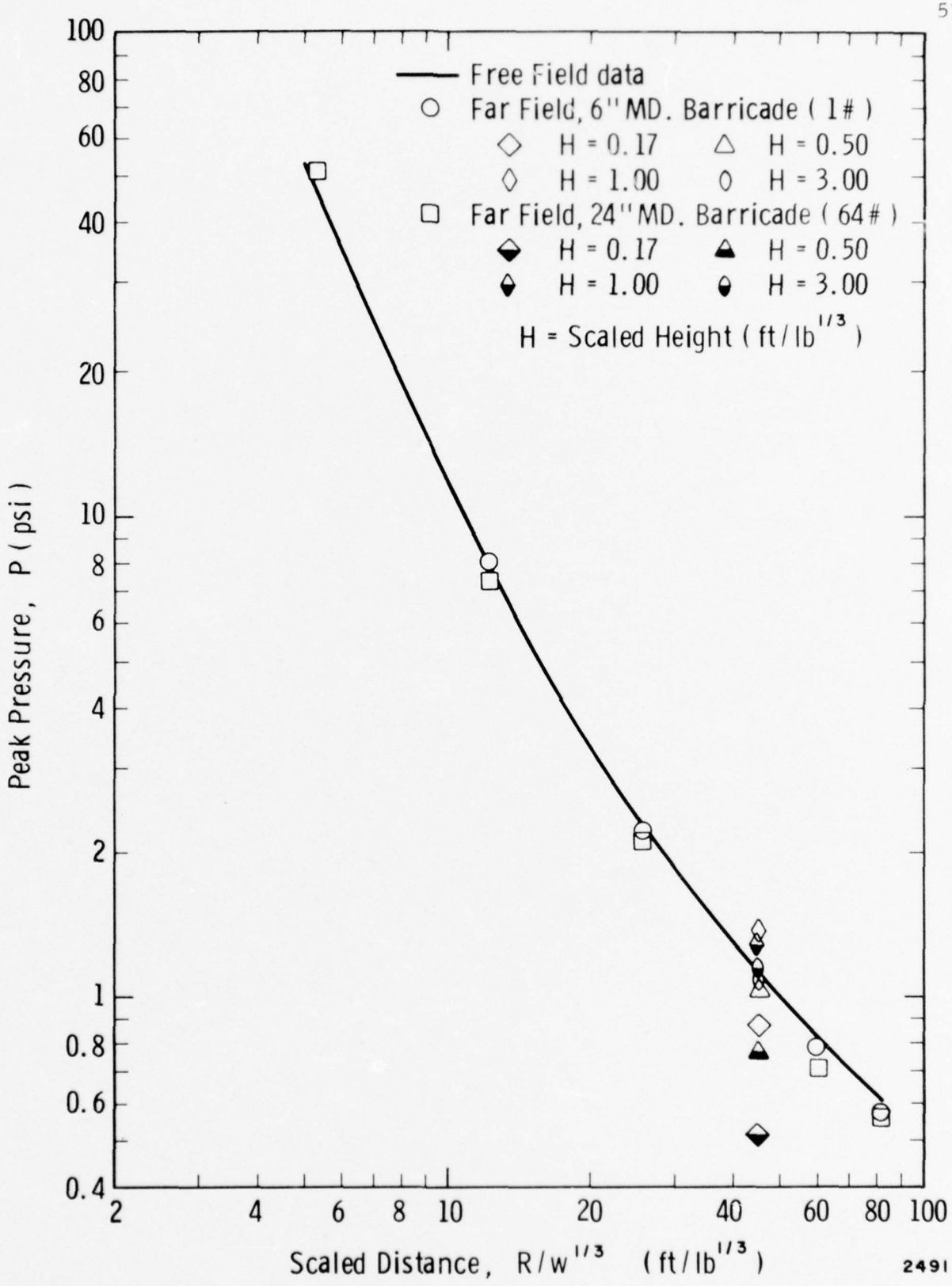

FIGURE 39. PEAK PRESSURE VS SCALED DISTANCE, MOUND, 6-IN. AND 24-IN. BARRICADES, FAR FIELD

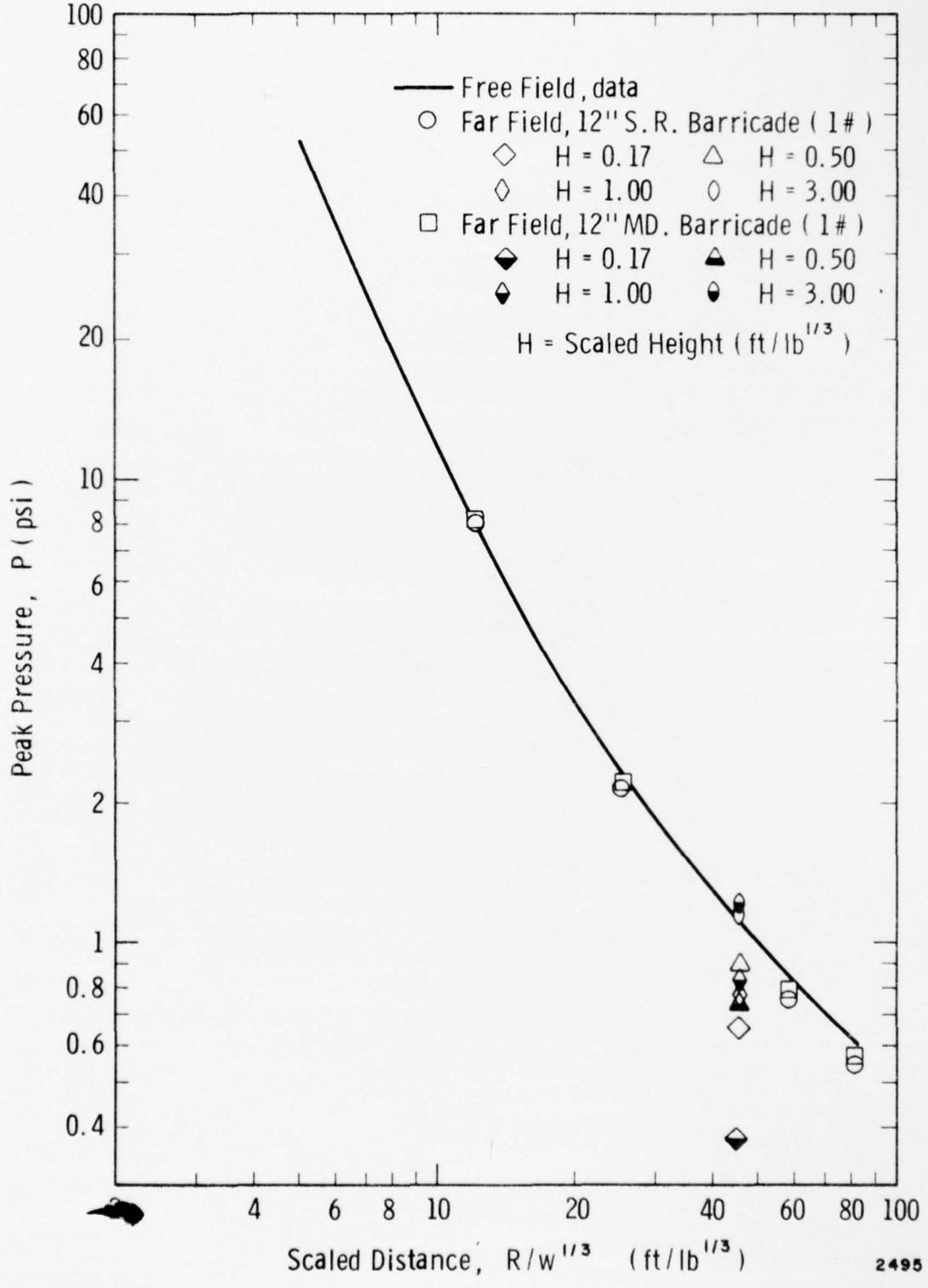

FIGURE 40. PEAK PRESSURE VS SCALED DISTANCE, SINGLE-REVETTED AND MOUND, 12-IN. BARRICADES, FAR FIELD (1-LB TESTS)

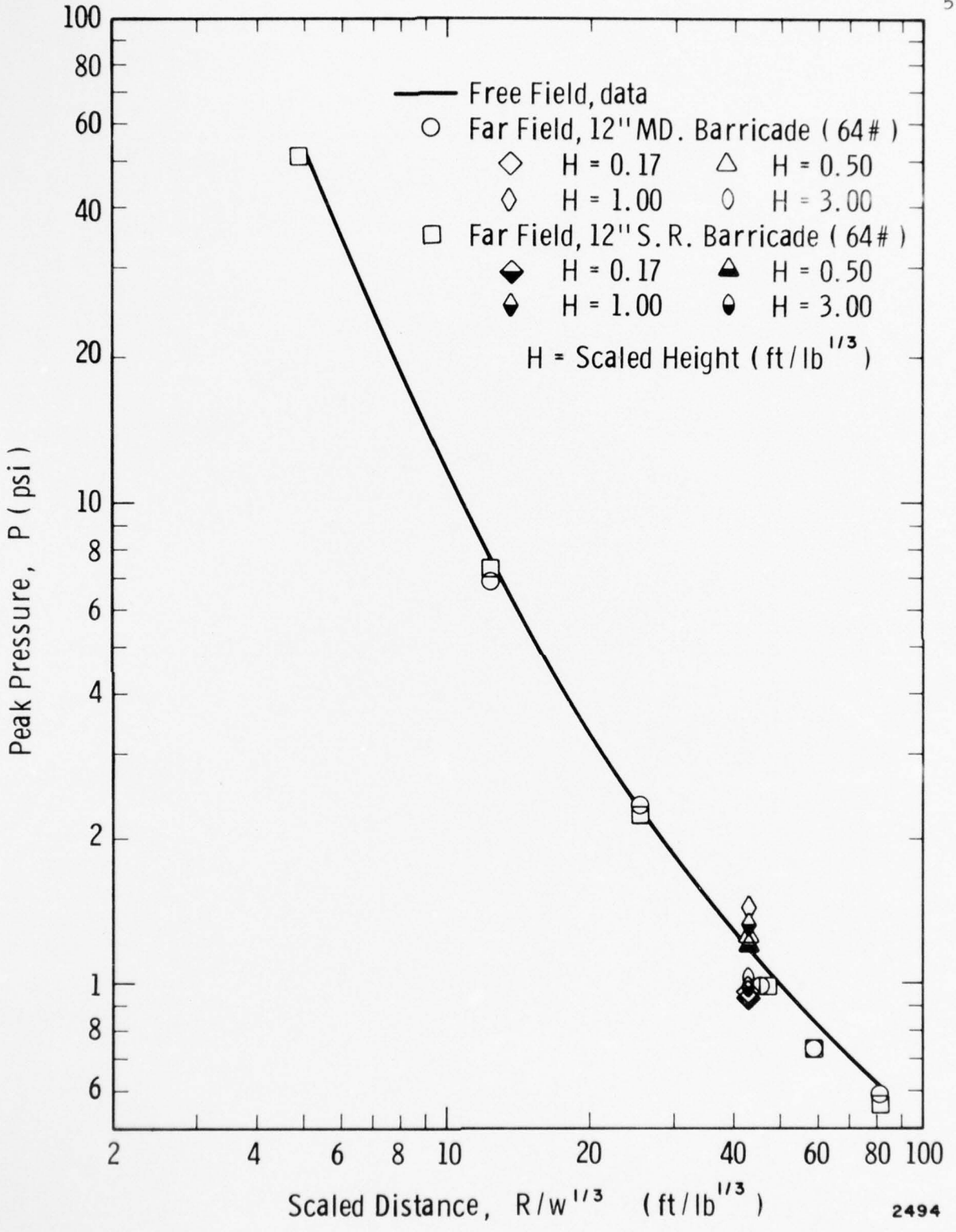

FIGURE 41. PEAK PRESSURE VS SCALED DISTANCE, SINGLE-REVETTED AND MOUND, 12-IN. BARRICADES, FAR FIELD (64-lb Tests)

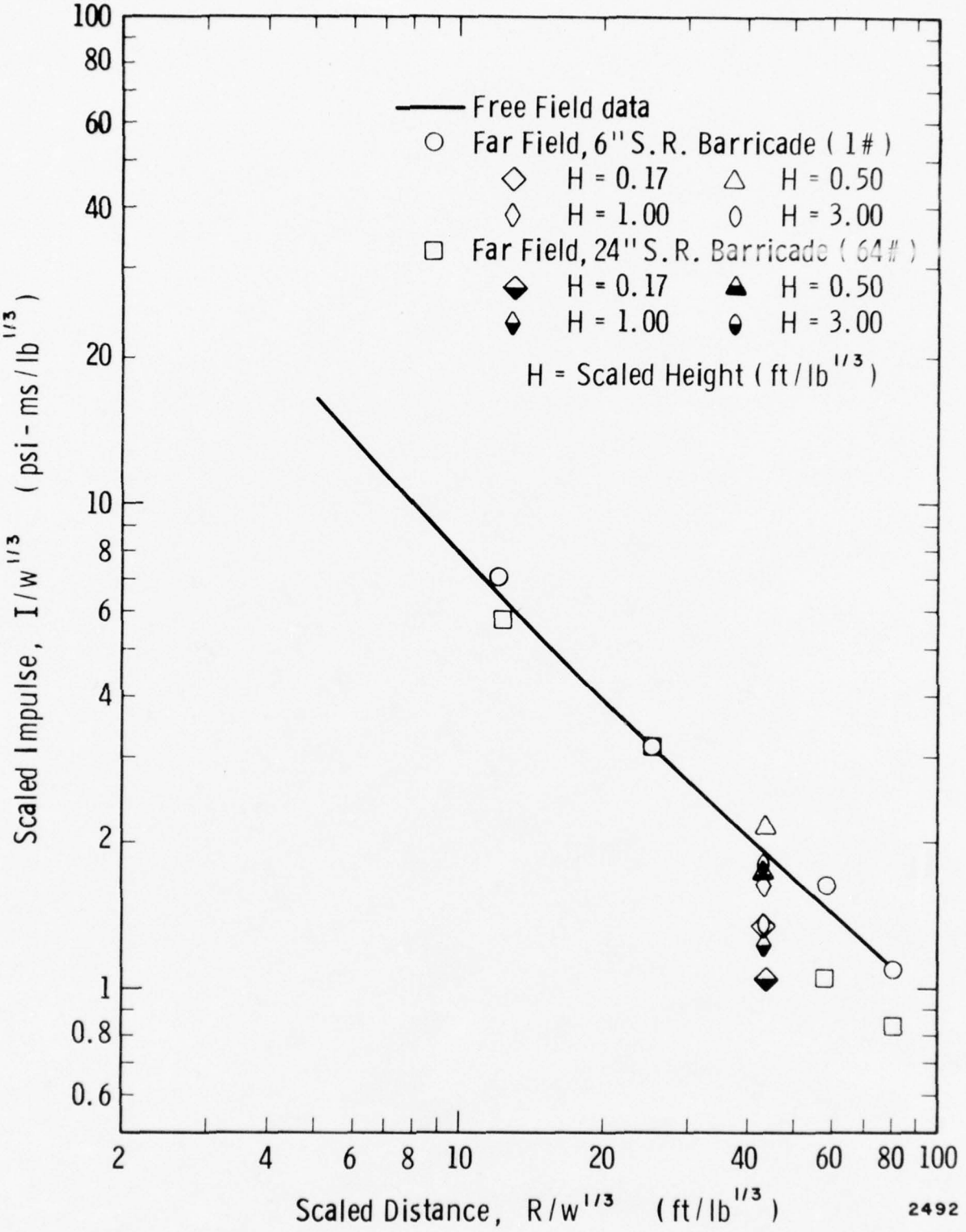

FIGURE 42. SCALED IMPULSE VS SCALED DISTANCE, SINGLE-REVETTED, 6-IN. AND 24-IN. BARRICADES, FAR FIELD

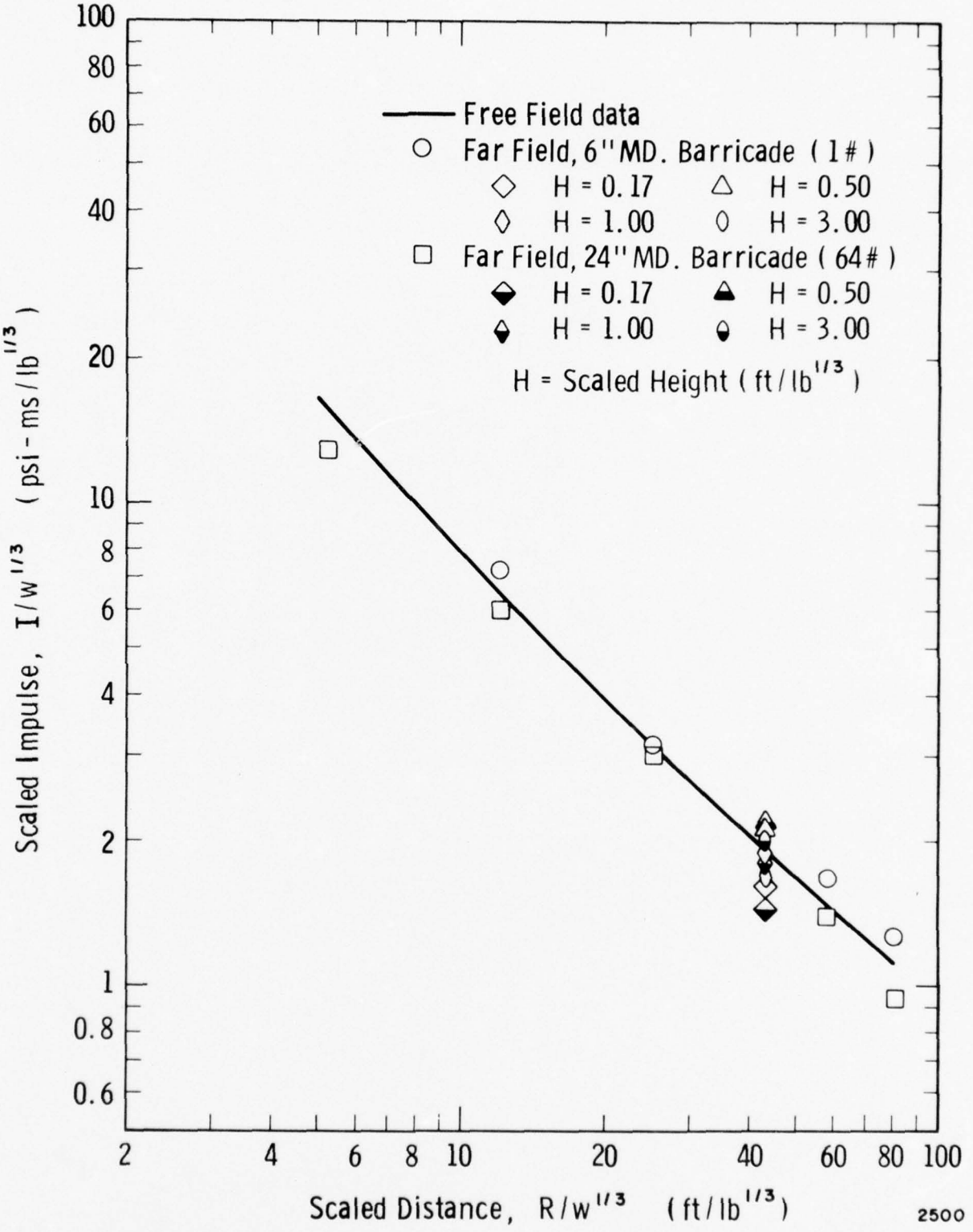

FIGURE 43. SCALED IMPULSE VS SCALED DISTANCE, MOUND, 6-IN. AND 24-IN. BARRICADES, FAR FIELD

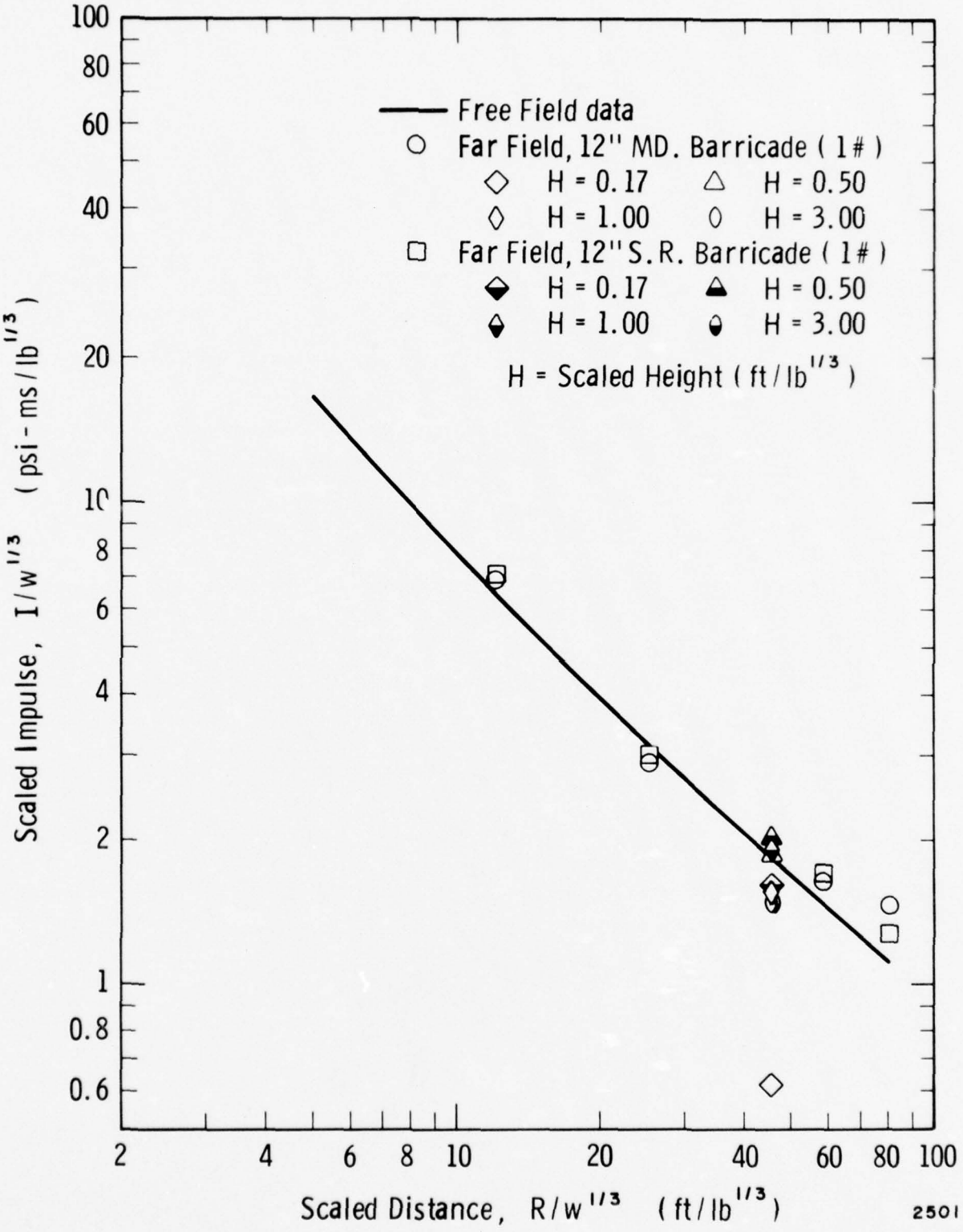

FIGURE 44. SCALED IMPULSE VS SCALED DISTANCE, SINGLE-REVETTED AND MOUND, 12-IN. BARRICADES, FAR FIELD (1-lb Tests)

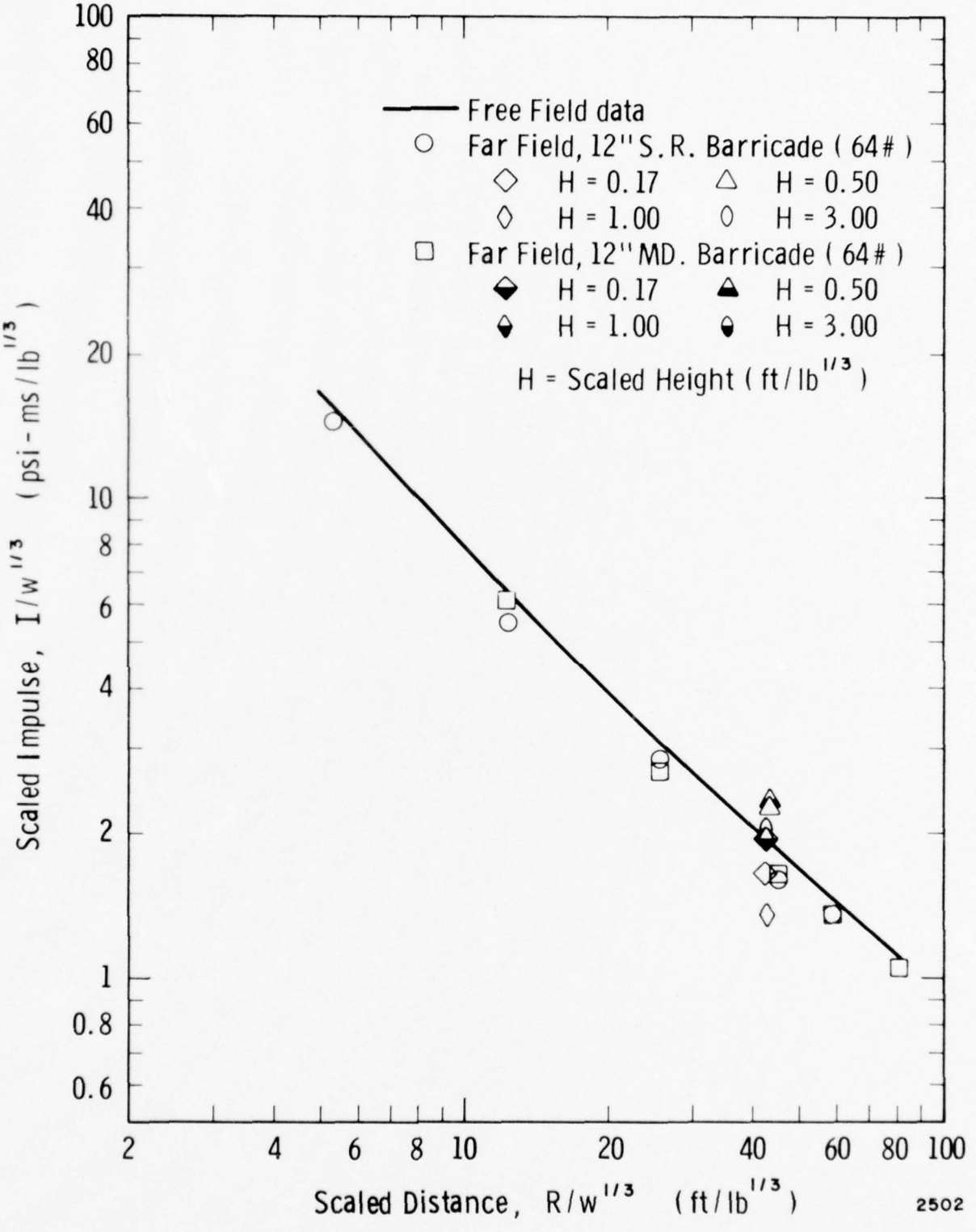

FIGURE 45. SCALED IMPULSE VS SCALED DISTANCE, SINGLE-REVETTED AND MOUND, 12-IN. BARRICADES, FAR FIELD (64-lb Tests)

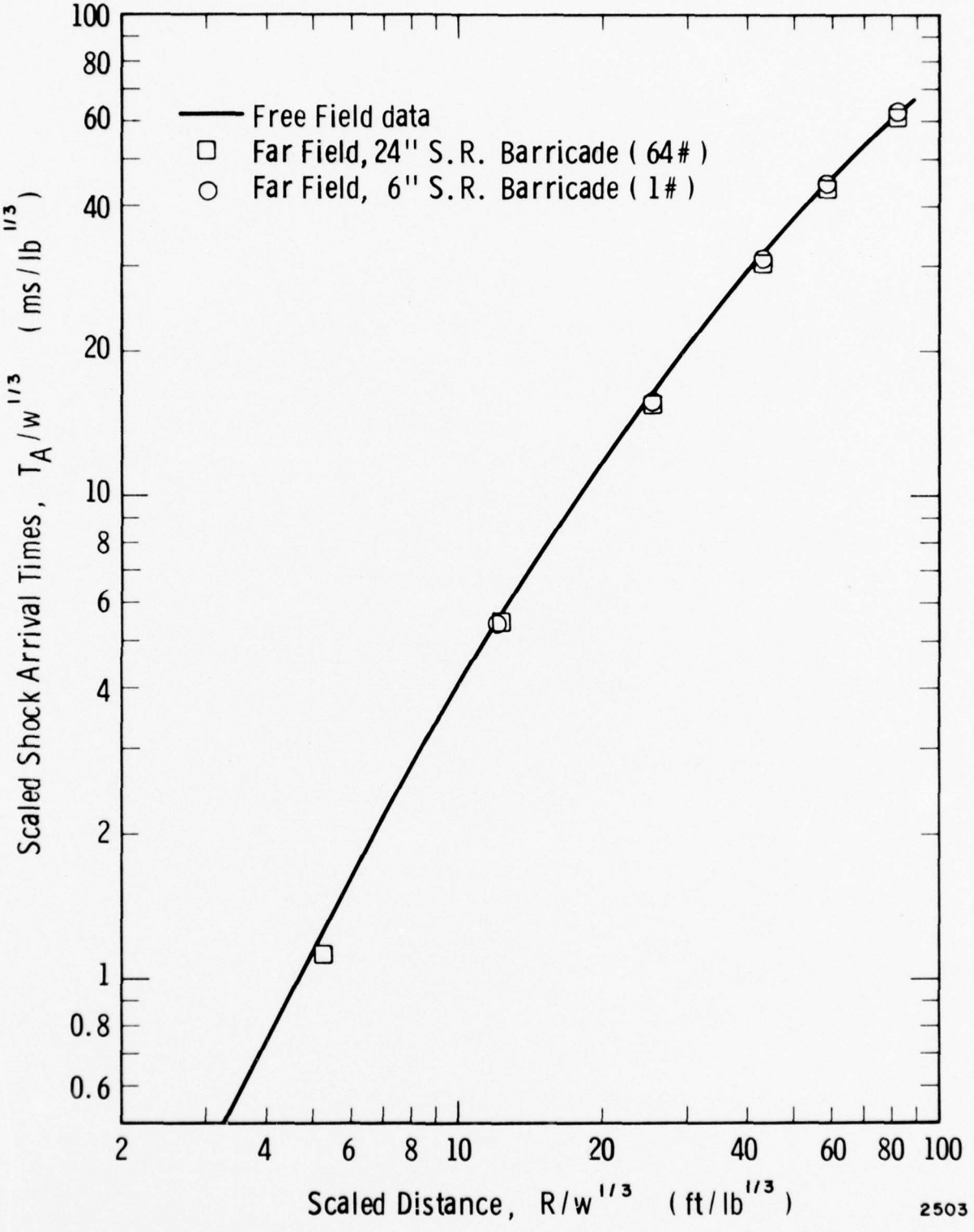

FIGURE 46. SCALED SHOCK ARRIVAL TIMES VS SCALED DISTANCE, SINGLE-REVETTED, 6-IN. AND 24-IN. BARRICADES, FAR FIELD

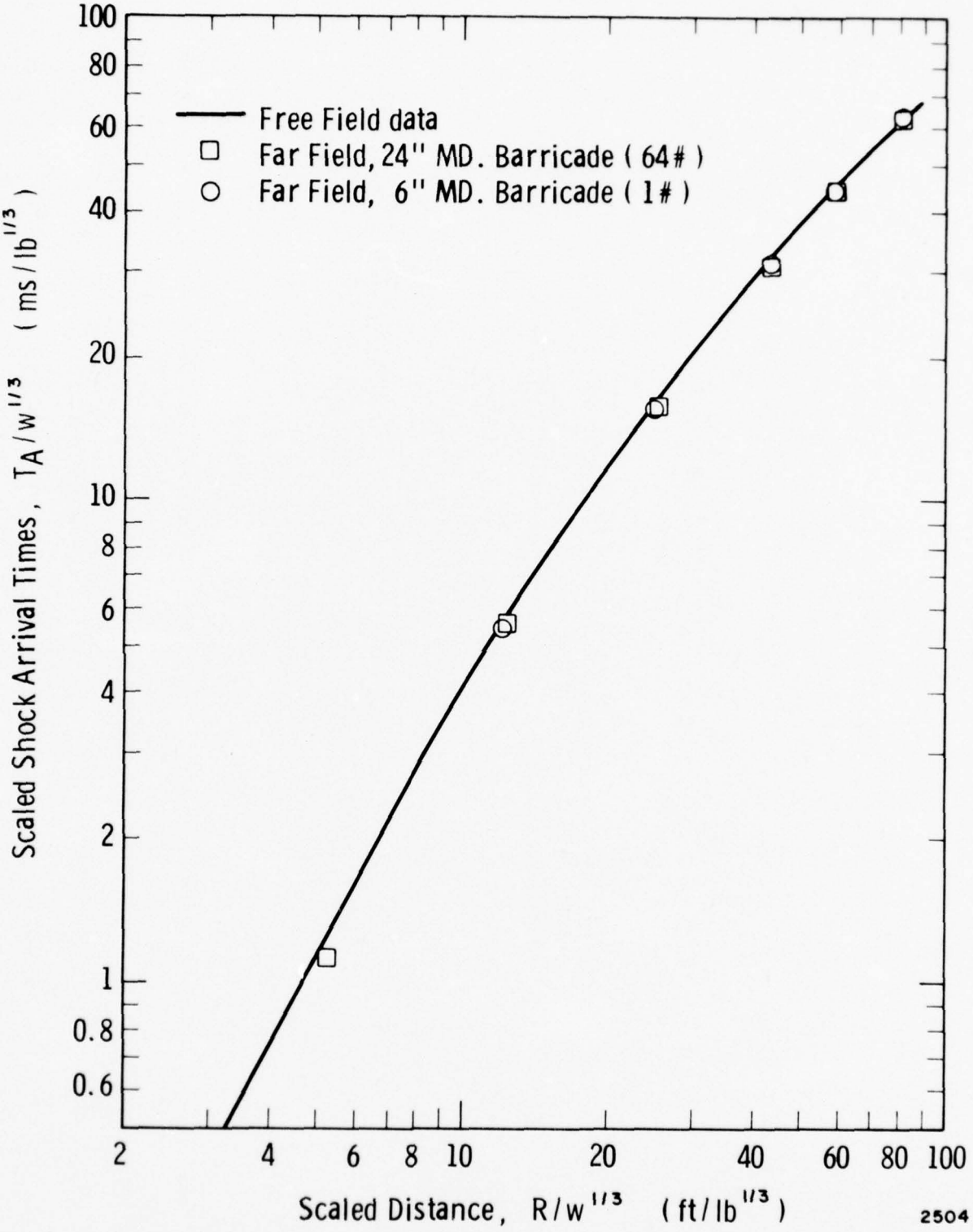

FIGURE 47. SCALED SHOCK ARRIVAL TIMES VS SCALED DISTANCE, MOUND, 6-IN. AND 24-IN. BARRICADES, FAR FIELD

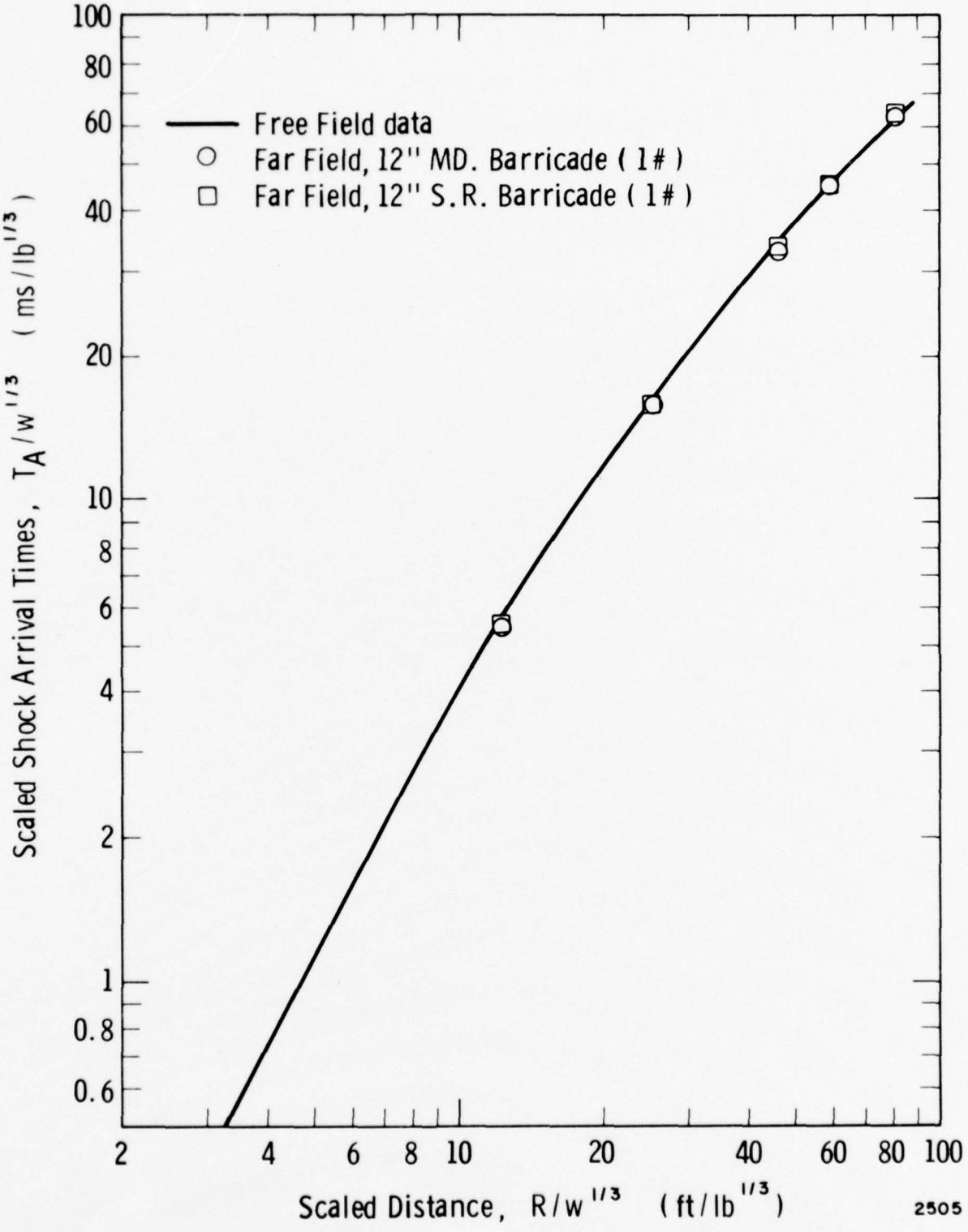

FIGURE 48. SCALED SHOCK ARRIVAL TIMES VS SCALED DISTANCE, MOUND AND SINGLE-REVETTED, 12-IN. BARRICADES, FAR FIELD (1-lb Tests)

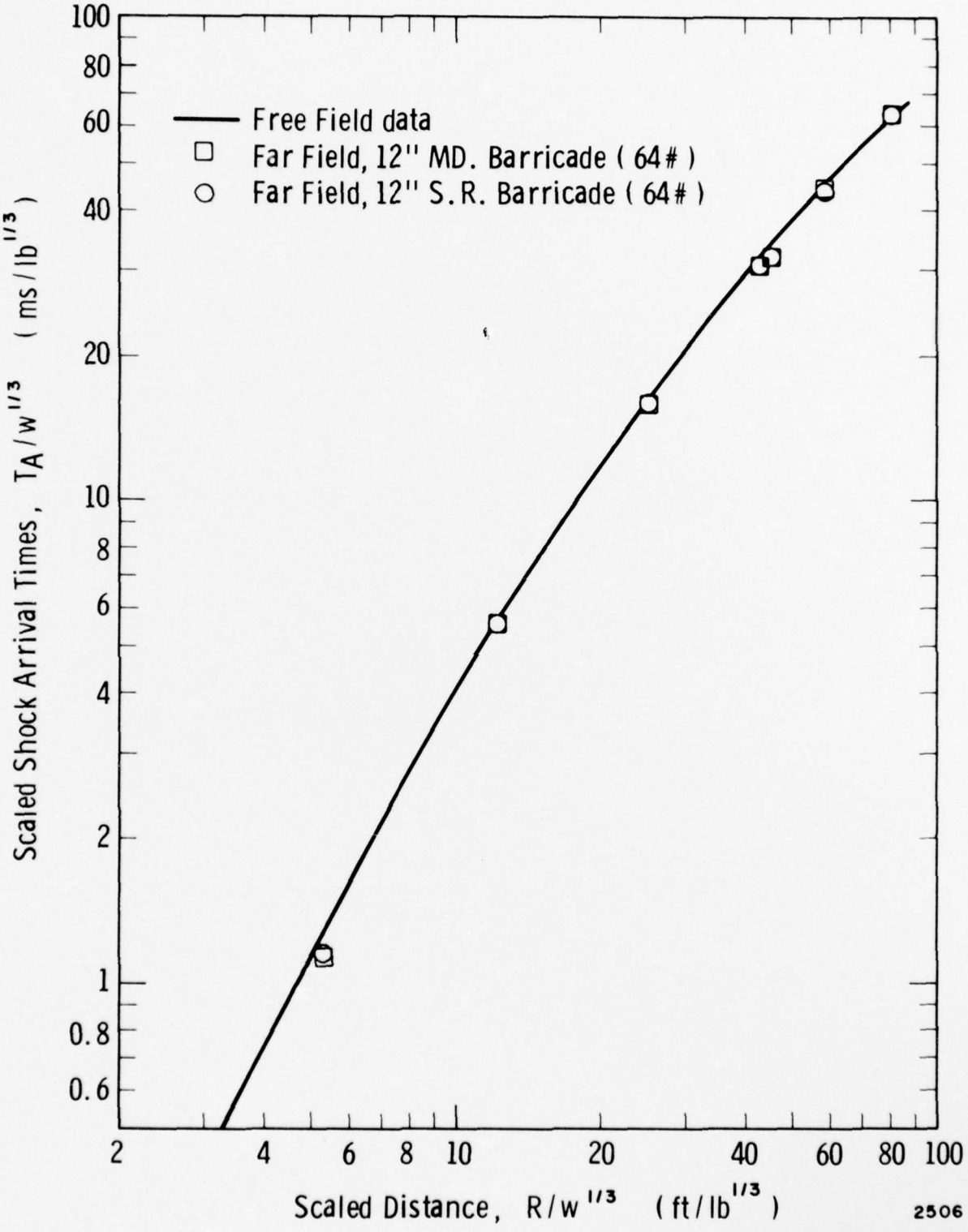

FIGURE 49. SCALED SHOCK ARRIVAL TIMES VS SCALED DISTANCE, MOUND AND SINGLE-REVETTED, 12-IN. BARRICADE, FAR FIELD (64-lb Tests)

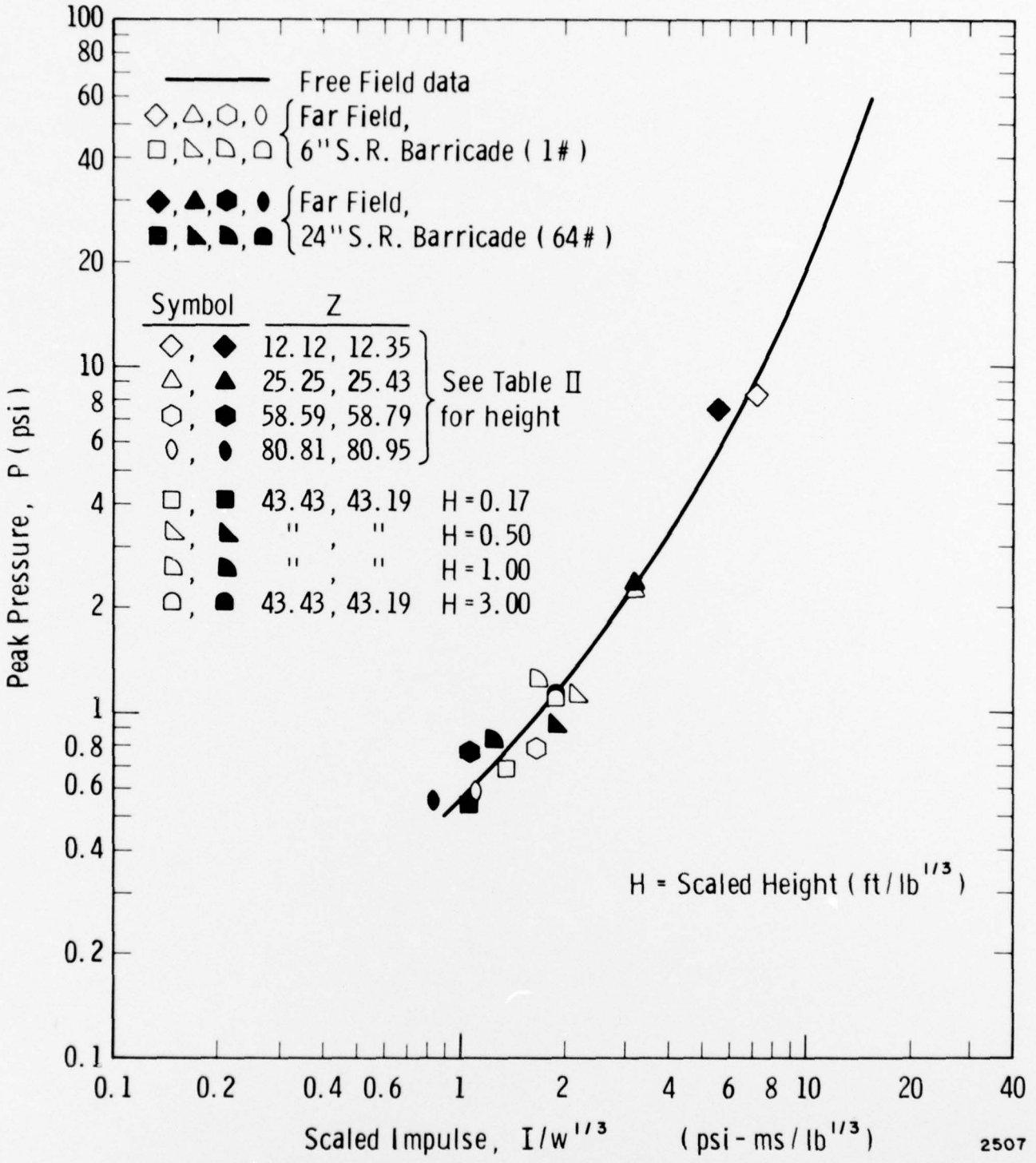

FIGURE 50. PEAK PRESSURE VS SCALED IMPULSE, SINGLE-REVETTED, 6-IN. AND 24-IN. BARRICADES, FAR FIELD

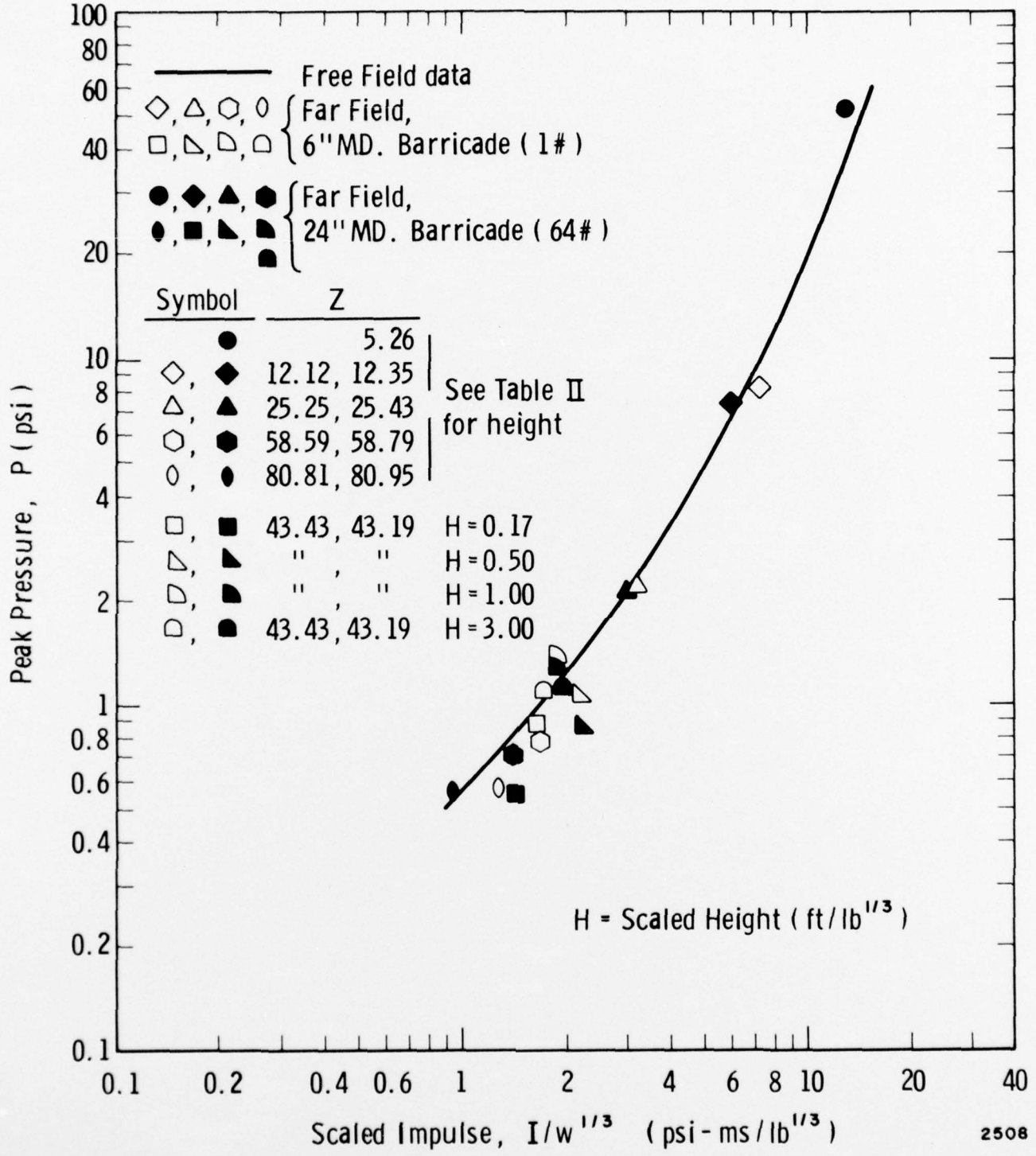

FIGURE 51. PEAK PRESSURE VS SCALED IMPULSE, MOUND, 6-IN. AND 24-IN. BARRICADES, FAR FIELD

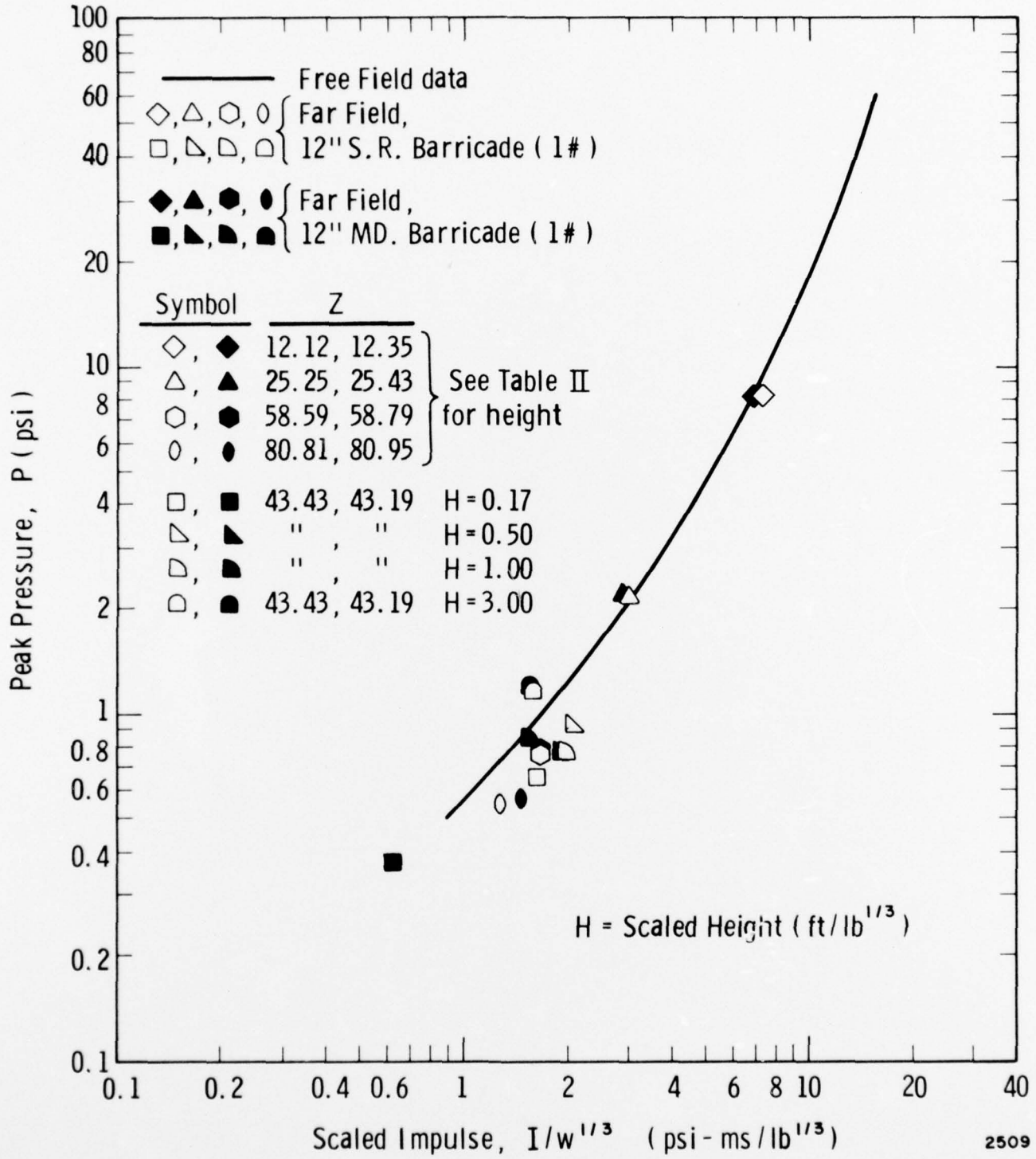

FIGURE 52. PEAK PRESSURE VS SCALED IMPULSE, SINGLE-REVETTED AND MOUND, 12-IN. BARRICADES, FAR FIELD (1-lb Tests)

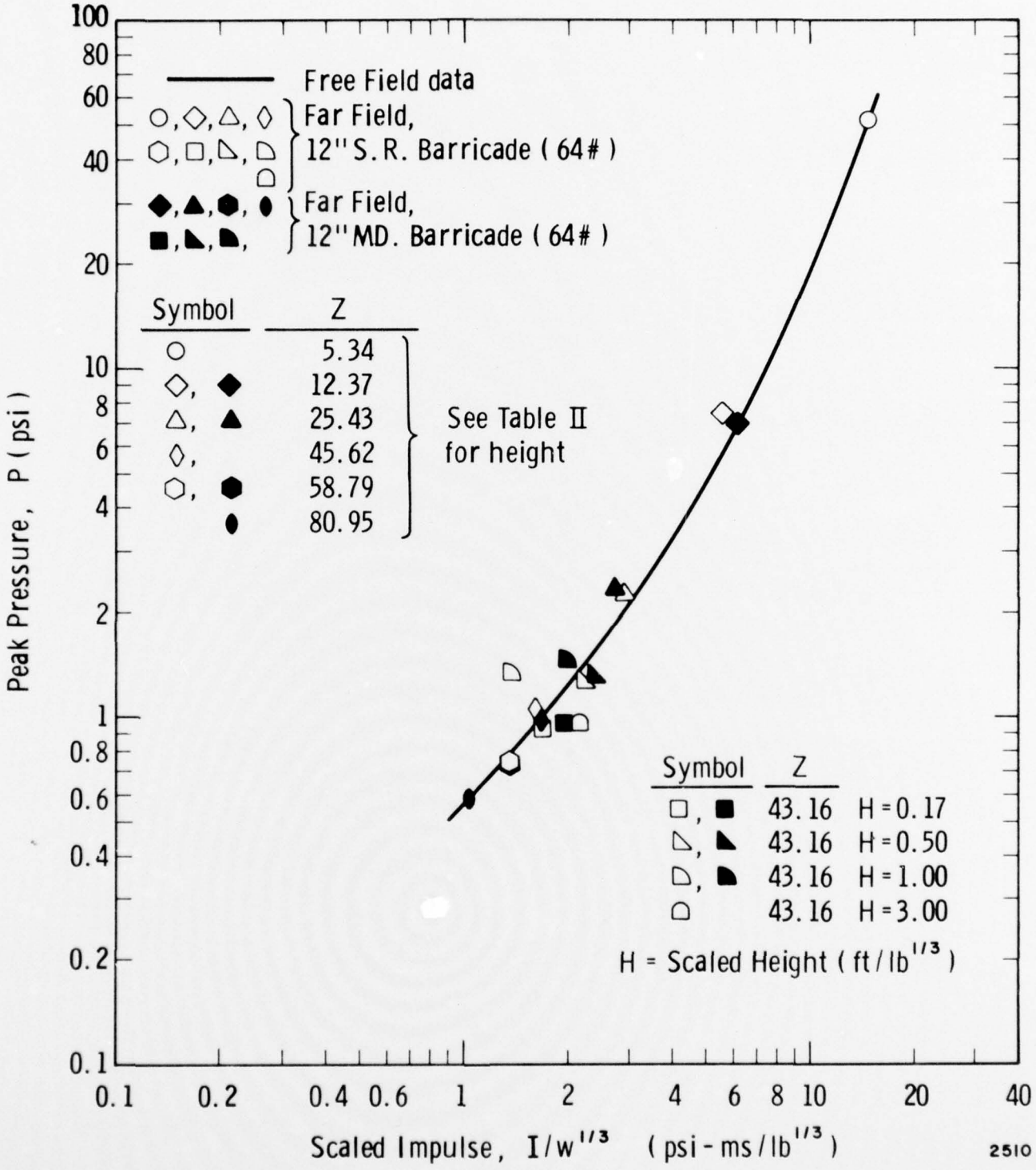

FIGURE 53. PEAK PRESSURE VS SCALED IMPULSE, SINGLE-REVETTED AND MOUND, 12-IN. BARRICADE, FAR FIELD (64-lb Tests)

V. CONCLUSIONS AND RECOMMENDATIONS

The principal conclusions reached as a result of the tests conducted on this program are:

- Barricades did reduce substantially the peak pressures and impulses immediately behind the barricades.

- Single-revetted barricades are more efficient in reducing peak pressures and impulses than mound barricades.

- Values of peak pressure and impulse are greatly influenced by the gage height relative to the ground, the location of the barricade, and the barricade dimensions and configurations.

- In the near field case for single-revetted barricade configurations, a significant reduction of pressure and impulse was observed out to scaled distances of Z = 10. Beyond the scaled distance of Z = 10, the peak pressures tend to approach those of the free field case very rapidly, and the impulses also tend to approach those of the free field case but not as rapidly as the peak pressures. The times of arrival in specific locations are greater than those of the free field case up to scaled distances of Z = 15. At scaled distances greater than Z = 15 they approach rapidly those of the free field case.

- In the near field case, mound configuration, the peak pressures and impulses are not greatly reduced, and actually are increased over the free field case at a scaled height of H = 0.17 and a scaled distance of Z = 4. However, the pressure and impulse observed at the scaled height of H = 0.5 at Z = 3 are both less than the free field values. There was a considerable decrease in pressure and impulse for the gage located at Z = 45 and scaled height of H = 0.75 as compared with the free field case and an identical gage located at Z = 45 and H = 0.150, respectively. The times of arrival were the same as those observed in the free field case for all scaled distances and scaled heights.

- For the far field case, single-revetted barricade configuration, the peak pressures and impulses were significantly reduced immediately behind the barricade; however, their individual values varied as a function of gage height. The times of shock arrival were the same as those observed in the free field case for all stations measured.

- For the far field case, mound configuration, the same observations as those made for the single-revetted case can be made here except that the effect of the barricade is considerably less than for the single-revetted configurations.

Reviewing the overall results of the program, one concludes that the repeated measurements for any one test case were quite reproducible, i.e., the standard deviations of the sets were small. Therefore, it was possible to detect small differences in blast parameters between free field and barricaded cases. However, any future experimental work in this field must pay close attention to the location of the gages relative to the barricades and their height from the ground. It is recommended that additional experiments be conducted to measure the pressure and impulse gradients as a function of gage height and distance from barricades, and also measure the effect of shock obliquity on the output of the pencil gages used.

VI. REFERENCES

1. Hopkinson, B., British Ordanance Board Minutes 13565, 1915.

2. Stoner, R. G. and Bleakney, W., "The Attenuation of Spherical Shock Waves in Air," Journal of Appl. Physics, 19, 7, pp 670-678, July 1948.

3. Kingery, C. N., et al, " Surface Air Blast Measurements From a 100-Ton TNT Detonation," Ballistic Research Labs Memo. Report No. 1410, Aberdeen Proving Ground, Md., June 1952.

4. Sachs, R. G., "The Dependence of Blast on Ambient Pressure and Temperature," Ballistic Research Labs Report No. 466, Aberdeen Proving Ground, Md., 1944.

5. Sperrazza, J., "Modeling of Air Blast," Use of Models and Scaling in Shock and Vibration, (W. E. Baker, ed), ASME, New York, pp 65-78, November 1963.

6. DOD Instructions 4145.23.

7. Turner, E. B., et al, "The Passage of Shock Waves over a Rectangular Block at Various Angles," Report No. 53-1, Engineering Research Institute, University of Michigan, August 1953, (AD 21421).

8. Turner, E. B., et al, "Three-Dimensional Observations on the Passage of Shock Waves over a Rectangular Block," Report No. AFSWP-703, Engineering Research Institute, University of Michigan, February 1954, (AD 34065).

9. Uhlenbeck, G., "Diffraction of Shock Waves Around Various Obstacles," Engineering Research Institute, University of Michigan, March 21, 1950, (ATI 194 476).

10. Turner, E. B., et al, "Diffraction of a Mach Stem Shock over a Square Block," Report No. AFSWP-704, Engineering Research Institute, University of Michigan, January 1956, (AD 87037).

11. Uppard, J. E., "Blast Protection," AWRE Report No. E 3/65, Atomic Weapons Research Establishment, Aldermaston, Berks., England, November 1965, (AD 479741).

12. White, D. R., et al, "The Diffraction of Shock Waves Around Obstacles and the Resulting Transient Loading on Structures," Technical Report II-6, Department of Physics, Princeton University, August 1, 1950.

13. Willoughby, A. B., et al, "Effects of Topography on Shock Waves in Air," AFSWC TR-57-9, Broadview Research and Development, Burlingame, California, August 1956.

14. Schleicher, A. R. and Wenzel, A. B., "Influence of a Barricade Upon Blast Wave Parameters," Armed Services Explosive Safety Board Seminars, Memphis, Tennessee, September 9-10, 1969.

15. Kingery, C. N., "Air Blast Parameters Versus Distance for Hemispherical TNT Surface Burst," Ballistic Research Laboratories Report No. 1344, September 1966.

16. Goodman, H. J., "Compiled Free-Air Blast Data on Bare Spherical Pentolite," Ballistics Research Laboratories Report No. 1092, Aberdeen Proving Grounds, Maryland, February 1960.

APPENDIX

TABLES OF DATA

TABLE A-1. BLAST PARAMETER DATA FROM 1-LB EXPLOSIVE CHARGES

Barricade Configuration	Z (ft/lb$^{1/3}$)	N_P	P (psi)	σ_P	N_I	$I/W^{1/3}$ (psi-ms/lb$^{1/3}$)	σ_I	$T/W^{1/3}$ (ms/lb$^{1/3}$)	σ_{T_A}	$\Delta T/W^{1/3}$ (ms/lb$^{1/3}$)	$\sigma_{\Delta t}$
Free Field											
None	5.05	20	52.84	2.44	20	16.47	1.66	1.03	0.05	1.41	0.15
	7.07	19	25.00	1.22	19	11.54	0.56	2.01	0.14	1.77	0.21
	12.12	18	8.42	0.61	18	7.33	0.96	5.34	0.06	2.42	0.45
	25.25	12	2.23	0.00	11	3.21	0.03	15.79	0.06	3.75	0.73
	45.45	11	1.09	0.00	11	1.73	0.00	32.77	0.09	4.31	0.69
	58.59	19	0.84	0.00	18	1.70	0.00	44.03	0.18	4.84	0.59
	80.81	14	0.59	0.00	14	1.19	0.00	63.21	0.67	4.73	0.33
Near Field, 6-In. Barricade											
Single-Revetted	5.05	20	23.85	1.70	20	10.58	1.43	1.57	0.02	1.25	0.05
	7.07	20	17.07	0.45	20	8.29	0.45	2.83	0.02	1.67	0.05
	12.12	20	6.57	0.27	20	5.22	0.50	6.44	0.03	2.26	0.27
	25.25	9	2.11	0.00	8	2.57	0.41	17.03	0.05	3.05	0.44
	45.45	16	0.98	0.31	16	1.57	0.01	34.07	0.12	3.70	0.33
	58.59	20	0.86	0.30	20	1.58	0.02	45.34	0.12	4.06	0.42
	80.81	15	0.60	0.02	15	1.13	0.00	64.59	0.56	4.28	0.23
Mound	5.05	18	33.15	1.62	14	13.16	1.46	1.14	0.02	1.12	0.17
	7.07	20	24.60	1.01	20	11.02	0.67	2.20	0.03	1.53	0.12
	12.12	20	8.44	0.56	20	6.52	0.36	5.61	0.05	2.16	0.15
	25.25	10	2.22	0.00	9	3.02	0.01	16.06	0.12	3.23	0.33
	45.45	18	0.99	0.21	18	1.68	0.00	33.10	0.18	3.98	0.64
	58.59	20	0.86	0.21	20	1.64	0.00	44.38	0.24	4.11	0.39
	80.81	15	0.60	0.20	15	1.20	0.00	63.65	0.38	4.28	0.79

TABLE A-I. BLAST PARAMETER DATA FROM 1-LB EXPLOSIVE CHARGES (Cont'd)

Barricade Configuration	Z (ft/lb$^{1/3}$)	N_P	P (psi)	σ_P	N_I	$I/W^{1/3}$ (psi-ms/lb$^{1/3}$)	σ_I	$T_A/W^{1/3}$ (ms/lb$^{1/3}$)	σ_{T_A}	$\Delta T/W^{1/3}$ (ms/lb$^{1/3}$)	$\sigma_{\Delta t}$
Near Field, 12-In. Barricade											
Single-Revetted	5.05	10	15.69	1.58	8	8.53	0.86	2.01	0.03	1.52	0.16
	7.07	16	10.91	0.53	16	5.99	0.86	3.23	0.06	1.69	0.13
	12.12	16	5.49	0.42	16	4.97	0.41	7.01	0.08	2.33	0.19
	25.25	8	1.88	0.00	8	2.68	0.03	17.60	0.08	3.64	0.59
	45.45	16	0.94	0.00	16	1.53	0.00	34.63	0.11	4.25	0.42
	58.59	16	0.80	0.00	16	1.41	0.00	45.74	0.14	4.14	0.47
	80.81	16	0.56	0.00	16	1.00	0.00	64.99	0.20	3.86	0.37
Mound	5.05	13	40.00	1.30	8	10.99	0.72	1.12	0.02	1.02	0.06
	7.07	18	19.50	1.12	17	8.45	1.01	2.23	0.03	1.62	0.16
	12.12	18	7.78	0.66	18	6.35	0.41	5.72	0.03	2.17	0.13
	25.25	9	2.14	0.00	8	2.90	0.00	16.17	0.06	3.06	0.22
	45.45	18	1.00	0.00	18	1.65	0.00	33.11	0.09	3.72	0.31
	58.59	18	0.89	0.00	18	1.55	0.00	44.39	0.08	3.90	0.40
	80.81	18	0.61	0.00	18	1.11	0.00	63.59	0.02	4.00	0.40
Near Field, 6-In. Barricade											
Single-Revetted	12.12	18	8.12	0.55	18	7.12	0.46	5.44	0.03	2.33	0.14
	25.25	9	2.21	0.00	9	3.17	0.00	15.85	0.08	3.46	0.28
H = 0.17	43.43	4	0.70	0.51	4	1.36	0.03	30.92	0.12	4.06	0.48
H = 0.50	43.43	9	1.11	0.00	9	2.17	0.00	31.13	0.14	3.94	0.13
H = 1.00	43.43	5	1.25	0.10	5	1.64	0.30	31.07	0.11	3.61	0.33
H = 3.00	43.43	4	1.09	0.00	4	1.84	0.00	31.13	0.12	4.22	0.20
	58.59	12	0.79	0.10	12	1.65	0.00	44.16	0.20	4.17	0.37
	80.81	10	0.59	0.10	10	1.10	0.00	63.34	0.30	4.23	0.45

TABLE A-I. BLAST PARAMETER DATA FROM 1-LB EXPLOSIVE CHARGES (Cont'd)

Barricade Configuration	Z (ft/lb$^{1/3}$)	N_P	P (psi)	σ_P	N_I	$I/W^{1/3}$ (psi-ms/lb$^{1/3}$)	σ_I	$T_A/W^{1/3}$ (ms/lb$^{1/3}$)	σ_{T_A}	$\Delta T/W^{1/3}$ (ms/lb$^{1/3}$)	$\sigma_{\Delta t}$
Near Field, 6-In. Barricade											
Mound	12.12	14	8.05	0.54	14	7.26	0.76	5.40	0.02	2.42	0.20
	25.25	7	2.20	0.00	7	3.17	0.02	15.79	0.03	3.47	0.30
H = 0.17	43.43	3	0.88	0.00	3	1.62	0.08	31.04	0.03	4.25	0.58
H = 0.50	43.43	7	1.04	0.00	7	2.19	0.00	31.08	0.03	4.20	0.08
H = 1.00	43.43	6	1.37	0.00	6	1.88	0.01	31.05	0.02	4.22	0.23
H = 3.00	43.43	6	1.10	0.00	6	1.70	0.00	31.02	0.02	4.03	0.20
	58.59	13	0.78	0.14	13	1.68	0.00	44.03	0.20	4.42	0.27
	80.81	11	0.58	0.17	11	1.27	0.00	63.12	0.22	4.64	0.47
Far Field, 12-In. Barricade											
Single-Revetted	12.12	12	8.11	0.64	12	7.06	0.67	5.48	0.03	2.42	-
	25.25	6	2.17	0.00	6	2.92	0.02	15.98	0.05	3.12	0.28
H = 0.17	45.45	6	0.66	0.14	4	1.62	0.00	33.13	0.06	4.33	0.13
H = 0.50	45.45	6	0.91	0.00	6	2.05	0.02	33.21	0.06	4.26	0.28
H = 1.00	45.45	6	0.78	0.00	6	1.91	0.00	33.05	0.05	4.33	0.12
H = 3.00	45.45	5	1.17	0.00	5	1.59	0.01	33.08	0.05	4.33	0.41
	58.59	12	0.76	0.00	12	1.71	0.00	44.45	0.08	4.31	0.41
	80.81	11	0.55	0.00	11	1.28	0.00	63.76	0.06	4.47	0.34
Mound	12.12	12	8.17	0.48	12	6.97	0.49	5.44	0.08	2.28	0.14
	25.25	6	2.20	0.00	6	2.88	0.00	15.81	0.06	3.14	0.25
H = 0.17	45.45	6	0.38	0.00	5	0.62	0.00	32.80	0.09	4.09	0.22
H = 0.50	45.45	6	0.76	0.00	6	1.86	0.00	32.83	0.14	4.11	0.33
H = 1.00	45.45	6	0.84	0.00	6	1.53	0.00	32.72	0.09	4.17	0.16
H = 3.00	45.45	6	1.20	0.00	6	1.52	0.00	32.76	0.05	3.98	0.31
	58.59	12	0.78	0.00	12	1.66	0.00	44.03	0.09	4.65	0.30
	80.81	12	0.57	0.00	12	1.46	0.00	63.14	0.16	4.92	0.41

TABLE A-II. BLAST PARAMETERS FROM 64-LB EXPLOSIVE CHARGES

Barricade Configuration	Z (ft/lb$^{1/3}$)	N_P	P (psi)	N_I	$I/W^{1/3}$ (psi-ms/lb$^{1/3}$)	$T_A/W^{1/3}$ (ms/lb$^{1/3}$)	$\Delta T/W^{1/3}$ (ms/lb$^{1/3}$)
Free Field							
None	5.26	2	50.31	-	-	1.08	-
	7.28	6	24.96	6	10.83	2.07	1.81
	12.35	6	7.74	6	6.06	5.43	2.39
	25.43	3	2.29	3	3.13	15.59	3.23
	45.65	6	1.10	6	1.65	32.32	4.31
	58.79	6	0.80	6	1.32	43.40	4.16
	80.95	6	0.59	6	1.02	62.28	4.19
Near Field, 24-In. Barricade							
Single-Revetted	3.31	6	31.43	6	14.13	0.72	1.32
	4.35	3	22.68	3	12.71	1.21	1.39
	5.26					1.72	
	7.28	6	11.34	6	5.71	2.93	1.42
	12.35	6	5.53	6	5.22	6.55	2.76
	25.43	6	2.06	4	2.37	16.88	2.73
	58.79	6	0.76	6	1.22	44.71	4.03
Mound	3.31	3	70.14	3	21.28	0.49	1.40
	4.35	3	74.60	3	28.32	0.86	1.76
	5.26	6	35.45	6	14.50	1.23	1.50
	7.28	6	16.13	6	9.46	2.30	1.79
	12.35	6	6.32	6	5.21	5.63	2.35
	25.43	6	2.22	6	2.68	15.75	3.08
H = 0.75	45.53	3	0.80	3	1.13	33.70	4.30
H = 1.50	45.53	3	1.10	3	1.57	33.56	3.92
	58.79	6	0.75	6	1.29	43.32	4.08
Far Field, 24-In. Barricade							
Single-Revetted	5.26					1.12	
	12.35	6	7.51	6	5.78	5.51	2.50
	25.43	3	2.36	3	3.15	15.79	3.68
H = 0.17	43.19	3	0.49	3	1.05	30.88	3.56
H = 0.50	43.19	3	0.91	3	1.87	30.58	3.45
H = 1.00	43.19	1	0.84	1	1.28	30.81	3.72
H = 3.00	43.19	3	1.15	3	1.84	30.67	3.86
	50.79	6	0.76	6	1.06	43.81	3.40
	80.95	6	0.56	6	0.84	62.78	3.68

TABLE A-II. BLAST PARAMETERS FROM 64-LB EXPLOSIVE CHARGES (Cont'd)

Barricade Configuration	Z (ft/lb$^{1/3}$)	N_P	P (psi)	N_I	$I/W^{1/3}$ (psi-ms/lb$^{1/3}$)	$T_A/W^{1/3}$ (ms/lb$^{1/3}$)	$\Delta T/W^{1/3}$ (ms/lb$^{1/3}$)
Far Field, 24-In. Barricade							
Mound	5.26	3	50.61	3	12.93	1.13	1.27
	12.35	8	7.31	8	6.00	5.54	2.53
	25.43	7	2.11	5	2.97	15.84	2.63
H = 0.17	43.19	4	0.55	4	1.43	30.70	4.39
H = 0.50	43.19	4	0.85	4	2.20	30.69	4.10
H = 1.00	43.19	4	1.27	4	1.82	30.67	3.56
H = 3.00	43.19	2	1.13	2	1.97	30.72	3.84
	58.79	8	0.72	8	1.40	43.99	4.26
	80.95	7	0.57	7	0.94	63.14	3.95
Far Field, 12-In. Barricade							
Single Revetted	5.34	2	50.10	2	14.60	1.15	1.53
	12.37	6	7.43	6	5.51	5.55	2.26
	25.43	6	2.26	6	2.86	15.85	3.37
H = 0.17	43.16	3	0.92	3	1.66	30.67	4.18
H = 0.50	43.16	3	1.24	3	2.28	30.61	3.69
H = 1.00	43.16	2	1.33	2	1.36	30.63	2.84
H = 3.00	43.16	1	0.96	1	2.02	30.70	3.86
	45.62	3	1.07	3	1.60	32.82	3.66
	58.79	6	0.74	6	1.35	43.90	4.11
	80.95	2	0.57	2	-	62.88	-
Mound	5.34	-	-	-	-	1.12	-
	12.37	6	6.95	6	6.12	5.55	2.71
	25.43	6	2.39	6	2.70	15.85	2.96
H = 0.17	43.16	3	0.97	3	1.96	30.66	3.90
H = 0.50	43.16	3	1.26	3	2.35	30.49	4.58
H = 1.00	43.16	2	1.46	2	1.96	30.67	2.40
H = 3.00	43.16	1	-	1	-	30.70	-
	45.62	3	1.00	3	1.68	32.80	3.82
	58.79	6	0.74	6	1.35	43.95	4.16
	80.95	3	0.59	3	1.04	62.94	4.08